

From Molecular Medicine and Surgery
Karolinska Institutet, Stockholm, Sweden

NOVEL BIOMARKERS IN REGULATING HUMAN DENSE CONNECTIVE TISSUE REPAIR

Junyu Chen

陈俊宇



**Karolinska
Institutet**

Stockholm 2022

All previously published papers were reproduced with permission from the publisher.

Published by Karolinska Institutet.

Printed by Universitetservice US-AB, 2022

© Junyu Chen, 2022

ISBN 978-91-8016-864-9

Novel Biomarkers in Regulating Human Dense
Connective Tissue Repair
THESIS FOR DOCTORAL DEGREE (Ph.D.)

By

Junyu Chen

The thesis will be defended in public Lecture Hall at Norrbacka, Eugeniavägen 27, Karolinska
Universitetssjukhuset, Solna, Sweden, 2022-12-09

Principal Supervisor:

Paul W. Ackermann, Professor
Karolinska Institutet
Department of Molecular Medicine and Surgery
Division of Orthopaedics

Opponent:

Gustav Andersson, Associate Professor
Umeå University
Department of Integrative Medical Biology

Co-supervisor(s):

Aisha S. Ahmed, PhD
Karolinska Institutet
Department of Molecular Medicine and Surgery
Division of Orthopaedics

Examination Board:

Ola Nilsson, Professor
Karolinska Institutet
Department of Women's and Children's Health

Thorpe Chavaunne, Lecturer
University of London
Department of Comparative Biomedical Sciences

Tomas Movin, Associate Professor
Karolinska Institutet,
Department of Clinical Science

致我的家人，爱人，朋友及所有爱我和我爱的人，谢谢你们的支持与包容！

POPULAR SCIENCE SUMMARY OF THE THESIS

Pain and degeneration in the musculoskeletal system cause immense individual suffering. One of the main reasons for the still not sufficient available therapies is the limited knowledge of the underlying key factors and different steps in the healing process responsible for the less than optimal and often varying healing outcomes of dense connective tissues (CTs). Dense CTs, such as tendons, ligaments and knee meniscus, have vital roles in supporting, protecting and transmitting forces in the human body. The overall aim of this thesis was to identify new biomarkers, such as proteins related to a good healing capacity, of dense CT healing. The thesis was designed to search for biomarkers during 1) the early healing phase with swelling and pain (inflammatory) as well as 2) the later healing phase with rapid growth of new parts (proliferative) in tendon tissue and in samples of tendon extracellular fluid, respectively, after Achilles tendon rupture (ATR) as a model of dense CT healing.

By using a highly sensitive technique for the detection and quantitation of messenger RNA (mRNA) of tendon tissue from early healing, the presence of potential biomarkers (*Col I, Col III, FGF, FN, MMP-9*) was identified. The mRNA levels of fibroblast growth factor (*FGF*) was positively associated with improved outcomes of the patients after 1 year. Higher collagen type III (*Col III*) mRNA expression was associated with patients perceiving better strength in their tendons at 1 year.

Analysis of the entire set of proteins of tendon tissue, using quantitative mass spectrometry, from early healing disclosed 769 proteins, including 51 proteins with different levels among patients with good- versus poor outcome after 1 year. Among these proteins a new biomarker, elongation factor-2 (eEF2), was identified as being highly associated with better patient clinical outcome after 1 year. Experimental studies revealed that eEF2 regulated cell renewal, cell growth and movement, as well as reduced cell death in dense CT healing.

Utilizing the entire set of proteins of tendon tissue from early healing phase together with analysis of a network the proteins, a biomarker, inter-alpha-trypsin inhibitor heavy chain (ITIH4), associated with improved patient 1 year healing outcomes was discovered. Experimental studies identified that ITIH4 in an intricate manner stimulated collagen type I production.

Further studies of the entire set of proteins from tendon fluid from the later proliferative healing phase discovered 1288 unique proteins, whereof 9 upregulated, and 23 downregulated proteins in patients with good- versus poor outcome after 1 year. Upregulated proteins were related mainly to the organization of new tissue, while downregulated proteins were associated with blood clotting. The most reliable biomarker to predict patient outcome was the downregulated inflammation-related, complement factor D (CFD).

Expanded studies of CFD demonstrated higher levels during early- and lower levels during later healing phases in the patients with good outcome. Further experimental

investigations demonstrated that CFD improved tissue repair by enhancing cell movement and production of collagen type I (Col1a1) during early healing, while exerting the opposite effects during later healing.

The results of this thesis have discovered new biomarkers eEF2, FGF, ITIH4 during the early healing phase and CFD mainly during the later healing phase. Measurement of the levels of these biomarkers predict if the patient will have a 1 year good- or poor outcome of their tendon repair, and these findings are presumably reflective of dense CT healing in general. These observations may lead to improved individualized treatment decisions, as well as to accelerate the development of improved therapies to promote good long-term healing outcomes of the patients.

ABSTRACT

Painful and degenerative disorders of the musculoskeletal system pose a tremendous burden on the healthcare system. One main reason is the limited knowledge of the underlying key factors and pathways responsible for the suboptimal and often varying healing outcomes of dense connective tissues (CTs), such as tendons, ligaments and knee meniscus, which have vital supportive, protective and force transmitting roles in the human body. The overall aim of this thesis was to identify novel biomarkers of dense CT healing. The thesis was designed to explore for biomarkers during the inflammatory- and proliferative healing phases in tissue biopsies and micro-dialysate, respectively, after Achilles tendon rupture (ATR) as a model of dense CT healing.

Using quantitative RT-PCR and immunohistochemistry of ATR tissue biopsies from the inflammatory healing phase the presence of potential biomarkers (*Col I*, *Col III*, *FGF*, *FN*, *MMP-9*) was identified. The gene expression of fibroblast growth factor (*FGF*) was positively associated with improved 1-year patient-reported- and functional outcomes. Higher *Col III* mRNA expression was associated with more perceived tendon strength at 1 year.

Proteomic profiling using quantitative mass spectrometry of ATR biopsies from the inflammatory healing phase disclosed 769 proteins, including 51 differentially expressed proteins among patients with good- versus poor 1-year outcome. Among them a novel biomarker, elongation factor-2 (eEF2), was identified as being strongly prognostic of the 1-year clinical outcome. Experimental exploration revealed that eEF2 regulated autophagy, cell proliferation and migration, as well as reduced cell death and apoptosis in dense CT healing.

Utilizing the proteomic profile from the inflammatory healing phase together with weighted co-expression network analysis a biomarker, inter-alpha-trypsin inhibitor heavy chain (ITIH4), associated with improved 1-year healing outcomes was discovered. Experimental explorations identified ITIH4 to stimulate collagen I production mediated by PPAR γ signaling pathways.

Further proteomic profiling of micro-dialysate from the proliferative healing phase discovered 1288 unique proteins, whereof 9 upregulated, and 23 downregulated proteins in patients with good- versus poor 1-year outcome. Upregulated proteins were related mainly to extracellular matrix organization, while downregulated pathways were associated with functions such as thrombosis formation. The most reliable predictive biomarker was the downregulated pro-inflammatory complement factor D (CFD).

Expanded characterization of CFD demonstrated higher expression during inflammatory- and lower expression during proliferative healing phases in the good outcome patients. Further experimental explorations demonstrated that CFD improved repair by enhancing cell migration and collagen type I (Col1a1) production during inflammation, while exerting the opposite effects during proliferative healing.

The results of this thesis have established biomarkers eEF2, FGF, ITIH4 during the inflammatory healing phase and CFD mainly during the proliferative healing phase, all prognostic of improved patient outcome in tendon repair, presumably reflective of dense CT healing in general. These findings may lead to improved individualized treatment decisions, as well as accelerate the development of improved therapies to promote good long-term clinical healing outcomes.

LIST OF SCIENTIFIC PAPERS

- I. **J Chen**, J Svensson, CJ Sundberg, AS Ahmed, PW Ackermann. FGF gene expression in injured tendons as a prognostic biomarker of 1-year patient outcome after Achilles tendon repair. *J Exp Orthop* 8, 20 (2021).
- II. **J Chen**, J Wang, DA Hart, AS Ahmed, PW Ackermann. Complement factor D as a predictor of Achilles tendon healing and long-term patient outcomes. *FASEB J* 36, e22365 (2022).
- III. **J Chen**, J Wang, X Wu, N Simon, CI Svensson, J Yuan, DA Hart, AS Ahmed, PW Ackermann. eEF2 improves connective tissue repair by regulating cellular death, autophagy, apoptosis, proliferation and migration. *Manuscript under review*
- IV. **J Chen**, J Wang, David A. Hart, AS. Ahmed, PW Ackermann. Complement factor D mediates human dense connective tissue repair by mediating collagen type I synthesis. *manuscript*
- V. X Wu, **J Chen**, W Sun, PW Ackermann, AS Ahmed. Network analysis identifies ITIH4 as a prognostic biomarker and therapeutic target of connective tissue regeneration. *Manuscript under review*

CONTENTS

1	INTRODUCTION.....	1
2	LITERATURE REVIEW	3
3	RESEARCH AIMS.....	19
4	MATERIALS AND METHODS	21
5	RESULTS AND DISCUSSION.....	33
6	CONCLUSIONS.....	57
7	POINTS OF PERSPECTIVE	59
8	ACKNOWLEDGEMENTS.....	61
9	REFERENCES.....	63

LIST OF ABBREVIATIONS

APOL1	Apolipoprotein L1
AT	Achilles tendon
ATR	Achilles tendon rupture
ATRS	Achilles tendon total rupture score
AUC	Area under the curve
BCA	Bicinchoninic acid
BMP	Bone morphogenetic protein
BMSCs	Bone marrow-derived mesenchymal stem/stromal cells
BSA	Bovine serum albumin
CFD	Complement factor D
CT	Connective tissue
CTGF	Connective tissue growth factor
Col I	Collagen type I
Col1a1	Collagen type I alpha 1 chain
Col III	Collagen type III
Col3a1	Collagen type III alpha 1 chain
CPN1	Carboxypeptidase N Subunit 1
DVT	Deep vein thrombosis
ECM	Extracellular matrix
eEF2	eukaryotic elongation factor-2
FAAM	Foot and Ankle Ability Measure
FAOS	Foot and Ankle Outcome Score
FGF2	Fibroblast growth factor-2
FN	Fibronectin
GAGs	Glycosaminoglycans
GO	Gene ontology
GSEA	Gene set enrichment analysis
H&E	Hematoxylin and Eosin
HRT	Heel-rise test
iBAQ	intensity-based absolute quantification

IDEAL	Iterative decomposition of echoes of asymmetrical length
IFM	Interfascicular matrix
IGFBP4	Insulin-like growth factor-binding protein-4
IGLV1-47	Immunoglobulin lambda variable 1-47
IL1	Interleukin-1
IL1	Interleukin-2
IL6	Interleukin-6
IF	Immunofluorescence
IHC	Immunohistochemistry
IPC	Intermittent pneumatic compression
ITIH4	inter-alpha-trypsin inhibitor heavy chain
KTN1	Kinectin 1
LC3	Microtubule-associated proteins light chain 3
LPS	Lipopolysaccharide
LSI	Limbs symmetry index
MMP3	matrix metalloproteinase-3
MMP9	matrix metalloproteinase-9
MS	Mass Spectrometry
MSD	Meso-scale discovery
NID2	Nidogen-2
PALLD	Palladin
PBS	Phosphate buffered saline
PDGF	Platelet derived growth factor
PINP	procollagen type I N-terminal pro-peptide
PIINP	procollagen type III N-terminal pro-peptide
PRP	Platelet-rich plasma
PROS1	Protein S-1
RCT	Randomized controlled trial
RIPA	Radioimmunoprecipitation
ROC	Receiver operating characteristic
RSA	Roentgen stereophotogrammetric analysis

SF-36	Short Form-36
SERPINB1	Serpin family B member-1
SERPINF1	Serpin family F member-1
TGF- β	Transforming Growth Factor Beta
TIMP1	Tissue inhibitor of metalloproteinase-1
TIMP3	Tissue inhibitor of metalloproteinase-3
TNF	Tumor necrosis factor
TSCs	Tendon stem cells
VEGF	Vascular endothelial growth factor
WB	Western blot
WGCNA	Weighted gene co-expression network analytical

1 INTRODUCTION

Dense connective tissues (CTs), such as tendons, ligaments and knee meniscus have vital supportive, protective and force transmitting roles in the human body. After injury, however, dense CTs exhibit impaired healing capabilities, which often lead to chronic pain and degenerative musculoskeletal disorders [1]. The limited reparative capability has been attributed to a relative avascular/aneuronal nature and low cellularity of dense CT leading to variable and frequently poor patient outcomes. Yet, the key factors and pathways responsible for the variable healing outcomes are mostly unknown.

Dense CTs are composed of three major components: elastic and collagen fibers, cells and ground substance [2]. The most common cell type of dense CTs is the fibroblast cells, which produce extracellular matrix (ECM). The repair of connective tissue after injury consists of three overlapping phases of inflammation, proliferative and remodeling. During dense CT repair, major cell types including fibroblasts, mast cells and macrophages play a vital role and are involved in a variety of biological pathways [3]. Additionally, collagen production, mainly by the fibroblasts, is a key process during ECM deposition and re-organization. Thus, essential proteins that influence or modulate cell types as well as collagen production could be seen as biomarkers of dense CT healing, and altered levels of these proteins may also promote the clinical outcome after injury.

Tendons are uniaxial and highly organized hypocellular dense CT. The Achilles tendon (AT) is the biggest tendon and also one of the strongest dense CT in human body [4]. The Achilles tendon connects the heel bone together with the calf muscles and can withstand a load of up to 12-times the body weight while running, jumping and skipping [5, 6]. The anatomical and physiological characteristics make AT the longest but also most frequently injured tendon [7, 8]. The reparative process after tendon or ligament injuries lead to high individual variations in long-term patient outcome, and the AT is no exception. One year after injury, 44% of the patients experience limitations due to pain and only four in ten patients with AT rupture have returned to their preinjury sport activities [9, 10].

This makes the study of AT healing a representative of dense CT repair. During dense CT repair fibroblasts produces collagen to maintain and protect the dense CT structure, as well as contributes to new dense CT formation. A deepened knowledge of how key biomarkers affect the molecular function of fibroblasts may contribute to a better understanding of dense CT repair. However, studies on the cellular and molecular biology of biomarkers in human dense CT healing are still lacking.

In this thesis, we used ruptured human AT as a model and combined with human primary fibroblasts and a fibroblast cell line to identify biomarkers, which can be used as predictors of tendon healing and clinical outcome, as well as a representative of dense CT repair. Identification of such biomarkers could lead to better individualized treatment regimens as well as to the development of new targeted treatments to improve dense CT repair.

2 LITERATURE REVIEW

1. *Connective Tissue (CT)*

Human movement is supported by the musculoskeletal system which mainly consists of bone, muscle and connective tissues. In general, CTs can be classified into dense CT (CT), loose CT and specialized CT. The load bearing structure of specialized dense CTs like tendons connects bone and muscle, and can therefore also transmit forces from muscle to bone [11]. The CTs build up a whole-body dynamic and mechanosensitive network which can be influenced by body movement [12]. The CT disorders are not only associated with muscle, skin and joint, but also related with numerous organs. Thus, gaining insight of the CTs network and their function may increase the understanding of body health and disease, and probably improve further treatment of musculoskeletal disorders.

1.1 *Dense CT*

Tendon, ligament, outer knee meniscus, sclera and the inner layer of the skin (dermis) are some major types of dense CTs. The function of dense CTs is to provide production of proteins and holding of muscles, bones and other organs. Dense CTs, also called as dense fibrous tissues consist of protein fibers. The most important and common component of dense CT is collagen type I (Col1) and the main cell type is fibroblasts.

1.1.1 *Tendon*

Tendons are a type of high-tensile-strength dense CT which connect muscle to bone. Healthy tendons generally consist of water, collagens, elastic fibers, proteins, polysaccharides and inorganic components (copper, manganese and calcium) [13]. The major subunit of tendon is the fascicle which is made up of different collagen fibers bound together (Figure 1). Fascicles are irregularly shaped in size with the diameter ranging from 150 to 500 μm . Interfascicular matrix (IFM) is the compartment that surrounds the fascicle, playing a role as an energy storage container [14]. Generally, five collagen molecules are linked by an intermolecular cross-linkage to form collagen microfibrils [15]. Collagen fibrils bound together to form collagen fibers, which are the most important components of the fascicle. Thus, the components of the fascicle make tendon a fibrous and soft tissue, which allows force from muscle to be applied to the bone.

Water constitutes 55-70% of the tendon wet weight. In contrast, collagens forms 60-85% of the dry weight of tendon, making collagen the most important element of tendon ECM [16]. The hierarchical collagen structure interacts with various non-fibrillar proteins, which results in a crucial function to maintain load with stability in tendons [11]. Among the collagens, type I (Col I) is the most important one which represents approximately 90% of all the collagen content. Collagen type III (Col III) makes up approximately 10% of the total collagen content in healthy tendon and participates in collagen fibrillogenesis and modifies the fibril size of Col I. In addition, collagens type V, VI, XI, XII and XIV are also present in tendons in a small amount [17-19]. On the cellular level, the molecules of tendon collagens

are formed by tenocytes, which are tendon specialised fibroblasts. Tenocytes are the major resident cells in tendons, displaying an elongated shape parallel with the collagen fibers. Tenocyte activity is mainly regulated by tendon loading. Subsequently tenocytes modulate the ECM, by regulating the degradation and formation of ECM [11]. An overview of different tendon elements on a molecular level is shown in Figure 1.

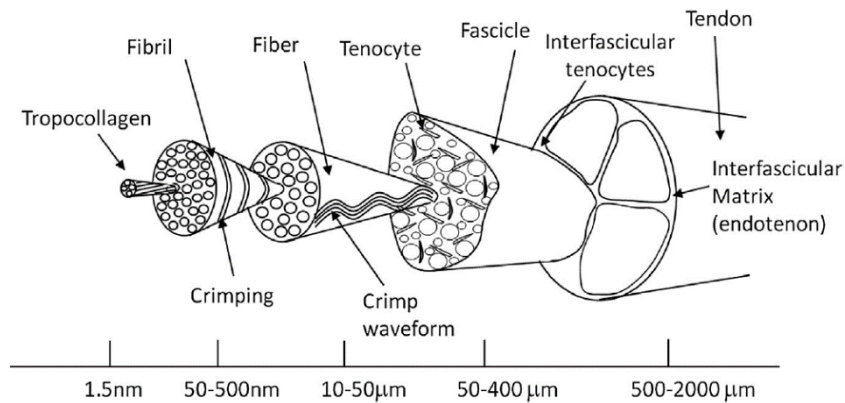


Figure 1. Tendon hierarchical structure, the increasing diameter formed by collagen molecules assemble (Tendon regeneration, Chapter 1, 1.1:5).

Tendons are traditionally considered as relatively inelastic musculoskeletal structures, which connect muscle to bone and functioning to convey power. The biomechanical and elastic properties of tendons depend partly on the diameter and orientation of collagen fibers which are parallel to each other and packed closely. During the past two decades, studies have focused on the elastic properties of tendons and their ability to act as springs. As a result, specific tendons like Achilles tendon (AT) and superficial digital flexor tendon were reported to exhibit additional functions as compared with other tendons, namely acting as elastic springs to store energy [20].

1.1.2 Ligament

Ligaments are another major type of dense CT, presenting its function in connecting bone to bone and help to maintain the structural stability. Although ligaments are considered to be inert, actually they response to internally systemic factors in order to impact their roles within the organism. There is a vascular layer called “epiligament” covering the surface of the ligament [21]. Although the ligament looks like a single structure, the internal collagen fibers tighten/loosen following movements of the joints. However, the structure of ligaments presents as fibroblasts surrounded by a matrix under the microscope. Compared with tendon tissue, the ligament is made up of lower ratio of collagens but higher percentage of proteoglycans, elastin and water. A schematic diagram of different ligament elements on a molecular level is shown in Figure 2.

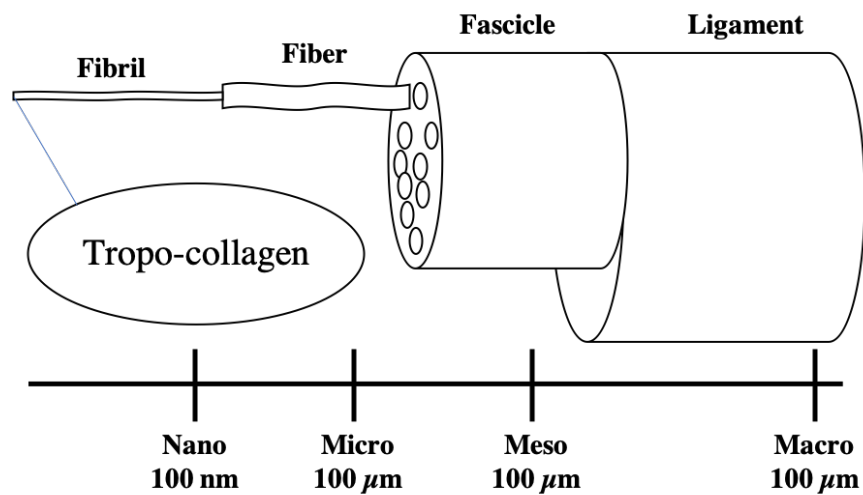


Figure 2. Ligament hierarchical structure (prepared by Junyu Chen based on the Reference [22]).

1.2 Loose CT

Loose CT, also known as areolar tissue, is a type of widely distributed CT in human body. Elastic and reticular fibers are the major component of the loose CT structure where fibroblasts, mast cells and adipocytes are the main cell types [12], while loose CT has lower ratio of fibers when comparing with dense CT. Since most of the cells in loose CT are migrated from blood vessels under special stimulation, loose CT is regarded as an area of inflammation and immune response. In general, adipose, basement membrane and areolar are the three major types of loose CT, showing their functions to protect body from overextending and help to save energy. Loose CT may be found surrounding tendons and can provide inflammatory- and immune reactions that can participate in healing.

1.3 Specialized CT

Special CT including adipose tissue, cartilage, blood, lymph, bone and reticular CT. Among these special CTs, blood and lymph are the most common specialized fluid CT in human body while bone and cartilage are considered as supportive CT. Generally, all the specialized CTs are included into the fascial system [23].

2. Dense CT Injurie

Generally, dense CT injuries can be divided into acute and overuse injuries. These injuries often occur during sports and training. Strains and contusions often lead to acute dense CT injuries, while overuse may lead to tendinopathy (previously known as tendinitis) and bursitis.

3. Dense CT Healing

After injury, a reparative process is initiated in dense CTs which is highly dependent on protein synthesis. The repair of dense CT injury consists of dynamic and overlapping phases, including the inflammatory, proliferative and regenerative phases [24]. After injury, the

immune system is activated, since the injuries also stimulate the fibroblasts and blood-derived cells to release collagen, pro-inflammatory cytokines and collagenases [25, 26]. Biomarkers may be released by several cell types, such as mast cells derived from tissue, which can increase the capillary permeability, leading the migration of white blood cells to the site of injury. Then the release of several growth factors (Transforming Growth Factor Beta (TGF- β), Connective Tissue Growth Factor (CTGF), Fibroblast Growth Factor (FGF)) stimulate the cellular migration, angiogenesis and cell growth [27, 28]. The production of these growth factors can lead to the synthesis and balance of matrix metalloproteinases (MMPs) and tissue inhibitor of metalloproteinases (TIMPs). The balance between MMPs and TIMPs is a vital factor of pro- and anti-angiogenesis. In CT healing, blood- and tissue-derived cells demonstrate their functions through deposition of ECM which is rich in collagen type I (Col I) and III (Col III) [29]. During the remodeling phase, which is still not fully understood, the ratio of collagen type I is increased while collagen type III is decreased [30]. However, more comprehensive studies are needed to explore the underlying mechanisms of dense CT remodeling.

The reparative process after dense CT injury is complex and can lead to considerable individual variation in long-term patient outcomes. Such variations often result in compromised function, chronic pain and degenerative musculoskeletal diseases for many patients [1]. Knowledge of the regulatory mechanisms responsible for such variability in regenerative outcomes, as well as identification of validated biomarkers that can be used as predictors of dense CT healing are still mostly lacking [31-33] but could be used in development of optimized treatments and to understand mechanisms of tendon healing. Since AT is one of the largest and most frequently injured dense CT, we used a human AT as a model to identify novel prognostic biomarkers and their molecular mechanisms of healing, as representative of dense CT repair.

4. Achilles Tendon

AT is the strongest and thickest tendon in human body [4]. It starts near the middle of the calf, spans the ankle joints, making AT the longest but most frequently injured tendon [7, 8]. The triceps surae (soleus muscle, the medial and lateral head of the gastrocnemius muscle) unite into a band of CT at the low end of calf. The AT connects the triceps surae and the calcaneus, pulls the calcaneus cranially when it contracts, allowing human to stand at the tip of toes, walk, jump, run and go up/downstairs. During physical activities, AT acts as an elastic spring, which save energy and then return it to the AT.

The average length of AT is approximately 15 cm and ranges from 11 to 26 cm [34, 35]. The AT is gradually narrowing from proximal to distal and then becomes thicker at 2-6 cm above the calcaneal tuberosity. Blood supply of the AT mainly comes from three sources: paratenon perforators, muscle-tendon and tendon-calcaneus junctions [36, 37]. However, the number of blood vessels decreases with age [38]. Approximately 2-6 cm above the insertion of AT is a relatively avascular region with poor blood supply, which is the area where most injuries occur [39, 40]. The tibial nerve supplies the gastrocnemius and soleus muscles, while

the innervation of AT mainly comes from the sural nerve with a minor contribution from other smaller branches of the tibial nerve.

4.1 AT Disorders

Disorders of AT generally include tendinosis, paratenonitis, tendinitis, retrocalcaneal bursitis and rupture [41]. Most of the tendon problems are associated with overuse and have a multifactorial origin [42]. Most of AT disorders are today collectively called tendinopathy, which depicts the clinical syndrome of swelling, pain and impaired performance.

4.1.1 Achilles Tendinosis

Tendinosis is a degeneration of the AT with no clinical and minor histological signs of intratendinous inflammation. Tendinopathy can be classified as non-insertional tendinosis occurring in the main body of the AT or as insertional tendinopathy, which depicts isolated pain at the site of insertion from AT to calcaneus [43]. Previous studies suggest that loss of balance in matrix synthesis and degradation can be one reason of tendinosis [44]. The etiologic factors of Achilles tendinosis include both extrinsic and intrinsic factors. Some intrinsic factors that are regarded to influence the development of tendinopathy are imbalance or weakness of muscles, malalignment, decreased blood supply, overuse and lack of flexibility. Moreover, intrinsic factors include hereditary factor and metabolically related disorders. Among extrinsic factors excessive mechanical loading and training errors are the most common factors. However, also certain drugs are known to increase the risk of tendinopathy, including corticosteroids, aromatase inhibitors, quinolone antibiotics and statins. Interestingly, studies have found that most patients that suffer an Achilles tendon rupture exhibit underlying Achilles tendinosis [45, 46].

4.1.2 Achilles Tendinitis

Achilles tendinitis is an inflammatory process usually detected on biopsy specimen of disordered tendons. Tendinitis is mostly associated with underlying inflammatory disorders. Thus, the description of Achilles tendinitis is not commonly used today and has been replaced Achilles tendinopathy, which more accurately depicts the clinical problem for most patients with pain from the AT.

4.1.3 Achilles Paratenonitis

Achilles paratenonitis which is also known as peritendinitis, is a frequent tendon disorder especially in athletes, accounting for 2/3 of AT injuries among competitive athletes [47]. It is caused by inappropriate shoes, overuse and repeated movement, specifically among runners. Patients with paratenonitis exhibit symptom including tenderness, pain and swelling in Achilles region, however, these symptoms will become worse during physical activities.

4.2 Achilles Tendon Rupture (ATR)

ATR is a normal injury presenting as a break in the conjoined tendon between soleus and gastrocnemius muscle [48], with an increasing incidence worldwide [42, 49, 50]. ATR frequently occurs during a sudden force on AT, especially eccentric load. Other activities, including running, jumping and quick changes of direction are also main reasons of ATR. In European countries, badminton is the most common cause, especially in Sweden (leading 66%) [51]. In contrast, basketball causes the highest range of ATR in United States [52]. There is a huge sex difference among ATR patients, presenting as a ratio of male-to-female of 20:1 [53]. Meanwhile, ATR is also a bimodal age distributed disorder with the first peak at 25 to 40 years old and a second peak in those over 60 years [51]. Additionally, underlying Achilles tendinopathy has also been shown to be a very common etiological factor [54].

4.3 Diagnosis of ATR

The diagnosis of ATR mainly depends on the anamnesis and the clinical examination of the patient. Patients with ATR commonly feel that their ankles or tendon area were suddenly pushed or struck with pain during physical exercises, with sudden inability for plantar flexion. After ATR, patients feel swelling and bruising. The typical features after ATR are limping, difficulty in weight-bearing ambulation and plantar flexion weakness. Standard diagnosis of acute ATR can be defined by at least two of the following physical tests according to American Academy of Orthopaedic Surgeons clinical practice guidelines: i) palpable defect; ii) different traumatic sports injury with low-energy injury which is related with tendinosis, a history of steroid injection in recent or previous years; iii) a positive Thompson test; iv) weakness of plantar flexion and strength. Imaging of ATR is only performed in uncertain cases, then mainly with ultrasonography.

4.4 Treatment after ATR

The treatment of ATR can be generally categorized as either nonsurgical or surgical management:

4.4.1 Non-surgical Treatment

Nonsurgical treatment consists of a 6 to 12 weeks lower-limb immobilization in a plantar flexed position using a plaster cast or an orthosis. During the immobilization time the ankle is successively moved from 30 degrees plantar flexion to a neutral position. The nonsurgical treatment, however, been reported to result in more frequent re-ruptures, around 12.6%, compared to the surgical treatment with a re-rupture risk of around 3.5% [55]. Although recent studies demonstrated that decreased cast immobilization time or early functional rehabilitation can decrease the re-rupture rate [56, 57], further research is needed to further strengthen and validate these findings. Rehabilitation is critical during nonsurgical treatment. This term represents early controlled movement exercises and protected weight bearing after nonsurgical treatment. Recent studies has shown the benefit of early exercises on AT healing in animal models [58, 59]. Early motion during 8 to 14 weeks after ATR improved tendon strength and mechanical loading on the healing AT, resulting in increased

tendon callus. A clinical study with 35 ATR patients has reported that the tendon elastic modulus in patients who received early motion were better than in the patients who only got immobilized [60], indicating the importance of rehabilitation in tendon healing. Although early weight bearing hasn't been reported to have an association with increased re-rupture risk during recovery, most authors advocates at least dorsiflexion motion restrictions [61].

4.4.2 Surgical Treatment

Surgical repair of acute ATR can be generally classified as mini-open, open and percutaneous reconstruction [62].

Conservative surgery for ATR is an open operation performed with a posterior medial approach method with the patient in a prone position. It is also the most frequently used technique since the posteromedial approach is performed at the site between the posterior tibial and peroneal arterial, minimizing the vascular damage [63].

Percutaneous ATR repair is an updated technique to minimize devitalization of surrounding tissues and decrease the size of incision to reduce the risk for skin infections and necrosis. This technique was firstly reported by Ma and Griffith [64]. It is performed by using suture to weave between proximal and distal ends of AT through medial and lateral stab incisions. Interestingly, a decreased risk of sural nerve injury was reported among patients received percutaneous repair when compared to those treated with the conservative method [65, 66], indicating an improvement of this updated technique.

Mini-open surgery is another technique that combines the advantages of open and percutaneous repair. This technique was firstly devised by Kakiuchi in 1995 [67]. This method maximizes the contact of the ruptured edges of tendon during the operation and minimizes the complications such as wound infection and sural nerve injury. Mini-open surgery is performed through a small incision above the rupture site and then spreading the tissue bluntly by using a device. The suture is guided inside the tendon from the skin, and across to the opposite side. Commonly, three sutures are used to sew the edges of proximal and distal tendon. In the end, the suture and device will be pulled outside in order to mark the position of repaired tendon after tying in the plantar flexed position. Compared with the other two techniques, patients treated with mini-open surgery present with lower rates of wound complications and better cosmetic appearance. However, the overall complication rate among these techniques have been reported to be statistically non-significant [68].

4.4.3 Post-surgical Treatment

The conventional method of post-surgery treatment is immobilization with a cast during the first 6 weeks. Prolonged immobilization is however not desirable. Conversely, early weight bearing and motion exercises are also important for tendon healing, and was shown to result in better recovery than immobilization [69].

4.4.4 Other Approaches

During recent years, researchers continue to explore other approaches to minimize the rate of re-rupture and enhance clinical outcomes. The down-turned gastrocnemius fascia flap during open AT repair was demonstrated for the first time in 2009 by Pajala [70], however, no statistical difference was found between patients with and without augmentation. Bone marrow-derived mesenchymal stem/stromal cells (BMSCs) and platelet-rich plasma (PRP) have been considered and investigated as biological techniques, although clinical evidence of positive efficiency of PRP and BMSC on ATR is lacking. A case-control study demonstrated no significant difference of 1-year outcome between PRP and control group among 30 patients [71]. Another study reported better recovery with shorter time of returning to sports in the PRP treated athletes compared to open repaired with and without PRP [72]. However, studies with more validated data and larger sample sizes are needed to clarify the effects of PRP on tendon healing. The BMSC is another novel approach to be mentioned together with PRP. With no evidence from clinical studies, BMSC was shown to affect tendon repair in animal models. In an animal study, Okamoto et.al demonstrated that rats treated with bone marrow or mesenchymal stem cells showed increased strength in tendon failure among bone marrow cells and mesenchymal cells using group respectively [73]. Another study in 2014 observed that no outcome improvements were found in the mesenchymal cells injected group when compared to no injection. However, the study found improved strength to failure detected in rats with mesenchymal cell injections [74]. More translational studies of bone marrow stem cells and PRP treatment are needed before applying it to humans.

4.5 ATR Healing and Related Factors

The healing process after ATR is complex and presented and generally can be divided into three overlapping phases: inflammation, proliferation and remodelling. During the early inflammatory phase of healing, the interaction of blood-derived cells (leukocytes, platelets and monocytes) and tissue-derived cells (stromal stem cells, fibroblasts, myofibroblasts, mast cell and macrophages) is initiated. In the proliferative healing stage, tissue-derived cells are transformed and activate tendon callus formation [75], through deposition of ECM which is rich in Col III [29]. During the remodelling phase, Col III is replaced by Col I through a matrix metalloproteinase mediated process. In this process, the ratio of COL I/III returns to normal level. Thus, factors which are involved in different healing stages can be expected to influence AT repair.

A series of biomarkers are reported to impact AT healing: Wang et al (2019) reported that in a rat model of AT tendinopathy, tendon stem cells (TSCs) improved AT healing through down-regulating MMP-3, while increasing TIMP-3 expression, and adjusting the balance of tendon ECM degradation and synthesis [76]. Millar et al (2015) demonstrated that IL-33 miRNA which is regulated by miRNA-29, is a key mediator during the replacement of Col III with Col I in the remodelling stage [77]. A number of growth factors like TGF- β , vascular endothelial growth factor (VEGF), basic fibroblast growth-2 factor (FGF2) and platelet derived growth factor (PDGF) act as regulators during tendon remodelling [78, 79].

Furthermore, other factors like mechanical loading [80], immobilization [81] and intermittent pneumatic compression (IPC) [82] were demonstrated to be associated with tendon healing.

4.6 Healing Outcome after ATR

4.6.1 Outcome Measurement

Patients with ATR can exhibit chronic pain, limitations in running, jumping, walking on uneven surface and other physical activities, leading to unsatisfactory outcomes [83]. Thus, validated assessment tools are of importance for evaluating scientific research and guiding clinical therapy.

The well accepted and validated methods for testing healing outcome after ATR can be divided into 1) patient-reported and 2) functional outcomes [84]. Patient functional outcome can be assessed by a calf muscle endurance test. However, the importance of self-assessments of outcomes is becoming more and more important in the past decades[85]. Thus, patient-reported outcome which represents the patients' own feeling together with objective methods of examining healing outcome are now being used frequently.

4.6.2 Patient-reported Outcome

Patient-reported outcome is measured based on multi-item scoring scales, including Achilles tendon Total Rupture Score (ATRS), Leppilahti Score, Foot and Ankle Outcome Score (FAOS), Foot and Ankle Ability Measure (FAAM) and Sort Form-36 (SF-36).

The most validated method to evaluate management of ATR is ATRS [84], which has been translated to different languages [86-88]. ATRS questionnaire is a self-expressed system with 10 specific items to assess symptom and function of patients: limitation due to decreased strength/failure/stiffness/pain in tendon, limited activities of daily living, limitation when walking on uneven surface/jumping/running/walking quickly up the stairs/performing hard physical work. All the items are filled by the patients, each item ranges from 0 to 10 where 0 = worst and 10 = best outcome with no limitation. ATRS has a maximum scale of 100, a higher score represents relative better outcome.

The Leppilahti Score is not the most important but the first patient-reported outcome assessment questionnaire[89]. It contains a total score of 100, including pain, stiffness, calf muscle weakness, footwear restrictions, isokinetic muscle strength, subjective result and active range of motion difference between ankles. However, some categories still have limitations in measuring the outcome[90]. FAOS is another questionnaire which consists of 5 categories with validity and reliability, including pain, sport and recreation function, activity of daily living, foot and ankle-related quality of life and other symptoms. Every category ranges from 0 to 100 where 0 means worst and 100 means best result, a higher scale is equal to relatively better outcome. FAAM was first reported in 2005 [91], including 2 sections consisting 21 and 8 items respectively. A higher score represents better outcome.

4.6.3 Functional Outcome

In contrast, the functional outcomes are tested by objective measures such as Heel-rise test (HTR), Achilles tendon elongation, Calf muscle strength/size/endurance, Ankle range of motion and Achilles tendon mechanical properties.

The HRT is commonly used to evaluate functional outcome after ATR, indicating the outcome of strength and endurance of the affected gastrocnemius-soleus complex. The test is performed on one leg with the patient standing on a 10° decline box. The test contains four categories, including the number of heel-rises, the height of every single heel-rise, the total work in joules (total distance × body weight), the time and the power (work/time). A comparison between injured and contralateral healthy leg is recorded using limb Symmetry Index (LSI), where the results from injured side is divided by score from contralateral healthy leg.

Calf muscle size and muscle strength are parameters for measuring functional outcome as well. Calf muscle size based on the circumference of calf can be used to check trophic modification during tendon healing. CT and MRI techniques are reported to measure the circumference values [42, 92]. After ATR, permanent strength of muscle in the injured leg was reported to have approximately 30% reduction when compared to contralateral healthy side [57, 93]. Thus, muscle strength is not only a parameter of healing outcome, the recovery of calf muscle strength is also vital during tendon repair. The most validated method for calf muscle strength management is unclear. Although isokinetic and isometric dynamometry have shown high validation [94], other specific methods to assess functional outcome are needed to be used together with them. Additionally, tendon lengthening [95], Roentgen stereophotogrammetric analysis (RSA) [96] and plantar pressure distribution [97] are reported during the past few years as functional parameters, however, more specific parameters are still needed to detect functional outcome with higher reliability.

4.6.4 Clinical Outcome

Healing process after ATR is protracted with functional deficits, re-rupture, chronic symptom and variety of limitation in motion such as limitations in running and jumping [83, 98]. The outcome of surgical and nonsurgical treatment after ATR were reported based on previous randomized controlled trials.

Comparing functional rehabilitation with cast-immobilization, patients with early rehabilitation present a faster return to work and physical activity [99], and lower rate of re-rupture as well. Interestingly, recent studies reported no statistical difference of the re-rupture rate between non-operative treatment with accelerated rehabilitation versus surgical treatment [56, 57]. A meta-analysis based on 826 ATR patients showed no difference of re-rupture rate between non-surgical and surgical treatment patients [100]. Moreover, surgical patients with early mobilization were detected to have reduced risk of re-rupture when comparing with prolonged immobilization [100]. Further evaluation for long-term functional outcome showed

no difference between operative and non-operative treatment by using variety of assessment tools [101, 102]. However, comparison among short-term with long-term outcome showed opposite result, presenting that surgically treated patients at 6 month had better functional recovery (better heel-rise height and concentric strength) than non-surgically treated patients. However, during 1-year follow up, no difference in functional recovery was identified between surgical and non-surgical treated patients [57]. The time of returning to work and plantar flexion strength were reported to have differences between surgical and non-surgical treatment group. A meta-analysis observed a 19 days earlier return to work in surgical treated patients when comparing with patients who received non-surgical treatment [101]. In another study based on 144 patients, a small but statistical significant improved plantar flexion strength was detected in the surgical treated group both at 1- and 2-years follow up [102].

Other complications after rupture included a lower rate among non-surgical patients when compared with patients who received operative treatment. Wallace et al., reported a lower complications rate with less pain, deep vein thrombosis (DVT), ulcer and numbness in non-surgical group [103]. A meta-analysis conducted in 2012 concluded that the previous comparison between surgical and non-surgical treatment, reported an approximately 16% higher rate of complications except re-rupture in the surgical group [101]. However, orthosis-associated complications including skin-associated, blisters, fungal infection and wound infection mostly happened in non-surgical patients although the complication risk other than re-rupture was lower [104].

In conclusion, surgical treatment shows higher risk of complications. Although the difference of re-rupture rate between surgical and non-surgical treatment is unclear, there is a slightly lower risk in operative patients. More validated and comprehensive studies are still needed to clear the complication risk after treatment to improve the individual therapy.

4.7 Clinical Outcome Prediction after ATR

Until now, physical and mechanical factors such as iterative decomposition of echoes of asymmetrical length (IDEAL) [105], number of sutures/suture limbs/mattress stitches [106], preoperative function and the size of ruptured tear [107] has been the most commonly used predictors of tendon healing. However, the markers for ATR prediction are even less well defined [108, 109]. Specific factors which are associated with healing and patient outcome will increase our understanding of AT healing characteristics and may help to improve treatment and outcome prediction. However, specific and validated markers which can predict healing in human ATR are still lacking.

Previous studies have reported body weight, oral corticosteroid or the use of quinolone antibiotics as possible predictors of ATR [109]. Sex was also demonstrated as an impact factor of patient outcome, presenting as female sex showing more inferior functional outcome [110]. Activity level, previous AT symptoms, later return to physical exercise, deep vein thrombosis and male sex were subsequently found as additional predictors of patient outcome [89, 111]. Recently, Michael et al. reported that age was a negative predictor for patient

outcome after ATR [108]. Younger age was associated with better patient outcome. Clinical samples including tissue biopsies and micro-dialysate are essential tools to detect functional biomarkers for outcome. Previous studies from our research group have shown an increased expression of inflammatory mediators such as interleukin (IL)-6, 8 and 10 in human micro-dialysate (collected 2 weeks after surgery) from healing leg when compared to the contralateral side [112]. Alim et al, reported a higher expression of procollagen type I N-terminal pro-peptide (PINP) and procollagen type III N-terminal pro-peptide (PIIINP) were correlated with less pain (ATR sub-scale) and less fatigue (ATR sub-scale) in the injured leg 1-year after ATR [113], indicating collagens as predictors for partial patient-reported outcome. Furthermore, in my PhD project, it has been shown that gene expression of FGF was associated with better patient outcomes 1-year after ATR, identifying FGF as a novel biomarker for tendon healing prognosis [33]. Thus, the expression of biomarkers of tendon healing at early stage (2 weeks) can be used to detect and predict patient outcome. However, further studies are needed to identify a bigger landscape of tendon healing related biomarkers and their association with patient outcome.

5. Fibroblasts

In general, fibroblasts involve in the production of structural proteins and integrating these proteins into ECM, providing its function of maintaining the integrity of most tissues [114, 115]. In the recent decades, the understanding of fibroblasts is becoming more and more clear, presenting that fibroblasts exhibit some biomarkers' expression (like pro-collagen) [116]. However, these markers have been proven to not be specific only for fibroblasts, and are not expressed by all the fibroblasts [117]. Traditional understanding only consider fibroblasts are just collagen-production cells. However, the associations between inflammation/immune responses and fibroblasts is largely challenging this old opinion [118-120].

Fibroblasts exhibit heterogeneity, demonstrating that fibroblasts derived from different body areas may have different origins [121, 122]. Moreover, the differences of cellular morphology and biology among fibroblasts from different area are highly associated with the genetic expression of Hox gene [123]. There are several major factors to mediate the cellular characteristics of fibroblasts, including transcriptional network, signaling interaction among cells and ECM-related components [124, 125]. Most of these impact factors are unclear except a few transcriptional mediators, such as Sox2, IL-1 and FGF [126-129]. Furthermore, some biological pathways are also regarded to regulated the identity of fibroblasts, such as Wnt/ β -catenin, TGF- β and BMP signaling pathways [115, 130, 131]. Additionally, specific fibroblasts could have relationship with some diseases with excessive fibrosis such as keloids, pulmonary fibrosis and scleroderma. For instance, over proliferation of fibroblasts and excessive ECM deposition are associated with keloids [132, 133].

5.1 Fibroblasts in Connective Tissue

In connective tissues, fibroblasts are the most common cell type. Fibroblasts are generally large and elongated cells. Previously, fibroblasts were regarded as to be derived from epithelial or endothelial cells based on a biological process called epithelial-to-mesenchymal transition (EMT) [134-136]. EMT has been proved among some organs' fibrosis such as kidney and heart, demonstrating the origin of fibroblasts among organ fibrosis. However, during the last decade more and more findings demonstrated that EMT process cannot fully explain all the fibroblasts differentiation in the connective tissues and organ fibrosis [137]. In some dense CTs like tendon and ligament, there are no epithelial or endothelial cells, indicating that fibroblasts are derived either from the human bone marrow mesenchymal stem/stromal cells (MSCs) or from connective tissues by the stimulation of connective tissue growth factor (CTGF) [138]. A number of studies identified the existence of multi-potent mesenchymal cells in connective tissues strengthening this hypothesis [139-141]. Furthermore, CTGF involves in increasing the differentiation of MSCs to FSP1+, collagen type I and alpha-SMA-induced fibroblasts, indicating the fibroblasts differentiated by CTGF are the important factor in dense CT healing. After stimulating by CTGF, the MSCs expressed fibroblastic hallmarks, leading an increasing production of collagen type I [138]. When the commitment of fibroblast is ready, the capacity of MSCs differentiate into non-fibroblasts (such as chondrocytes and osteoblasts) is declined. In previous pre-clinical study, researchers identified that CTGF injection improved the postnatal dense CT to fibrogenesis, indicating that this cell type is highly involved in tissue scar formation and repair. The modulation of fibroblasts is generally considered as the essential process during dense CT healing, especially during the remodeling stage [142].

Generally, fibroblast is a type of large and elongated cell which produces ECM and collagen, forming the structure of tissues. When a fibroblast is activated, cells can be easily detected by the rough endoplasmic reticulum. However, the un-activated fibroblasts are smaller with lower number of rough endoplasmic reticulum when compared with the activated fibroblast (Figure 3).

Fibroblasts, together with other cell types in dense CT, are derived from primitive mesenchyme. All the precursors of the ECM components are produced by the fibroblasts. This characteristic of fibroblasts provides its common function to form and maintain the major structure of dense CTs. Moreover, fibroblasts are also involved in collagen and glycosaminoglycans synthesis, and participate in the production of elastic and reticular fibers. Furthermore, fibroblasts also are reported to be involved in regulating the immune response during tissue injury and healing by expressing immune-related genes [143].

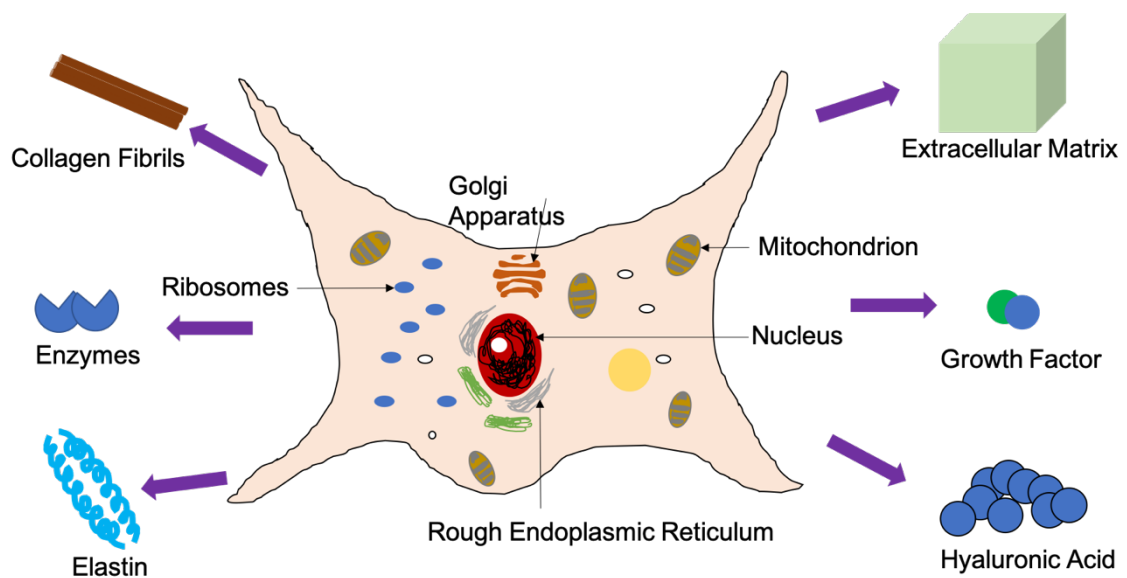


Figure 3. Schematic diagram representing fibroblast structure and function. (Prepared by Junyu Chen based on the references [108-147]).

5.2 Fibroblasts in Dense CT Repair

The general process of dense CT healing is to replace the injured/damaged tissue with granulation tissue to form healthy dense CT. Inside the granulation tissue, a large number of fibroblasts are proliferated, migrated and stimulated to produce the collagens and a new ECM formation.

Fibroblasts are important during dense CT repair and present from the late inflammatory stage to the whole healing phases [144-148]. After injury, fibroblasts are migrated to the site of injury, proliferate and become involved in other important activities such as protein secretion [149]. After the remodeling stage of healing, the number of fibroblasts will return to the normal level [150].

Fibroblasts are originally located in the ECM of tissue and are recruited to the injured area by chemoattractants such as IL-1 beta and tumor necrosis factor-alpha [151]. Fibroblasts are firstly migrated to the site of injury at the intersection of late inflammation and the early proliferation phase during dense CT repair [144]. At this transition point, MMPs are secreted by the fibroblasts, leading the replacement of the fibrin clot with molecular components including collagen type I, II, III, IV, XVIII, laminin, glycosaminoglycans (GAGs), proteoglycans and glycoproteins [152]. It was reported that fibroblasts are migrated into the injured area by a mechanism called “contact guidance” [153]. Unlike some other cells’ migration which is usually disordered, fibroblasts move along the collagen orientation during the migration process. At the site of injury, fibroblasts are not attached to the collagen fibers, but appear to adhere to the fibronectin (FN) instead [154]. The fibroblast migration is crucial for healing, too low activity can result in a delayed healing process whereas excessive activity can lead to defective repair and even cause complications [140].

6. Impact Factors in Dense CT Repair

Unsatisfactory dense CT repair, leading to prolonged healing time and poor clinical outcome, is becoming a big issue for millions of patients all over the world. Patients suffering with chronic pain and wounds will result in higher costs for economic and medical resources [155, 156]. The core aim of clinical treatment after dense CT injuries is still to minimize the aesthetic influence of patients and maximize tissue restoration. Thus, poor dense CT healing is mainly due to an un-mediated repairing response, including angiogenesis, un-controlled ECM deposition, inflammation-/proliferation-/remodeling-related disorders and pathological scarring. Extending the knowledge of impact factors affecting single or multiple stages of dense CT repair can be a great help to complete the understanding of healing mechanisms, improve clinical outcome and develop target treatment. However, these functional markers are still lacking.

6.1 Biomarkers during Inflammation

Major cells during the inflammatory stage are fibroblasts, T-lymphocytes, neutrophils and macrophages [157]. After getting injured, the damage will activate the clotting cascade, initiating the migration of inflammatory and healing-related cells. Furthermore, the platelets inside the clots also involve in secreting growth factors and these factors will be transferred to the site of wound. These platelets and their productive factors were reported to present positive influence on the tissue healing in both pre- and clinical models [158, 159]. At the same time with hemostasis, early inflammatory reaction also has a role of attracting defense factors to the site of wound. Any kind of factors which affect and prolong the inflammatory stage will lead to a chronic and failed dense CT repair during the early phase. It was reported that an up-regulated infiltration of macrophages and neutrophils can cause prolonged wound healing [160, 161]. Thus, uncontrolled expression of mediator of inflammatory infiltration mediator such as IL-1 β and tumor necrosis factor-alpha (TNF) [162, 163] can delay inflammation phase, leading a delayed tissue repair. Some macrophage-secreted biomarkers like platelet-derived growth factor (PDGF), fibroblast growth factor-2 (FGF2), IL-6 and TGF- β are also involved in proceeding tissue healing from inflammatory to proliferative phase [33, 157]. Additionally, IL-2 whose synthesis is highly associated with lymphocytes [164] helps to attract fibroblasts to the site of a wound.

6.2 Biomarkers during Proliferation

Proliferation including fibroplasia, granulation and epithelialization is the subsequent phase in wound healing [165, 166]. This stage initiates with the migration of fibroblasts to the site of wound under a PDGF-stimulated process. The major functional cells during proliferation are platelets, macrophages and fibroblasts. Unlike their roles in inflammation, platelets and macrophages are the producer of PDGF in this stage, and the released PDGF involves in increasing fibroblast proliferation and collagenase synthesis. Fibroblasts present a vital role of producing structural proteins, including collagens, fibronectin (FN), thrombospondins and vitronectin. Moreover, fibroblasts also involve in producing MMPs and demonstrate an interaction with MMPs. Briefly, MMPs promote fibroblast movement inside the matrix and fibroblast subsequently decline the proteolytic activity of MMPs to initiate

protein deposition. Among these biological processes, TGF- β and CTGF are the regulator of the fibroblast-MMPs interaction [167], and vitamin C is involving in mediating collagen production. TIMPs, the inhibitor of MMPs are also playing key role in proliferation by regulating the activity of MMPs and balance of MMPs/TIMPs. Additionally, a novel biomarker complement factor D (CFD) was identified as a predictive marker and prognostic factor in human dense CT [30].

Fibroblasts, macrophages and epidermal cells promote angiogenesis through releasing numerous growth factors such as FGF2, TGF- β and VEGF to replace the damaged tissue with new granulation tissue. Adenosine, which is an intermedator of hypoxia, has been reported as an important factor in regulating tissue healing [168]. Furthermore, epidermal growth factor (EGF), TNF and keratinocyte growth factor (KGF) are the mediators of the epithelialization process.

6.3 Biomarkers during Remodeling

Remodeling is the last stage of dense CT repair. In this phase, the inflammatory cells are decreased together with numerous growth factors. Although the number of fibroblasts is declined at the same time, these cells still involve in promoting collagen deposition [157]. Collagen deposition and collagen-collagen cross-linking are vital processes in dense CT remodeling. Thus, all the regulators of these processes are the major impact factors regarding dense CT repair. However, these collagen-related biomarkers are still limited [32, 169].

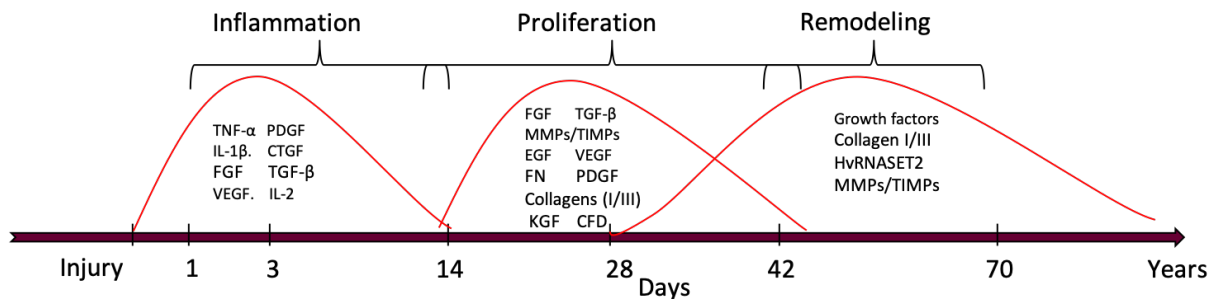


Figure 4. A summary of biomarkers during dense CT repair.

3 RESEARCH AIMS

The overall aim of the present thesis was to identify novel biomarkers of dense connective tissue (CT) healing. The thesis was designed to explore for biomarkers during the inflammatory- and proliferative healing phases in tissue biopsies and micro-dialysate, respectively, after Achilles tendon rupture (ATR) as a model of dense CT healing. A second aim was to investigate the molecular functions of these healing-related biomarkers during inflammatory and proliferative conditions in regulating dense CT repair.

To reach the overarching aims of the present thesis, we included five continuous studies with the following goals:

- 1) To explore whether the expression pattern of potential biomarkers of healing (FGF, COL III, FN, COL I and MMP-9) during the inflammatory healing phase (in ATR tissue biopsies) were associated with the long-term clinical patient outcome after ATR.
- 2) To investigate the proteomic profile during AT proliferative healing phase and to identify reliable biomarkers of dense CT healing in patients with ATR in terms of their long-term clinical outcome.
- 3) To characterize the proteomic profile during AT inflammatory healing phase and to investigate for novel prognostic biomarkers of dense CT healing in patients with ATR in terms of their long-term clinical outcome. Further, to explore the regulatory mechanisms for the identified biomarkers during the repair process.
- 4) To investigate a healing- and outcome-related biomarker, complement factor D (CFD), during the inflammatory and proliferative healing stages of dense CT repair in patients with ATR in terms of their long-term clinical outcome in terms of collagen synthesis.
- 5) To identify potential biomarkers of dense CT healing during the inflammatory healing phase using a network proteomic analysis in patients with ATR.

4 MATERIALS AND METHODS

All the methods used in this thesis were listed below and marked with paper and manuscript. General information of all the techniques will be described in the following text and detailed information can be found in the individual papers.

Patient Cohort

In this thesis, we collected 55 patients with acute ATR from two different cohorts included in prospective, randomized controlled trials (RCT). Micro-dialysate from both healing and contralateral healthy legs were collected 2 weeks after surgery. Patient outcomes based on patient-reported and functional outcome were assessed by using the Achilles tendon Total Rupture Score (ATRS), Foot and Ankle Outcome Score (FAOS), and the Heel-rise test (HRT) at 1-year post-operation. Characteristics of all the subjects are listed in Table 1.

Table 1. Patient characteristics for patients with tendon biopsies and micro-dialysates

	Group	Good Outcome	Poor Outcome	p-value
Micro-dialysate (Paper II)	35	n=16	n=19	
Gender (M:F)	26:9	13:3	13:6	ns
Age	37 (32-42)	35 (29-39)	39 (33-48)	0.049
BMI	25.4 (24.1-28.1)	25.2 (26.7-24.2)	26.2 (28.1-23.7)	ns
ATRS	75 (62-92)	93 (91-97)	64 (57-73)	<0.0001
Limitation in calf strength	7 (5-9)	9 (8-10)	5 (3-7)	<0.0001
Tiredness in the calf	8 (7-9)	10 (9-10)	7 (5-8)	<0.0001
Stiffness in the calf	9 (6-10)	10 (9-10)	7 (5-9)	0.001
Pain in the calf	9 (7-10)	10 (10-10)	7 (4-9)	<0.0001
Activity of daily life	9 (7-10)	10 (10-10)	7 (5-9)	<0.0001
Walking on uneven surface	9 (7-10)	10 (9-10)	8 (6-9)	0.003

Limitation on walking in stairs	9 (8-10)	10 (9-10)	8 (6-9)	0.001
Limitation on running	8 (4-10)	10 (9-10)	5 (3-7)	<0.0001
Limitation on jumping	7 (4-9)	9 (8-10)	5 (3-6)	<0.0001
loss in physical work	8 (8-10)	10 (10-10)	8 (5-8)	<0.0001
FAOS				
Pain	97 (83-100)	100 (94-100)	89 (81-97)	0.011
Symptom	93 (93-100)	96 (89-100)	89 (79-93)	0.036
Activity of daily life	99 (93-100)	100 (100-100)	96 (90-99)	0.002
Sport and recreation	85 (75-95)	95 (90-100)	75 (64-81)	<0.0001
Foot-and ankle-related QOL	66 (56-85)	88 (75-94)	56 (44-63)	<0.0001
HRT				
LSI Time and power %	81 (73-93)	89 (79-97)	78 (66-83)	ns
LSI Total work %	71 (60-89)	85 (69-102)	70 (55-78)	ns
LSI Repetition %	92 (73-101)	100 (96-104)	81 (68-94)	0.018
LSI Average height %	80 (13-88)	88 (79-98)	78 (68-83)	ns
Tendon biopsies (Paper III, IV, V)				
Gender (M:F)	40 (32:8)	20 (17:3)	20 (19:1)	ns
Age	40 (26,65)	40 (26,65)	39 (28,59)	ns
BMI	25.4 (19.6,34.7)	24.6 (19.6,34.7)	25.4 (20.6,30.6)	ns
TTS (h)	85.8 (24.5,158.7)	87.5 (24.5,158.7)	85.3 (41.0,135.6)	ns

ATRS	76 (40,100)	95 (87,100)	63 (40,78)	<0.001
Limitation in calf strength	8 (1,10)	9 (7,10)	5 (1,8)	<0.001
Tiredness in the calf	8 (3,10)	10 (7,10)	5 (3,8)	<0.001
Stiffness in the calf	8 (2,10)	10 (5,10)	5 (2,8)	<0.001
Pain in the calf	10 (3,10)	10 (9,10)	9 (3,10)	<0.001
Activity of daily life	9 (4,10)	10 (9,10)	8 (4,10)	<0.001
Walking on uneven surface	10 (3,10)	10 (7,10)	8 (3,10)	<0.001
Limitation on walking in stairs	9 (4,10)	10 (9,10)	8 (4,10)	<0.001
Limitation on running	8 (0,10)	10 (8,10)	6 (0,9)	<0.001
Limitation on jumping	7 (2,10)	10 (7,10)	4 (2,9)	<0.001
loss in physical work	9 (3,10)	10 (9,10)	8 (3,10)	<0.001
<hr/>				
FAOS				
Pain	100 (69,100)	100 (89,100)	93 (69,100)	0.007
Symptom	93 (39,100)	100 (75,100)	89 (39,100)	0.009
Activity of daily life	100 (88,100)	100 (91,100)	98 (88,100)	0.012
Sport and recreation	88 (45,100)	100 (75,100)	75 (45,90)	<0.001
Foot-and ankle-related QOL	69 (31,100)	91 (69,100)	56 (31,88)	<0.001
<hr/>				
HRT (%)				
Concentric power	80.8 (23.5,189.9)	80.6 (52.9,115.9)	82.1 (23.5,189.9)	ns

Total work	71.5 (24.3,288.0)	77.7 (57.5,119.6)	68.2 (24.3,288.0)	ns
Repetition	90.5 (45.8,275)	96.7 (71.4,114.3)	82.7 (45.8,275.0)	ns
Average height	81.8 (37.6,110.5)	81.8 (65.1,110.5)	81.9 (37.6,104.0)	ns

Table 1. BMI=Body mass index TTS= Time from injury to surgery DS=Duration of surgery DVT=Deep venous thrombosis, IQR=Interquartile range. P-values from Mann-Whitney u-test / Student's t-test or Fishers exact test*

Ethical Approval and Consent to Participate

This study was conducted with the approval from the Regional Ethical Review Committee in Sweden and followed all guidelines according to the Declaration of Helsinki. Written consent was obtained from all patients.

Inclusion and Exclusion Criteria for the Patients

The inclusion criteria were; patients diagnosed with acute Achilles tendon rupture at the Karolinska University Hospital. The exclusion criteria was; 1) unable to give verbal and/or written consent for participating in the study; 2) currently treated with anticoagulants; 3) allergic to contrast liquid; 4) planned follow up on other hospital than Karolinska University Hospital Solna; 5) unable to follow instructions; 6) patients suffering from renal failure; 7) patients with symptomatic chronic heart failure; 8) patients with thrombophlebitis or known coagulation disorder; 9) patients had received other surgery during the month before tendon rupture; 10) patients with known malignancy or pregnancy.

Surgical and Biopsy Procedure

Local anesthetic was administered (20 ml of Marcain® and adrenalin 5 mg/ml, AstraZeneca, London, UK) in the dermis, subcutis and peritendinous space prior to surgery. The patients were then placed in prone position and a medial incision was made through the skin, fascia cruris and paratenon. The rupture was located by the surgeon and a 10 mm Achilles tendon biopsy was taken from the ruptured area, another 10 mm biopsy was taken 3-4 cm away from the rupture side as a control, from a visibly intact tendon area.

A modified Kessler suture with two 1-0 polydioxanone (Ethicon, Somerville, New Jersey, USA) sutures, was used to bring the tendon ends together. The paratenon and fascia cruris were then closed with 3-0 Vicryl (Ethicon, Somerville, New Jersey, USA) and the skin was sutured with 3-0 Ethilon (Ethicon, Somerville, New Jersey, USA). The same anesthetic and surgical techniques were used for all patient using a predefined study protocol.

Post-operative Treatment

All patients were prescribed paracetamol 500 mg or codeine 30 mg for administration if necessary, one to two pills at a maximum of four times per day. Patient included participated

in two randomized trials evaluating post-operative treatments the first two post-operative weeks. None of the different post-operative treatments altered patient outcome at 1-year post surgery [31, 170, 171]. The first study evaluated treatment in a below-knee plaster cast for 2 weeks compared to orthosis and adjuvant intermittent pneumatic compression [31]. The other study evaluated treatment in a below-knee plaster cast for 2 weeks compared to early weight bearing in an orthosis [170]. The remaining 4 weeks of immobilization all patients were prescribed full weight bearing in an orthosis.

Clinical Outcome Assessment

Patient-reported outcomes were collected by using ATRS, FAOS and HRT 1-year post-surgery during the follow up:

Patient-reported Outcome. Patient-reported outcomes were assessed by validated questionnaires; ATRS and Foot and Ankle Outcome Score (FAOS) one-year post-surgery during the follow up.

ATRS consists of 10 specific sub-scales which includes strength in tendon, tiredness in the tendon, stiffness in tendon, pain in tendon, limitations in activity of daily life (ADL), limitation in uneven surface, stairs, running, jumping and loss in physical work. Each sub-scale ranges from 0 to 10 where 0 = worst and 10 = best outcome with no limitation. The maximum total score of ATRS is 100 and a score higher than 80 was regarded as good subjective outcome [172].

FAOS is a 42 items questionnaire assessing of 5 separate categories including pain, symptoms, activities of daily living, sport and recreational activities, and foot-and ankle-related quality of life. Each category ranges from 0 to 100 where 0 = worst and 100 = best outcome, and a score higher than 80 was regarded as good subjective outcome.

Functional outcome. At 1-year post-surgery, functional outcomes of all patients were evaluated by using the heel-rise test (HRT), a validated method which has been used previously [113, 173, 174]. The HRT was performed on one leg with patients standing on a box with 10° incline, test sequence was 30/min by using a metronome. Patients were told to perform as high as possible during each heel-rise, and also to perform as many times as they could. The test was stopped when the patients could not perform a complete heel-rise or could not maintain the sequence of 30/min. All results, including the number of heel-rise, height of every single heel-rise, total work in joules (total distance × body weight), time and the power (work/time) were recorded for further data analysis. The Limb Symmetry Index (LSI) which was used to show the ratio between injured and contralateral healthy leg and presented in percentage (injured/contralateral healthy).

Micro-dialysates collection

To assess the AT healing, micro-dialysates were collected 2-week post-surgery from the operated and non-operated healthy leg as described previously [175]. Briefly, a micro-dialysis

catheter (CMA Micro-dialysis AB, Sweden) with 100 kDa molecular cut-off, was introduced into the peritendinous space 2-5 mm ventral to the Achilles tendon. A perfusion fluid (Macrodex) was pumped through the catheter at 1.0 $\mu\text{L}/\text{min}$ speed and collected in vials every 30 min for 2 hours. Owing to the lingering effect of the insertion trauma and the possible differences due to pump adjustment the first of the four vials was not considered reliable and therefore was not included in the analysis. Earlier studies have verified that this methodology can assess increased metabolism, as well as matrix deposition[113] in the healing compared to the contralateral healthy Achilles tendon.

Histological Staining

Fixation. The injured and intact human tendon biopsies from 5 ATR patients were collected and fixed in Zamboni's fixative consisting of 4% paraformaldehyde diluted with 0.2 mol/L Sörensen phosphate buffer (PH = 7.3), including 0.2% picric acid at 4 °C. Subsequently, a 20% sucrose in 0.1 mol/L Sörensen phosphate (PH = 7.2), including sodium azide and bacitracin (Sigma Chemicals, St. Louis, MO, USA) was used to soak the fixed biopsies. In the next step, a Leitz® 1720 cryostat (Ernst Leitz, Wetzlar, Germany) was used to prepare tendon biopsies sections to a thickness of 7 μm and then mounted on SuperFrost/Plus slides. One section from the injured and another one from the uninjured area of tendon was attached to each slide. All the sections were stored at -20°C for further biological analysis.

Hematoxylin and Eosin (H&E) Staining

The H&E staining is the foundation of the anatomical pathology diagnosis. The H&E process stained the nucleus and cytoplasm with high contrast color in order to apart cellular components. The nuclear chromatin and other acidic cellular components were stained by hematoxylin solution. We stained the sections with hematoxylin for 15 min and then washed by 1x PBS for 5 min x 3. Then dropped eosin on each slide to cover the tissue section and incubated for 10 min. After dyeing, distilled water was used to wash the slides before differentiation by using 1% hydrochloric acid ethanol. Washing process should ensure that the excessive dye bound with nucleus and cytoplasm were completed cleaned. A weak alkaline blue reagent was used to dye the hematoxylin for anti-blue process. Distilled water was used again to wash the slides and remove extra dye on the sections before start dehydration. The 80%, 95% and absolute ethanol were used step by step to remove water inside the sections, each step of dehydration spent 2-3 mins. After drying the stained samples in the air, the slides were covered with xylene for 5 mins and dried again in at room temperature without light. A light microscope was used to capture the images.

Immunohistochemistry (IHC)

Biopsies were cut into 7 μm sections and then marked with pap-pen and soaked in 1% PBS for 5 min before incubation with 1% H_2O_2 for 30 min. Sections were then blocked with 2% goat or horse serum, washed with 1% PBS for 3 \times 5 min and incubated with Avidin and Biotin before overnight incubation with antibodies against FGF, COL III, FN, COL I and

MMP-9 at room temperature. Sections were washed with 1% PBS for 3×5 min before incubating with 100 μ l secondary antibodies (1:250, PBS-0.1% BSA) for 40 min. Secondary antibody, horse anti mouse was used for MMP-9, FN, FGF while for COL I and III, goat anti rabbit antibody was used. Slides were washed with 1% PBS for 3×5 min and incubated with 100 μ l of ABC solution (Vector Laboratories, Inc. Burlingame, CA, USA), stained with DAB solution (Vector Laboratories, Inc. Burlingame, CA, USA) and counterstained with Hematoxylin (Vector Laboratories, Inc. Burlingame, CA, USA). This step was followed by dehydration in 70%, 96% and 100% alcohol and with the Xylene before mounting with pertex. To demonstrate specificity of staining, primary antiserum was either omitted or replaced by normal rabbit IgG. All the images were saved by the computer connected to the light microscope (DEI 750; Optronics Engineering, Goleta, CA, USA).

mRNA Extraction and Tissue Homogenization

RNA was extracted from both injured and uninjured tendon biopsies among 20 ATR patients collected from Karolinska University Hospital, following the previous description [176]. Generally, tendon biopsies were cut into small pieces under -20 °C and transferred to pre-cooled tubes with steel beads including 1ml of tri-reagent (Sigma, Stockholm, Sweden). The tubes were immediately homogenized 30s x 2 using a bead homogenizer which can shake the tubes vigorously and keep a fully-completed homogenization [171]. Samples were centrifuged to split into an aquatic and an organic stage after additional chloroform. We kept the aquatic step to separate and precipitate with isopropanol to obtain RNA as pellet. Furthermore, glycogen was also added to make better visualized RNA pellet. The RNA pellet was subsequently washed 2 times by ethanol, dried and re-dissolved in 10 μ l RNase-free water.

mRNA Purification and Quantitative Real Time-PCR (qRT-PCR) analysis

We used a Nanodrop ND-1000 spectrophotometer software (Isogen Life Science, Sweden) to quantify the extracted RNA. The quality of RNA was measured as the RNA quality index (RQI) with the Experion electrophoresis system (BioRad, Sweden). First-strand cDNA was synthesized from 50 ng of total RNA using a first-strand cDNA Synthesis Kit (Roche, Germany).

For the qRT-PCR-analysis, RT-qPCR was performed using TaqMan Gene Expression Assays (Applied Biosystems, Carlsbad, CA) with the GeneAmp 7500 Fast Sequence Detection system (Applied Biosystems, Carlsbad, CA). Specific primers for FGF, COL III, FN, COL I, and MMP-9 (MWG Biotech, Ebersberg, Germany) were used to detect target genes (Table 1). Data was normalized by using GAPDH as the reference gene and $\Delta\Delta C_t$ method was used for analysis. All the basic information of primers were shown in Table 2.

Table 2. Primers sequences during qRT-PCR

Genes	Forward Primer	Reverse Primer
<i>FGF</i>	TGACGGGGTCCGGGAGAAGA	ATAGCCAGGTAACGGTTAGCACACAC
<i>Col 1</i>	GGCAACAGCCGCTTCACCTAC	GCGGGAGGACTTGGTGGTTTT
<i>Col 3</i>	CACGGAAACACTGGTGGACAGATT	ATGCCAGCTGCACATCAAGGAC
<i>FN</i>	TTTGCTCCTGCACATGCTTT	TAGTGCCTTCGGGACTGGGTTC
<i>MMP-9</i>	AGCGAGGTGGACCGGATGTT	AGAAGCGGTCCTGGCAGAAATAG
<i>GAPDH</i>	CCTCCTGCACCACCAACTGCTT	GAGGGGCCATCCACAGTCTTCT

Mass Spectrometry (MS)

Preparation of Samples.

The protein concentration in micro-dialysates was determined by BCA assay (Thermo Scientific, Sweden) and sample aliquots of 5 µg were supplemented with 50 mM AmBic solution to the total volume of 50 µL. Proteins were reduced with 4 µL of 100 mM dithiothreitol in 50 mM AmBic, incubated at 37°C for 45 min and alkylated with 10 µL of 100 mM iodoacetamide in 50 mM AmBic and incubated at room temperature for 30 min in dark. Proteolytic digestion was performed by adding 1.5 µL of 0.2 µg/µL trypsin (sequencing grade, Promega) and incubated at 37°C overnight. The reaction was stopped with the addition of 3.5 µL of concentrated formic acid. Samples were cleaned on a C18 Hypersep plate (bed volume of 5-7 µL, Thermo Scientific) and dried in a vacuum concentrator (miVac, Thermo Scientific).

Pulverized patient tissue samples were solubilized in 8M urea and 100 mM NaCl with 1% ProteaseMAX (Promega) in 100 mM ammonium bicarbonate (AmBic) and mixed vigorously. Low binding silica beads (400 µm, Ops Diagnostics, Lebanon NJ) were added to each sample and vortexed at high speed. Subsequently, samples were quickly frozen and subsequently then thawed and subjected twice to disruption of the tissue on a Vortex Genie disruptor for 2 min before addition of AmBic, urea and NaCl. Following centrifugation, the supernatant was transferred to new tubes and 50 mM AmBic was added and the mixture was vortexed vigorously. Proteins were reduced with 100 mM dithiothreitol in 50 mM AmBic, incubated at 37°C and alkylated with 100 mM iodoacetamide in 50 mM AmBic in the dark. Proteolytic digestion was performed overnight. The reaction was stopped with concentrated formic acid and the samples were then cleaned on a C18 Hypersep plate (bed volume of 40 µL, Thermo Scientific) and dried in a vacuum concentrator (miVac, Thermo Scientific).

RPLC-MS/MS Analysis

Reversed phase liquid chromatographic separation of peptides was performed on a 50 cm long C18 EASY-spray and C18 trap columns connected to an Ultimate 3000 UPLC system (Thermo Scientific, USA). The gradient was 120 min long at a flow rate of 300 nL/min: 2-26% of buffer B (2% AcN, 0.1% formic acid) in 90 min and up to 95% of buffer B in 5 min. Mass spectra were acquired on an Q Exactive HF mass spectrometer (Thermo Scientific) in m/z 350 to 1600 at resolution of $R=120,000$ (at m/z 200) for full mass, targeting 5×10^6 ions with maximum injection time of 100 ms, followed by data-dependent higher-energy collisional dissociation (HCD) fragmentations from precursor ions with a charge state $2+$ to $7+$ of the top 17 most intensive precursors. The tandem mass spectra was acquired with a resolution of $R=30,000$, targeting 5×10^4 ions with maximum injection time of 54 ms, setting isolation width to m/z 1.4 and normalized collision energy to 28%.

Proteomic Data Analysis, Protein Identification and Quantification

Raw files were imported to Proteome Discoverer v2.3 (Thermo Scientific) and analyzed using the SwissProt protein database with Mascot v 2.5.1 (MatrixScience Ltd., UK) search engine. The MS/MS spectra were matched with The Human Uniport database (last modified: 3 September 2020; ID: UP000005640; 75,777 proteins) using the MSFragger database engine[177]. Searching parameters for MS/MS spectra were chosen as follows: up to two missed cleavage sites, peptide mass tolerance of 10 ppm, 0.02 Da for the HCD fragment ions. Carbamidomethylation of cysteine was specified as a fixed modification, whereas oxidation of methionine, deamidation of asparagine and glutamine were defined as variable modifications.

For quantification, both unique and razor peptides were requested. Only unique peptides $\geq 2\%$ and false discovery rate (FDR) $< 1\%$ were set for identification of protein and peptide. LFQ algorithm implemented was used for protein quantification through MaxQuant software, statistical analysis was performed by Perseus v1.6.14.0, SPSS 26.0 and Graph Prism v8.0 software. Protein identification was then performed, reverse sequences, contaminants and the “only by site” entries were excluded. Protein abundance was calculated based on normalized spectrum intensity (LFQ intensity), and an intensity-based absolute quantification (iBAQ) algorithm was used for normalization[178]. In order to normalize the difference among samples, the iBAQ value of each identified protein was converted to an FOT (fraction of total) value by dividing it by the sum of the LFQ intensity values of all the identified proteins[179]. No expression markers and empty value among samples were marked with 0 for the LFQ intensity values to make the data validated. Differentially expressed proteins between healing and healthy tendon were identified by paired Wilcoxon test and unpaired Mann-Whitney U test was used for identifying significance between good and poor outcome subgroup, a p value < 0.05 and fold change (FC) > 2 were set as significant threshold. Heat maps performed with z-score of \log_2 LFQ intensity values and volcano plots were performed by R. Common and shared proteomic files between each subgroup were showed with Venn plot performing in InteractiVenn tool [180]. Gene Ontology (GO) annotation database was

used to identify the biological functions of enriched proteins. Enrichment analysis was performed with GO annotations (biological process/pathways, molecular function, cellular component) on STRING v11.0 (<http://string-db.org>) database for the confirmation of protein-protein interaction network among subgroups.

Immunofluorescence (IF)

For fluorescence staining, slides were blocked with 2% BSA in 1 mol/L phosphate buffered saline (PBS) and subsequently incubated with the primary antibody against eEF2 overnight at 4°C and then incubated with Alexa Fluor 488-labeled Goat anti-rabbit IgG secondary antibody at room temperature. All the slides were stained with antifade reagent (with DAPI) and mounted. Negative controls were prepared by omitting the primary antibody or including a rabbit IgG1 (M5284, 1:100 dilution) isotype control. Data analysis was performed using ImageJ software.

Meso Scale Discovery (MSD) Analysis.

Micro-dialysates were analyzed using commercially available Uniplex immunoassay kit for CFD (Meso Scale Discovery, USA). All samples were randomized before assay procedure and diluted into 1:5 dilutions in assay diluents and added to the plate. The method followed the protocol as set by the manufacturer. Briefly, the MSD 96-well plate (Meso Scale Discovery) was coated overnight with 25µl of coating capture solution under constant shaking at 2-8 °C. The plate was then washed (3x5 min) with 150µl of 1x MSD Tris washing buffer before addition of 25µl each of assay diluent and calibrator standard or samples, sealed and incubated at room temperature for 1 hour with shaking. The plate was then washed (3x5 min) with 150µl of washing buffer and added 50µl of detection antibody in a dilution of 1:200, sealed and incubated at room temperature for 1 hour. After which, plate was washed (3x5 min) before addition of 150µl of detection buffer and read on the MSD reader. Micro-dialysate from 22 patients were used for MSD analysis which included 15 patients analyzed by the MS analysis and due to the limited volume of the rest, additional 7 micro-dialysate samples were included.

Western Blot Analysis

Human tendon biopsies were cut into small pieces and incubated in radioimmunoprecipitation (RIPA) assay buffer mixed with EDTA-free protease inhibitor and phosSTOP for 40 mins at 4°C. Concentration of protein in the biopsies was tested with a BCA assay detection kit (Thermo Fihser Scitific), and stored in -80°C for further western blotting analysis. Briefly, 5µg of protein per well was loaded, separated by gel electrophoresis (4-12% Bis-Tris, Invitrogen), and transferred to nitrocellulose membranes. The membranes were incubated with 5% nonfat milk in 1x tris-buffered saline with 0.1% tween (TBST) to block unspecific binding sites, and the membranes were subsequently covered with different primary antibodies overnight at 4°C (eEF2 0.1µg /ml, Colla1 0.1µg /ml, β-actin 0.02 µg /ml, GAPDH 0.01µg /ml, Cell Signaling). After washing the membranes, they were incubated

with secondary antibody conjugated to HRP (anti-rabbit IgG and anti-mouse IgG; Cell Signaling). The chemiluminescence signal was initiated by using SuperSignal West Pico PLUS kit (Thermo Fisher Scientific). Chemiluminescence was identified and quantified by using biorad ChemiDoc MP Imaging and analysis was performed in Image Lab. Immunopositive bands were normalized with the bands of GAPDH or β -actin and final results were presented as fold change from control values.

Cell Culture

Previous study has shown the use of fibroblasts in connective tissue (CT) research [181]. Thus, in the further *in vitro* studies we used both primary fibroblasts (#C-12302, Promo Cells) and fibroblast cell line (fHDF/TERT166 human foreskin fibroblast cell line, #CHT-031-0166, Evercyte, Austria) to confirm the molecular function and mechanisms of more biomarkers for human CTs repair based on our tendon model. Cells were cultured in Dulbecco's Modified Eagle Medium/F12 (DMEM/F12, Gibco) supplemented with 10% fetal bovine serum (FBS, Gibco) and 1% penicillin-streptomycin (PEST) (Gibco) at 37°C in a humidified atmosphere containing 5% CO₂. When the cells reached 80 to 90% confluency, we dissociated them by using 0.25% trypsin- ethylenediaminetetraacetic acid (Trypsin-EDTA) (Thermo Fisher Scientific). The split cells were subsequently seeded in 12-well plats with a concentration of 2.5×10^5 cells/well supplemented with DMEM/F-12 medium for the following investigations.

Inflammatory Injury and Proliferative Fibroblast Model Creation

The inflammatory injury fibroblast model was created by using recombinant human tumor necrosis factor alpha (TNF) (#300-01A, PeproTech) in both primary fibroblasts and fibroblast cell line. Meanwhile, an unchallenged fibroblast model was created to simulate the proliferative stage of CT healing. Bovine serum albumin (BSA), 0.2% was used for dissolving the TNF, and 10 ng/ml was used for fibroblast stimulation [182].

Cell Transfection

Cells were seeded in 12-well plates and then transfected with silencing RNA (si-RNA) to detect the potential role of target biomarker in tendon healing as representative of dense CT repair. Cells were then stimulated with 10 ng/ml TNF for 24 hours before being transfected with si-RNA. Then, cells exposed to silencing RNA and negative controls were transfected for 48 hours at a final concentration of 100 nM in each well using Lipofectamine™ 3000 transfection reagent (Thermo Fisher Scientific) and diluted with Opti-MEM reagent.

Cell Proliferation Assay

A Click-iT® EdU AlexaFluor 488® Imaging Kit (Thermo Fisher Scientific) was used to identify the changes in proliferation rates of human fibroblast primary cells and the cell line. Normal, transfected and 3-MA stimulated cells were incubated with EdU media for 2

hours before fixation with 4% PFA. Each section was incubated with freshly prepared Click-iT[®] reaction cocktail as instructed in the kit. BSA (3%) in PBS was used to wash the slides twice for 5 min. Cell nuclei were stained with Hoechst 33342 for 5 min and the slides were subsequently washed with PBS for 2 x 5 min. All the steps of the EdU assay were performed while avoiding light and the slides were never allowed to dry out.

Cell Apoptosis Assay

Live/Dead[™] Cell Imaging Kit and CellEvent[™] Caspase-3/7 Green Detection Reagent (Thermo Fisher Scientific) were used for detection of cell apoptosis based on the manufacturer instructions. Cells were treated with si-eEF2, fixed with 4% PFA (specifically for caspase-3/7) and stained using an annexin V-FITC, PI and Caspase-3/7 green detection reagent in dark. Hoechst 33342 was used for cell nucleus staining. Finally, cells were assessed and quantified using the fluorescence microscope. Image J and SoftMax Pro 7.0.3 were used to perform the data analysis.

Scratch Wound Assay

A cell scratch assay was used to explore the role of eEF-2 on cell migration. Based on an unchallenged fibroblast model, cells were seeded in 6-well plates and a scratch was created using a pipette tip on the confluent monolayer cell culture. Next, cells were transfected with si-eEF2 and compared with a subgroup exposed to normal FBS free medium. After 24 hours, light microscopy and ImageJ were used to assess the results.

Confocal Immunofluorescent Detection for Cells

Cells were plated on the glass chamber slides and treated with starved stimulation for autophagy, eEF2 siRNA and 3-Methyladenine (3-MA), respectively. Next, the cells were washed, fixed with 4% paraformaldehyde (PFA), blocked with 5% BSA in PBS, permeabilized with 0.1% Triton X-100, incubated with anti-Coll1a1 antibody (CST) and followed by Alexa-Fluor-488 conjugated secondary antibody (#A-11008; Thermo Fisher Scientific). All the slides were stained with the antifade reagent (with DAPI) and mounted. The single-stained and merged images were performed using a Zeiss LSM 880 confocal microscopy (without AiryScan, CMM Karolinska Institutet), and the data was analyzed using ImageJ software.

Gene Set Enrichment Analysis (GSEA).

GSEA, an aggregate score and running sum statistical approach focusing on gene sets which share common biological function, chromosomal location or regulation, was used to provide the molecular signature based statistical significance. An entire gene set including a ranked list of all expression values in a data set without requiring a cut-off of differentially expressed values for functional analysis was used [183]. In our study, we supplied a pre-ranked list of up and down-regulated fold changes to be analyzed for healing and contralateral healthy groups, and good versus poor outcome subgroups. Molecular Signatures

Database was used to understand the functional enrichment profiles of proteomic data. GSEA was performed in R and a loading gene set collection from gmt files from BROAD Institute were used according to GSEA documentation [183, 184]. Normalized enrichment score (NES) with the total protein list was used as a background. Adjusted p value and FDR < 0.05 were regarded as statistical significance.

Clinical Model of Prognosis

Receiver operating characteristic (ROC) curve analysis is a highly proofed approach to assess how well a factor is capable of discriminating between subjects who experience disease onset and those who do not [185]. The area under a ROC curve (AUC) is a validated method with high sensitivity and specificity to test and predict the clinical/treatment outcome of patients [186, 187]. The value of AUC ranges from 0 to 1 where 0 value means completed inaccurate test and 1 means a test with perfect accuracy [188]. Briefly, for a factor, an AUC = 0.5 is equal to no discrimination, AUC = 0.7-0.8 means considerable predictor, AUC = 0.8-0.9 is regarded as excellent and AUC higher than 0.9 is considered as perfectly accurate [188].

Statistical analysis

Statistical analysis and graphing were performed with SPSS (IBM SPSS, v26.0), GraphPad Prism 8.0 and R. Skewness was checked for all the variables. Standard descriptive statistics were used to summarize clinical variables. Differential comparison of protein expression between healing and contralateral healthy tendon was identified by paired Wilcoxon test while unpaired Mann-Whitney U test was used for identifying significance between good and poor outcome subgroups. A p value < 0.05 and FC > 2 were considered as statistical significance. The outcome measurements were associated with proteomic files by univariate analysis. Non-parametric Spearman's rank correlation was used for severely skewed variables, while Pearson correlation was used among skewed variables. Outcome measurements which were significant in univariate analysis were subsequently tested in a linear regression model. Correlation between protein LFQ intensity and clinical data was calculated with confounders by linear regression analysis to identify the most specific proteomic file which can be used as predictors for longer term patient outcome, an adjusted p value < 0.05 was set as significant threshold.

5 RESULTS AND DISCUSSION

5.1 FGF gene expression in injured tendons as a prognostic biomarker of 1-year patient outcome after Achilles tendon repair (Study I)

In this study, we aimed to identify biomarkers in tissue biopsies which potentially can be used as predictor of long-term clinical outcome after ATR.

5.1.1. Patients and tissue collection.

This study included 25 patients diagnosed with ATR. During the ATR reconstruction surgery tissue biopsies were collected from both the injured area and from a visibly intact area 3-4 cm proximal to the rupture and the tissues were taken for histological and biochemical analysis.

Our histological analysis revealed apparent structural differences among injured and intact area. The collagen fibers were continuous and aligned in a parallel manner in intact tendon section (Figure 5a, b) while disordered and broken fascicles were observed in the injured tendon (Figure 5c, d).

5.1.2 Biomarkers expression at mRNA level

The quantitative RT-PCR reported higher expression of all studied genes (*FN*, *MMP-9*, *FGF2*, *Col I*, *Col III*) in tendon biopsies collected from the injured in comparison to uninjured tissues. However, no statistically significant differences could be detected at the mRNA levels for any of the studied biomarker among injured and intact tendon biopsies (Figure 6).

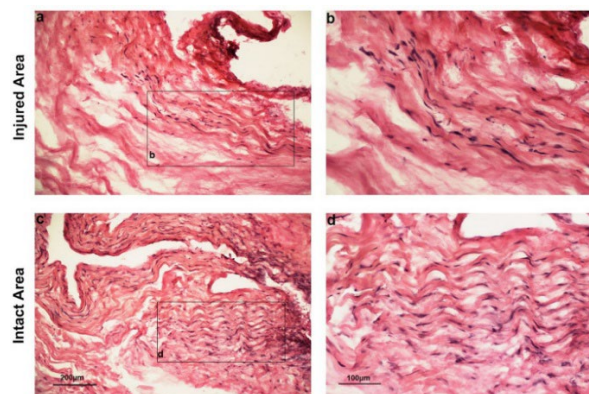


Figure 5. Histological structure of human Achilles tendon stained with hematoxylin and eosin (a-d). All the images are representatives from 5 patients. Original magnification is either 10x (a, c) or 20x (b, d). Adapted from **Paper I**, Figure 6.

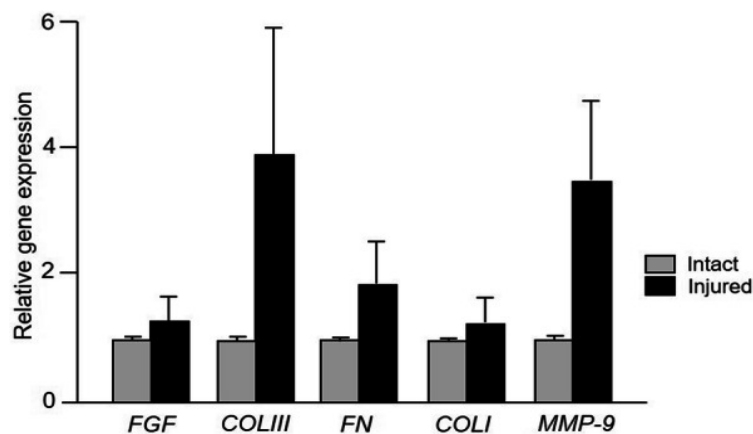


Figure 6. Relative gene expression of *FGF*, *Col III*, *FN*, *Col I* and *MMP-9* in human tendon biopsies collected from injured and intact area. Values are normalized with house-keeping gene, GAPDH and reported as mean \pm SEM, n = 12. Adapted from **Paper I**, Figure 1.

5.1.3 Biomarkers Expression in relation to Clinical Outcome

In the next step, the relationship between the mRNA expression of all studied genes and 1-year post-operative clinical outcome was studied. Our analysis identified *FGF2* mRNA expression to be positively associated both with functional (LSI height and LSI power) and patient-reported outcome as measured by ATRS (*FGF2* and LSI height: $r = 0.8$, $p = 0.031$; *FGF2* and LSI power: $r = 0.758$, $p = 0.048$; *FGF2* and ATRS: $r = 0.711$, $p = 0.003$, Figure 7a-c).

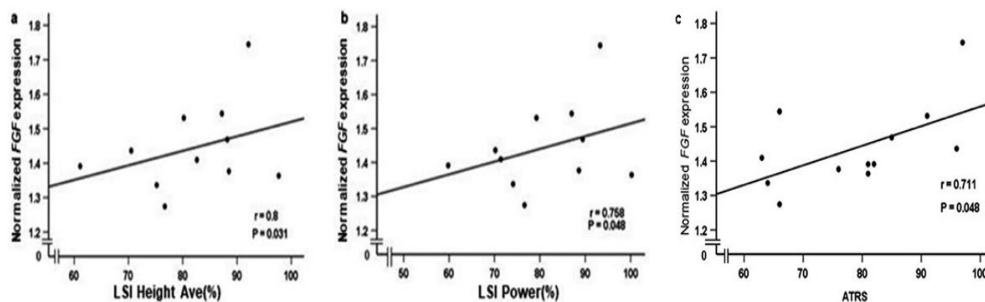


Figure 7. Associations among *FGF2* mRNA levels and a) LSI average height; b) LSI power; and c) total ATRS in injured tendon tissues. Data analyzed by Spearman's rank correlation coefficient. *FGF2* mRNA levels were normalized by GAPDH. ATRS ranges from 0 to 100 where 100 = best outcome, HRT ranges from 0, where higher ratio means better outcome, n = 12. Adapted from **Paper I**, Figure 2 and 4.

Further analysis revealed that *FGF2* gene expression was positively correlated with less running limitation ($r = 0.733$, $p = 0.007$), less pain ($r = 0.558$, $p = 0.02$) and less loss in physical activity ($r = 0.778$, $p = 0.007$) (Figure 8a-c) in injured tissues. Moreover, *Col III* expression was associated with higher tendon strength ($r = 0.71$, $p = 0.032$) (Figure 8c). There was no effect of age, gender, body mass index (BMI) or time to surgery (TTS) on these correlations. No significant correlations were found between *MMP-9*, *Col I* or *FN* mRNA levels and 1-year clinical outcome.

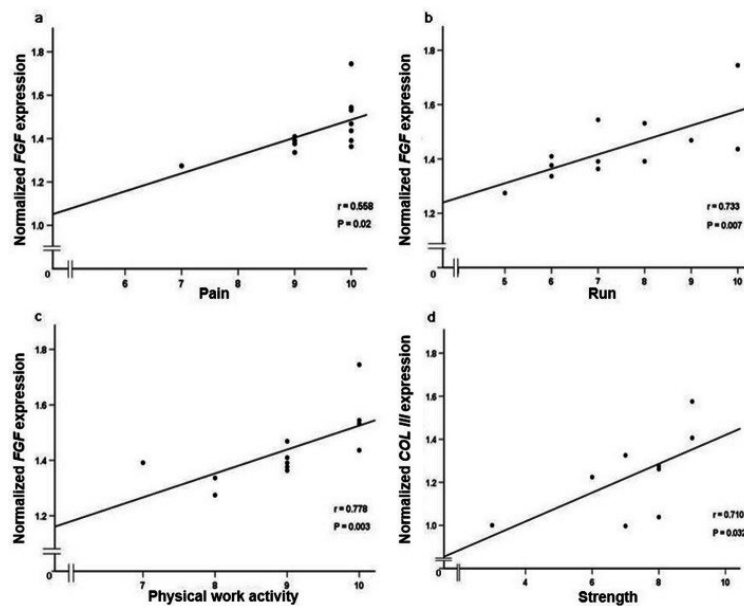


Figure 8. Associations between mRNA levels and ATR sub-scales. Correlation between a) *FGF* gene expression and pain; b) *FGF* gene expression and running limitation; c) *FGF* gene expression and physical work activity; d) *Col III* gene expression and strength. Statistical analysis was performed by a Spearman's rank correlation coefficient. ATRS sub-scale ranges from 0 to 10 where 10 = best outcome, n = 12. Adapted from **Paper I**, Figure 3.

5.1.4 Localization and Expression of Biomarkers at Protein Level

We further analyzed these biomarkers at the protein level with immunohistochemistry. The differential expression pattern and localization was observed for all studied biomarkers. The FGF2 expression was observed to be in proximity to blood vessels within interfascicular CT and matrix in the injured tendon (Figure 9 a-b), while in uninjured area, it was mostly expressed in interfascicular matrix (Figure 9 c).

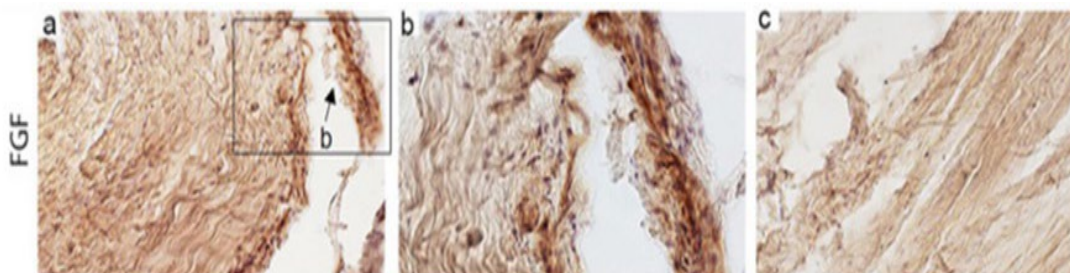


Figure 9. Protein expression of FGF in Achilles tendon biopsies. Representative images from (a, b) injured and c) intact tissues, n = 5. Magnification 20x in a, c while 40x in b. Adapted from **Paper I**, Figure 7.

The most important finding from the study was that higher *FGF2* gene expression was positively associated with better 1-year clinical outcome suggesting an overall improved tendon healing. Tendon healing is affected by various biological processes, including cellular proliferation, migration and ECM formation, all mediated by variety of biomarkers [189, 190]. FGF2 is the most important growth factor in the FGF family. Our findings of FGF2 as an important growth factor with positive effects on human tendon repair are novel as previously the role of FGF on healing has only been reported in pre-clinical studies [191,

192]. Further, it has been reported that FGF2 can initiate and/or stimulate fibroblast proliferation and migration, leading to collagen production. In addition, it has been reported that FGF can stimulate stem cells to induce Col I and III [193]. The increased FGF expression in injured Achilles tendons as identified in the present study, potentially by activating collagens synthesis might regulate the balance between degradation and production of ECM, leading to improved healing. This is supported by an earlier study in a rat model in which FGF2 was shown to strengthen the biomechanical properties of healing tendon by increasing Col I and III synthesis [194, 195].

Taken together, these findings extend the potential role of FGF2 from animal to human and present a positive association between FGF2 gene expression and clinical outcome. These findings also provide a basis for the development of FGF2 based novel therapies to promote healing after dense CT injuries.

5.2 Complement factor D as a predictor of Achilles tendon healing and long-term patient outcomes (Study II)

Studies on proteomic profiles and their associations with pathogenesis have been reported previously [196, 197]. However, only a few previous studies, have explored the proteomic landscape of dense CT healing especially in relation to human Achilles tendon repair [198]. The study was designed to investigate the proteomic profile of healing, identify potential biomarkers, and assess their association with the patient's long-term outcomes after ATR.

For the study, micro-dialysates were collected from healing Achilles tendon two weeks post-surgery, and from the contralateral healthy side at the same timepoint. Micro-dialysates were analyzed by the quantitative MS technique. Patient long-term clinical outcomes were assessed by ATRS one-year post-surgery. The clinical parameters for all patients are presented as **Table 1**.

5.2.1 Proteomic Landscape of Healing Achilles Tendon

By using MS technique, we detected the largest landscape of proteomic profile of healing Achilles tendon, including 1891 unique proteins from which 1423 proteins passed the quality filter (peptides > 1%, unique peptides > 1%, coverage >50%, contaminant = False). Specific clusters of proteins, with both increased and decreased expression, were presented in the healing compared with the healthy tendon (Figure 10a). Among all the proteins, a total of 821 shared proteins were identified within the healing and contralateral healthy tendon, including 388 up-regulated and 17 down-regulated proteins in the healing in comparison to healthy micro-dialysates (Figure 10b-c).

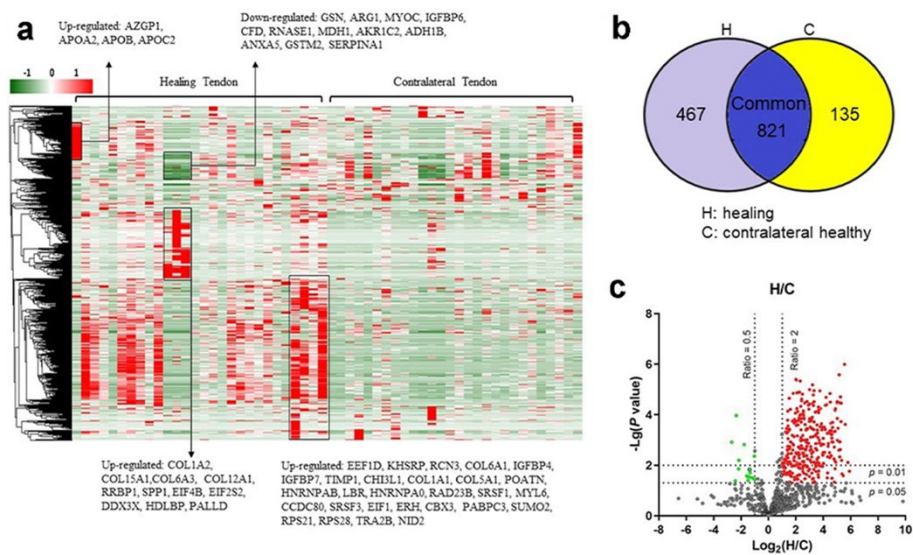


Figure 10. Proteomic landscape identification of healing tendon. a) Heat map of 1423 proteins that passed through the quality filter across all patients. Fold change (FC) > 2 was set to show the differentially expressed proteins in healing and healthy samples with p-value < 0.05 as the cut-off standard to control the error detection rate and to represent a statistical significance. Scale bar shows the expression level with red = up-regulated, green = down-regulated, and white = unchanged proteins as measured by the paired Wilcoxon test. n = 28 in each group. b) Venn plot of overlapping and distinct proteomic profiles of healing and healthy micro-dialysates. c) Volcano plot with differentially expressed proteins in healing compared to healthy micro-dialysate. The X coordinate represent Log₂ (FC) and the Y coordinate to -Log₁₀ (p-value). Each dot represents a protein with red = up-regulated (n = 388), green = down-regulated (n = 17) and, black = non-differentially expressed proteins. Adapted from **Paper II**, Figure 1.

To understand the potential role of these 405 (388 up- and 17 down-regulated proteins) differentially expressed proteins, we analyzed the top 50 up-regulated and all the down-regulated proteins by STRING and GO databases. Three highly enriched protein-protein networks were identified, including two networks among up- and one in the down-regulated proteins, pointing out the potential healing-related processes. The enrichment factor analysis reported that up-regulated proteins were mostly involved in ribosomal structural constituent and RNA binding, while the down-regulated proteins were contributor in exocytosis, wound repair response, immunity initiation and oxidative response.

5.2.2 Proteomic Landscape of Outcome related Biomarkers in Tendon Healing

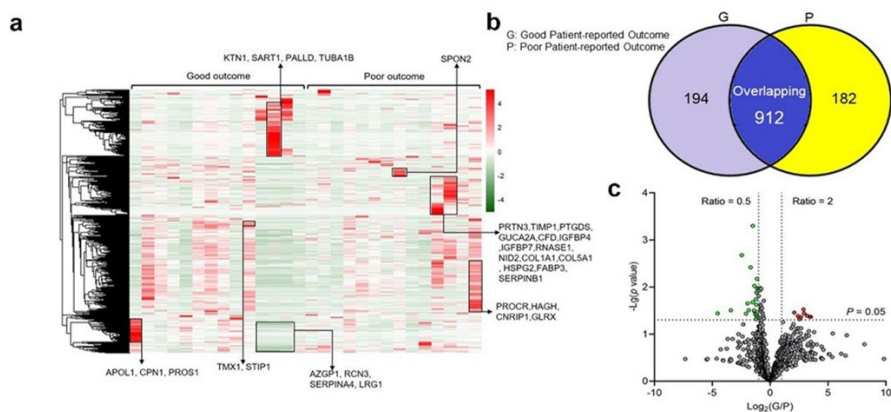


Figure 11. Quantitative proteomics of healing micro-dialysates grouped into good and poor patient outcome. a) Heat map of 1288 proteins that passed through the quality filter across all samples. Fold change (FC) > 2 was set to show the differentially expressed proteins in good and poor outcome groups with p -value < 0.05 as the cut-off standard to control the error detection rate and represent a statistical significance. Scale bar shows the expression level with red = up-regulated, green = down-regulated, and white = unchanged proteins as measured by the Mann-Whitney U -test. $n = 14$ in each group. b) Venn plot of overlapping and distinct proteomic profiles of good (G) and poor (P) outcome. c) Volcano plot with differentially expressed proteins. The X coordinate represents Log_2 (FC) and the Y coordinate to $-\text{Log}_{10}$ (p -value). Each dot represents a protein with red = up-regulated ($n = 9$), green = down-regulated ($n = 23$) and, black = non-differentially expressed proteins. Adapted from **Paper II**, Figure 2.

To explore the proteins prognostic of tendon healing, we analyzed the proteomic profile by re-grouping the samples according to their 1-year clinical outcome. Hierarchical cluster analysis reported the distinct proteomic file of good and poor clinical outcome from a total of 1288 unique proteins (Figure 11a). As a result, we found 912 shared proteins among good and poor outcome subgroups, including 9 up- and 23 down-regulated proteins (Figure 11b, c). Enrichment analysis detected protein-protein interactions in down-regulated proteins indicating that these proteins were mainly involved in ECM organization, wound healing, vesicle-mediated transport, and exocytosis. Although, no interactive network was identified among the up-regulated proteins, four up-regulated proteins Apolipoprotein L1 (APOL1), Kinectin 1 (KTN1), Carboxypeptidase N Subunit 1 (CPN1) and Protein Si (PROS1) presented significant interactions with down-regulated proteins. Additionally, we identified that the potential role of these differentially expressed proteins were mainly associated with ECM organization, exocytosis, and wound healing.

5.1.2 Detection of Predictive Biomarker

Next, by overlapping the healing- and outcome-related proteomic files, we identified 9 proteins which included APOL1, Collagen alpha-1 (I) (Col1a1), Collagen alpha-1 (V) (Col5a1), Insulin-like growth factor-binding protein-4 (IGFBP4), Complement factor D (CFD), Nidogen-2 (NID-2), Palladin (PALLD), Serpin family B member-1 (SERPINB1) and Metalloproteinase inhibitor-1 (TIMP-1). All these proteins, except CFD, exhibited elevated levels in healing compared to the healthy tendons. CFD was the only biomarker with lower levels in patients with good clinical outcome as well as reduced levels in healing tendons.

A linear-regression model was used to identify proteins associated with patients 1-year clinical outcomes. We detected that CFD and SERPINB1 were negatively associated with ATRS while a positive relationship was identified between APOL1 and ATRS (Figure 12a-c).

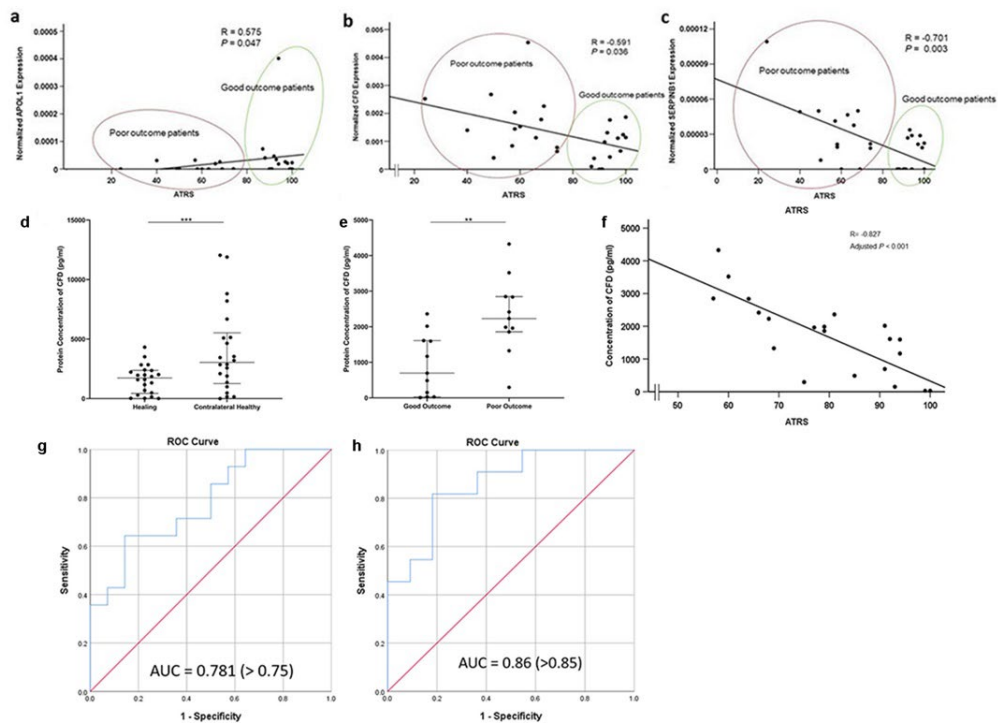


Figure 12. Predictive biomarker identification and confirmation. Association between protein expression and healing outcome assessed by ATRS (a-c) through a linear regression model. Protein expression was normalized and ATRS ranges from 0-100, An adjusted p value < 0.05 was considered as statistical significance. $n = 28$. d, e) CFD expression as measured by MSD in healing and contralateral healthy micro-dialysate and analyzed by d) paired Wilcoxon test. $n = 22$ in each group and, e) by Mann-Whitney U test with $n = 11$ in each group. f) correlation between CFD level and ATRS measured by linear regression. $n = 22$. $**p < 0.01$ and $***p < 0.001$. g) ROC curve and AUC value of CFD and patient 1-year outcome, $AUC > 0.75$ means CFD shows a relevant good significance to predict patient outcome. h) ROC curve and AUC value of CFD and patient 1-year outcome, $AUC > 0.85$ means CFD shows a great significance to predict patient outcome. Adapted from **Paper II**, Figure 4.

An area under the receiver operating characteristic (ROC) curve (AUC) is a validated tool to examine the reliability of the predictive biomarkers [87, 199, 200] for effective healing. Our analysis showed an AUC for CFD = 0.78 (Figure 12g), APOL1 = 0.71 and SERPINB1 = 0.74, highlighting CFD as the most effective biomarker of tendon healing. Further confirmative analysis by MSD repeated the findings from MS data, demonstrating a lower expression in the healing tendon and better outcome patients (Figure 12d, e) and a negative association with 1-year clinical outcome (Figure 12f). The AUC analysis on MSD data with values 0.86 (Figure 12h), further highlighted a strong reliability of CFD with a predictive role in tendon repair.

CFD is mainly produced and released by the adipocytes, monocytes and macrophages, and is considered as an important trigger of inflammatory response [201]. A previous study reported that lower CFD levels in fibroblasts can increase the TIMP1 production leading to improved Col1a1 synthesis [169]. Fibroblasts play an important role during tendon repair through synthesizing Col [202]. Therefore, we speculate that lower CFD expression might mediate tendon repair by up-regulating TIMP1, which by down-regulating the biological activity of MMPs leads to increased Col1a1 expression. Interestingly, our results showed

lower CFD while higher TIMP1 and Col1a1 levels in the micro-dialysates from healing- compared to the healthy side, supporting our hypothesis. Further bioinformatic analysis of the MS data showed a relationship between CFD and granule secretion and leukocyte mediated activity. In an earlier rat model, leukocytes were showed to improve inflammatory cytokines, leading to delayed tendon healing [203, 204]. Another human study reported that CFD can inhibit granule secretion via polymorphonuclear neutrophil leukocytes [205]. These processes can be driven in part by exocytosis. However, the accurate mechanisms involved need to be further investigated in detail. Thus, our findings highlight the role of a novel biomarker CFD in CT healing and provide this protein as a specific target for further interventions.

5.3 Biomarkers of Early Healing and Their Function on Dense CT Repair (Study III, manuscript submitted)

The study was designed to investigate the proteomic profile of injured human Achilles tendon, identify potential biomarkers, and assess their association with the patient's long-term outcomes after ATR. Further, the regulatory mechanisms of the identified biomarkers on Col 1, as a marker of dense CT repair, were investigated in *in-vitro* models based on primary fibroblast and fibroblast cell line.

The study included a total of 40 patients with ATR undergoing tendon reconstruction surgery. Tendon biopsies were collected during surgery and were analyzed by MS. At the one-year post-surgery follow-up, all patients were assessed for healing outcomes based on their ATRS. To explore the underlying mechanism of dense CT repair, patients were divided into groups of good (ATRS > 80; n = 20) and poor healing outcomes (ATRS < 80; n = 20). No statistically significant differences were noted among good and poor outcome groups regarding age, sex and BMI. However, the ATRS for the good outcome group (95.3+/- 4.0) was significantly higher ($p < 0.001$) than the ATRS for the poor outcome group (61.5 +/- 9.7). The clinical parameters for all patients are presented as **Table 1**.

5.3.1 Detection of Predictive Biomarkers for Dense CT Repair

The computational data analysis detected a total of 855 unique proteins, including 769 shared proteins across the good and poor outcome groups. Among the shared proteins, 51 differentially expressed proteins were detected with 10 down- and 41 up-regulated proteins in good compared to poor outcome subgroup (Figure 13a, b).



Figure 13. Quantitative proteomic file of injured human Achilles tendon. a) Venn plot of overlapping and distinct proteomes of patients with good (G) and poor (P) outcome. $n = 20$ in each group; b) Volcano diagram with differentially expressed proteins. The X coordinate represents Log_2 fold change (FC) and the Y coordinate to $-\text{Log}_{10}$ (p -value). Each dot represents a protein with red = up-regulated, green = down-regulated and, black = non-differentially expressed proteins;

Subsequent linear-regression analysis based on the proteomic data and 1-year post-surgery clinical and functional data identified two proteins: eukaryotic elongation factor-2 (eEF2) and fibrillin-2 (FBN2). Both eEF2 and FBN2 were positively associated with ATRS (Figure 14a, d) and average heel rise height (Figure 14b, e). The expression of both markers was up regulated in good compared to the poor outcome patients (Figure 14c, f). The eEF2 and FBN2 were then subjected to AUC analysis which identified eEF2 as a strong predictor of good clinical outcome with the value of 0.86, as compared to FBN2 with an AUC value of 0.69.

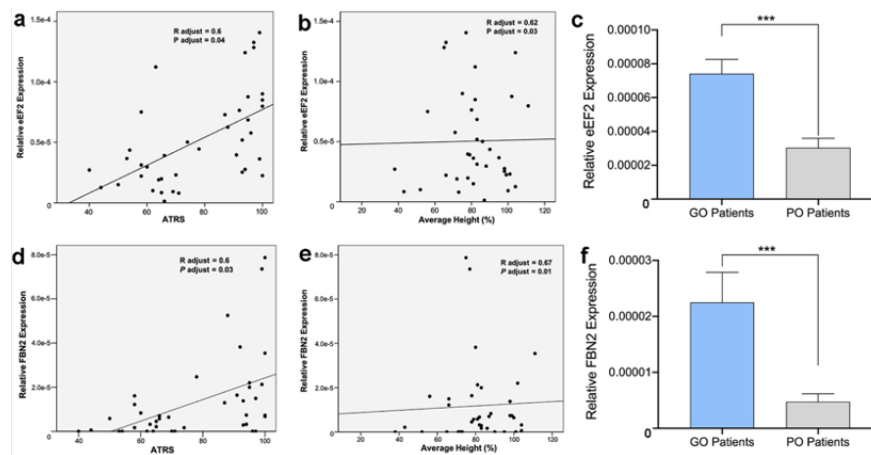


Figure 14. Association of eEF2 with a) ATRS and, b) average heal rise, $n = 40$; c) eEF2 expression between good outcome (GO, $n = 20$) and poor outcome (PO, $n = 20$) patients, data presented as mean \pm SD, *** $p < 0.001$; Association among FBN2 and d) ATRS, e) average heal rise, $n = 40$; f) FBN2 levels among good outcome (GO, $n = 20$) and poor outcome (PO, $n = 20$) patients, data presented as mean \pm SD, *** $p < 0.001$; g). Adapted from Paper III, Figure 2.

5.3.2 eEF2 Regulates Collagen Expression during Dense CT Repair

To explore the underlying mechanisms of eEF2 on healing, the association between eEF2 and Collagen type I $\alpha 1$ (Coll1a1) was analyzed. Western blot analysis from protein lysates generated from biopsies used for the MS analysis were used for eEF2 and Coll1a1 expression in patients with good and poor outcome. The analysis demonstrated higher Coll1a1 levels among patients with better outcome (Figure 15b), in accordance with the findings for eEF2 (Figure 15a). Interestingly, a strong association among eEF2 and Coll1a1 (Figure 15c) was observed suggesting that eEF2 may mediate Coll1a1 production to enhance tendon repair. We further observed higher Coll1a1 levels in good compared to the poor outcome patients (Figure 15d).

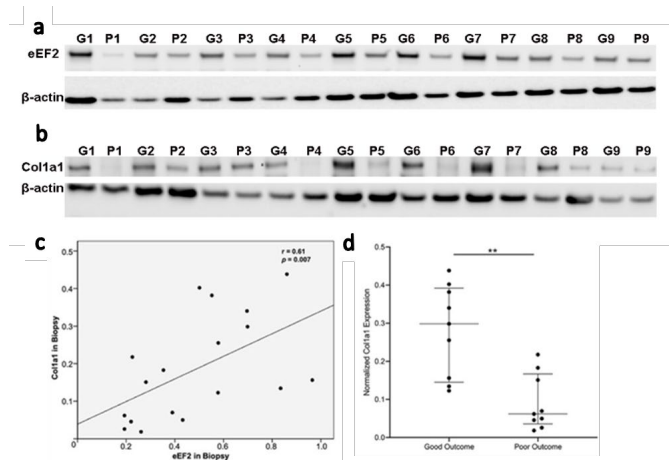


Figure 15. The eEF2 and Col1a1 expression in tendon biopsies. Western blot images from a) eEF2 and beta-actin (β -actin) and b) Col1a1 and β -actin expression in good (G, n = 9) and poor (P, n = 9) outcome patients. c) Association among eEF2 and Col1 expression based on western blot analysis, n = 18. d) Col1a1 expression in good and poor outcome patients, n = 9. For western blot analysis, band signal intensity was used and normalized by the intensity of the house-keeping gene (beta-actin). Adapted from **Paper III**, Figure 2 and 3.

5.3.3.1 eEF2 Enhances Dense CT Repair during Inflammation by Improving Autophagy and Apoptosis.

Autophagy, which is a self-renewal mechanism that can degrade and recycle cellular components, plays an essential role during various phases of wound healing [206-208]. It has been shown that autophagy can prevent excessive inflammation and also regulate collagen synthesis during the inflammatory phase of healing [209].

The bioinformatic analysis of our MS data also identified strong associations among eEF2 and autophagy induced markers: DCN (Decorin) and SOGA3 (suppressor of glucose by autophagy) (Figure 16a, b), highlighting a potential role of autophagy during the inflammatory stage of tendon repair in humans. Thus, inflammatory fibroblast injury models based on human primary fibroblasts and fibroblast cell line were used to confirm and further explore whether eEF2 regulate collagen production by mediating autophagy during inflammatory stage.

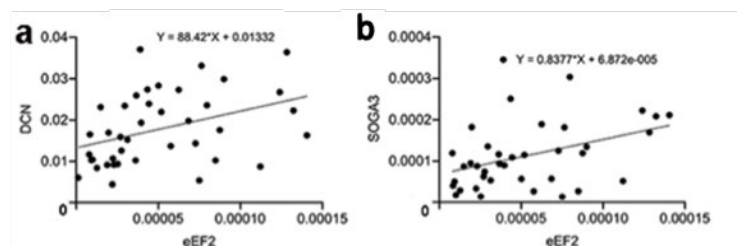


Figure 16. Association among eEF2 and autophagy related markers a) DCN, and b) SOGA3. Adapted from **Paper III**, Figure S2.

Autophagy was induced in the fibroblast primary cells and cell line, leading to an increase in microtubule-associated proteins light chain 3-II (LC3-II) expression and LC3-II/I ratio. The LC3-II expression and LC3-II/I ratio were significantly reduced when eEF2 was silenced, suggesting a positive effect of eEF2 on autophagy (Figure 17a-d). Further

exploration of this relationship demonstrated that autophagy leads to increased Col1a1 expression and that this up-regulation was controlled by eEF2 (Figure 17e-f).

After tissue injury, the inflammatory stage of healing is comprised of multiple biological processes that are crucial towards tissue repair [210-212]. Among these processes, our bioinformatic and statistical analysis identified that eEF2 not only improved autophagy but also promoted apoptotic processes during tissue repair. To confirm the findings from the bioinformatic and statistical analysis, the ratio of dead/live cells was assessed in inflammatory fibroblast models. Our experimental data demonstrated that inflammation increased the ratio of dead/live cells in fibroblasts (Figure 17g-h). Further, TNF-induced up-regulation of dead/live ratio that was even higher when eEF2 was silenced. In addition, the increased ratio of dead/live fibroblasts led to higher ratio of apoptotic cells as observed by caspase-3/7 activity (Figure 17i-j). These findings highlight eEF2 as a multi-functional biomarker of tissue repair by reducing cell death/apoptosis during the inflammatory phase of dense CT repair.

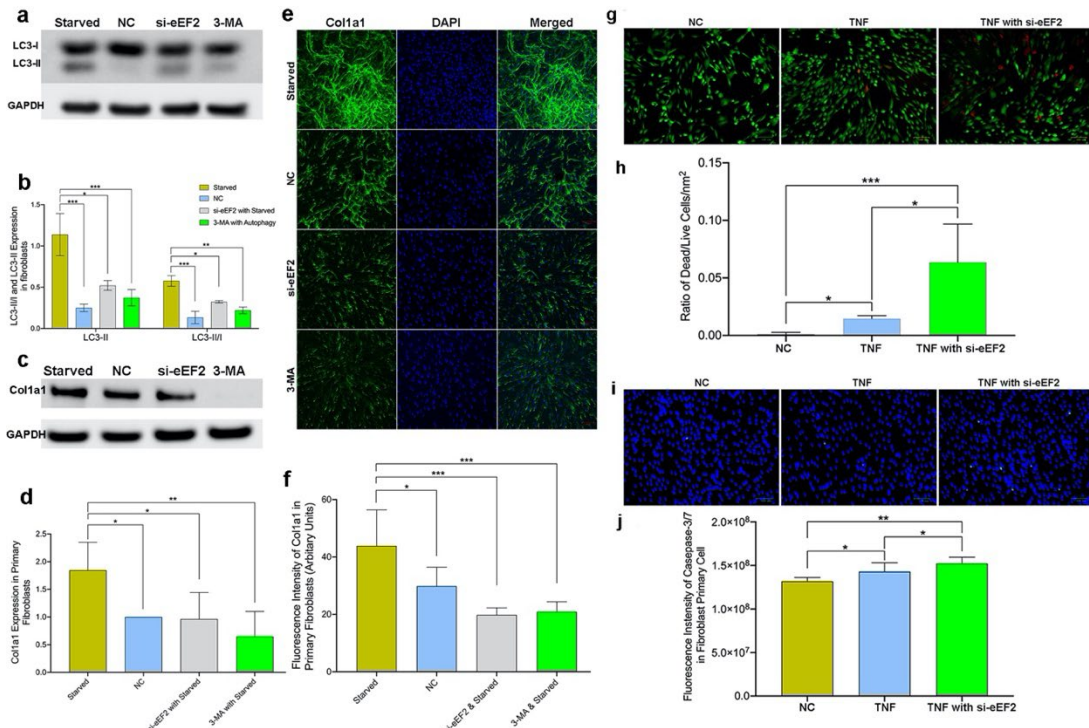


Figure 17. eEF2 enhances healing processes in TNF-induced inflammatory fibroblasts. a-f) eEF2 affects Col1a1 expression through autophagy in primary fibroblasts. a, b) Representative Western blot images and semi-quantitative analysis of LC3-II and LC3-II/LC3-I ratio, c-f) Representative Western blot (c) and confocal images (e) along with semi-quantitative analysis of Col1a1 (d, f) in cells treated with normal medium, starved medium for autophagy, si-eEF2 and by autophagy inhibitor (3-MA) incubation based on autophagy; g-j) Representative images captured by fluorescent microscope demonstrated the cell death and apoptosis when treated with normal condition, TNF and si-eEF2, (g, h); si-eEF2 positively associate with cell apoptosis among fibroblasts (i, j); The ratio of dead/live cells was reported by percentage and the apoptotic level of cells was presented by fluorescent green intensity. Data reported as mean \pm SD, * $p < 0.05$, ** $p < 0.01$, *** $p < 0.001$, scale bars = 100 μ m, 3 replicates were used for quantitative analysis. Adapted from **Paper III**, Figure 4.

5.3.4.1 eEF2 Enhances Dense CT Repair by Enhancing Cell Proliferation

The inflammatory phase of healing is successively replaced by proliferative healing processes and matrix deposition. Our recent finding based on the proliferative stage of healing [30] also detected an increased eEF2 expression in the healing tendons at two weeks post repair surgery. To further investigate the role of eEF2 on proliferative healing processes, the effects of si-eEF2 on fibroblast proliferating was studied in unchallenged cell line as well in primary fibroblasts. Our analysis showed a decline in Colla1 production by knocking down eEF2 (Figure 18a-b), confirming the role of eEF2 on collagen synthesis. Quantitative image analysis demonstrated an eEF2-induced cell proliferation among cells treated with si-eEF2 (Figure 18c-d). Taken together, these observations confirmed and extended the potential role of eEF2 from inflammatory to the early proliferative stages of dense CT repair.

5.3.4.2 eEF2 Enhances Dense CT Repair by Reducing Cell Death and Apoptosis during Proliferation

Cell death is an essential yet opposing biological process in relation with proliferation [213, 214], while apoptosis is the outcome of cell death. In the next step, the impact of eEF2 on the coordinated cell proliferation and apoptosis leading to dense CT repair was explored in unchallenged fibroblasts. The experimental observations indicated an opposite effect of eEF2 on cell death when compared with cell proliferation as demonstrated by increases in the ratio of dead/live cells when cells were treated with si-eEF2 (Figure 18e, f). The pathway to cell death was corroborated by demonstrating an increased apoptotic ratio of cells following treatment with si-eEF2 (Figure 18g, h). These findings for the first-time reported that eEF2 induced fibroblast proliferation, and at the same time reduced cell death and apoptosis to improve dense CT repair.

5.3.4.3 eEF2 Enhances Dense CT Repair by Enhancing Cell Migration during Proliferation

During wound healing, fibroblast migration to the site of injury is a crucial step to initiate healing processes [215]. Thus, we assessed the role of eEF2 on cell migration in *in-vitro* wound model where a scratch was created in monolayer cultured fibroblasts. The findings confirmed the earlier bioinformatic analysis by demonstration of a reduced cell migration area and ratio among cells transfected with si-eEF2 (Figure 18i-k). Quantitative analysis of the results demonstrated a significantly ($p = 0.01$) slower (30%) migration rate in eEF2 knock down cells in comparison with a 47% rate in normal cells supporting a mechanistic role for eEF2 in cell migration during dense CT repair.

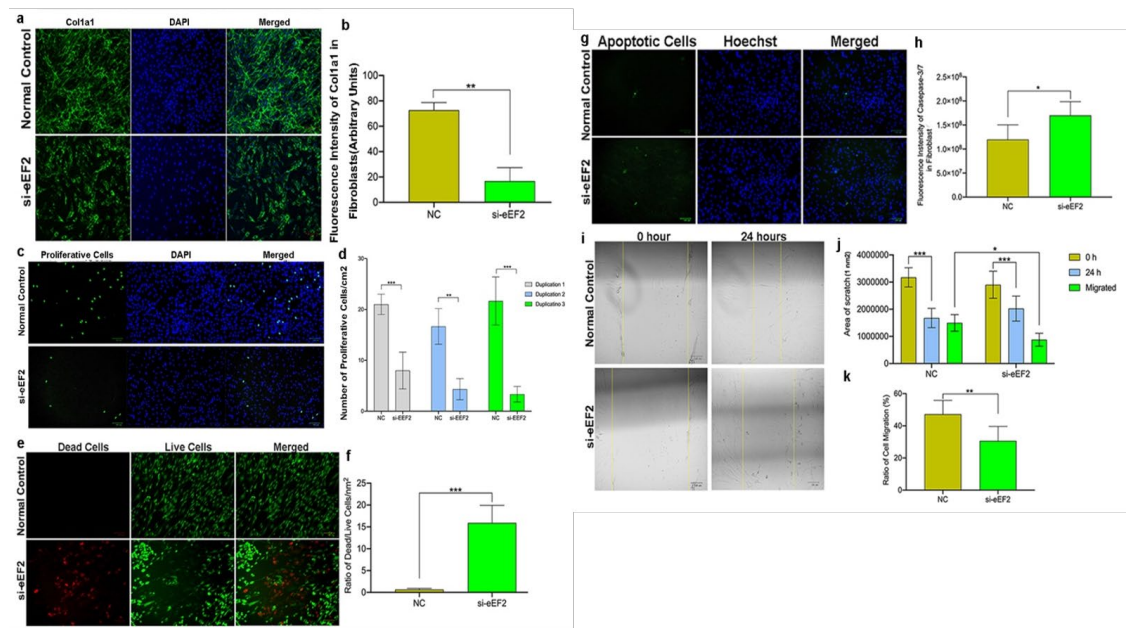


Figure 18. eEF2 enhances fibroblast proliferative processes. a-b) Representative confocal images and semi-quantitative analysis of Coll1a1 in fibroblasts, with and without si-eEF2; c-d) Representative immunofluorescence images and number of proliferating fibroblasts, with and without si-eEF2; e-f) Representative immunofluorescence images and ratio of dead/live cells in fibroblasts, with and without si-eEF2; g-h) Representative immunofluorescence images and number of apoptotic fibroblasts with and without si-eEF2; i-k) Representative images and quantitative analysis of cell migration rate assessed at 0 and 24 hours in fibroblasts, with and without si-eEF2. Data reported as mean \pm SD, * $p < 0.05$, ** $p < 0.01$, *** $p < 0.001$, scale bars = 100 μ m, n = 3 replicates. Adapted from **Paper III**, Figure 5.

Dense CT repair consists of dynamic and overlapping phases, including inflammatory, proliferative and regenerative phases [24]. To understand the mechanisms of eEF2 in dense CT repair we, in a stepwise manner, investigated how this biomarker regulates tissue healing from the inflammatory to the early proliferative healing processes. The finding that eEF2 increases Coll1a1 production by positively regulating autophagy during inflammation is supported in the literature among different cell types showing an association between autophagy and Coll1a1 production [208, 216-218]. eEF2 is an elongation factor, which promotes the GTP-dependent translocation of the ribosome, and thus presumably also promotes Coll1a1 synthesis during CT repair [219, 220]. Coll1a1, produced by fibroblasts, encodes the major component of Col I, the most abundant collagen in the ECM of healthy CT [221-223]. Moreover, higher expression of Col I leads to improved dense CT repair [224]. Thus, our combined bioinformatics analysis and mechanistic approaches using inflammatory fibroblast models confirmed that eEF2 enhances dense CT repair during the inflammatory phase of healing by increasing autophagy and thereby promoting the production of Coll1a1.

Cell proliferation is the subsequent phase in wound healing [157, 165, 166], in which eEF2 has been reported to act as a promoter [225], presumably by improving the cell proliferative process through the PI3K pathway [226]. The identification of increased eEF2 levels at 2-weeks post Achilles tendon surgery [30], suggests a role in the early proliferative healing phase in accordance with previous studies of Achilles tendon healing [112, 113]. Here, we used both unchallenged human primary fibroblasts and a fibroblast cell line,

mimicking aspects of the proliferation phase of healing, to investigate the mechanistic role(s) of eEF2 in tissue repair. The combined bioinformatic and mechanistic analysis confirmed that eEF2 enhanced fibroblast proliferation and increased Coll1a1 production. In addition, the positive association between eEF2 and Coll1a1 extends our understanding of the role of this protein in tissue healing. The coordination between cell proliferative and apoptotic activity also plays a key role in tissue development and homeostasis in the human body [213]. The current findings that eEF2 increases cell proliferation and migration, and at the same time reduces cell death and apoptotic processes, suggest that eEF2 can regulate and enhance dense CT repair during the proliferative healing phase.

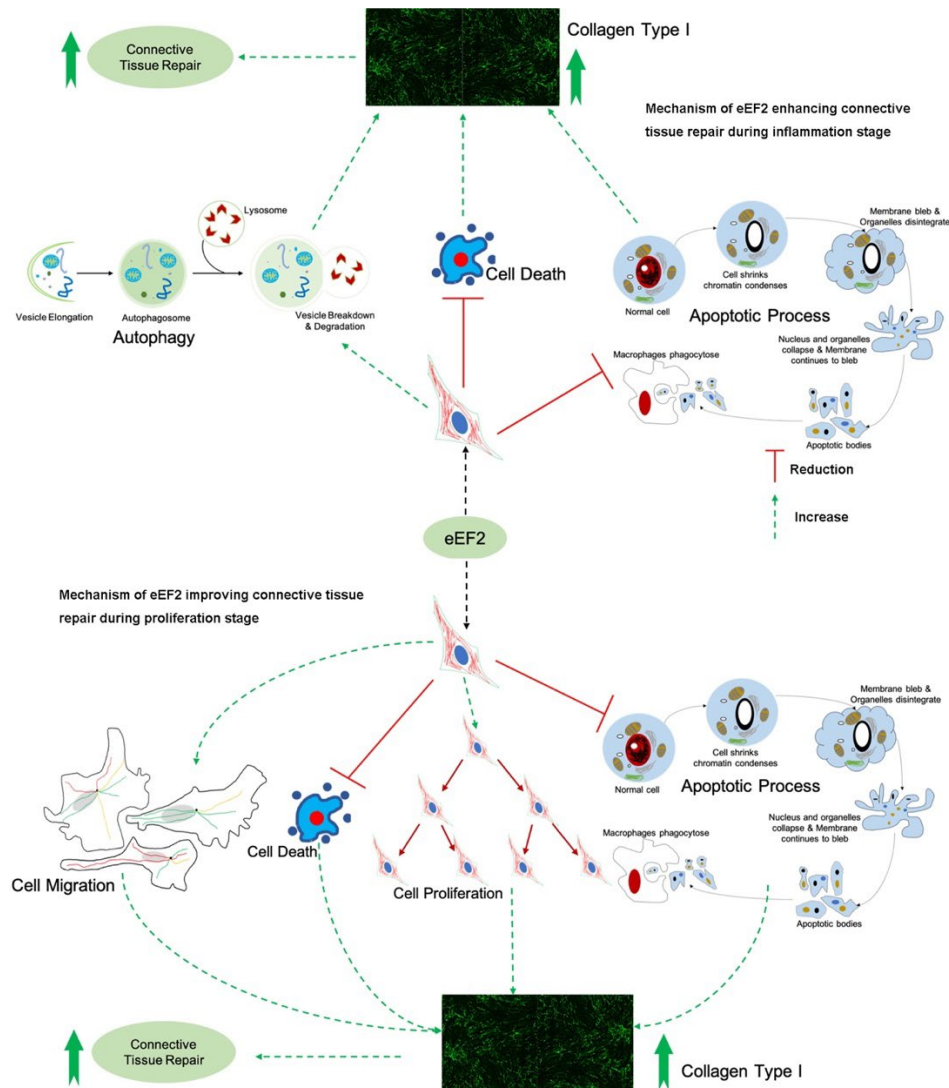


Figure 19. Potential mechanisms and mode of action of eEF2 during inflammation and proliferation phases of connective tissue repair. Adapted from **Paper III**, Figure 6.

5.4 An Inflammatory Biomarker Complement Factor D in Human Dense CT Repair Based on Achilles Tendon Model (Study IV, Manuscript)

The study was designed to investigate and explore the role of CFD on injured AT repair both at the inflammatory and early proliferating phases of healing. Further, the regulatory mechanisms of CFD on Col1a1 synthesis were investigated in primary fibroblast and fibroblast cell line.

In the previous study (study II) we presented that CFD plays a vital role in healing and showed that CFD has a prognostic capacity for long-term clinical outcome after ATR injury. In this study, we further explored the role of CFD in tendon repair by combing MS-based proteomic profile obtained at the time of surgery and at 2-weeks post-surgery from healing AT.

5.4.1 Detection of Complement Factor D during Dense CT Repair

Since CFD was identified with an AUC value equal to 0.78 in micro-dialysate (Study II), demonstrating its predictive role in dense CT healing. To identify the long-term role of CFD in dense CT healing, we compared proteomic data from tendon biopsies collected at the time of surgery, and from micro-dialysates collected 2-weeks post-surgery. The regression model followed by an AUC analysis detected the prognostic role of CFD with high reliability and sensitivity. We identified lower CFD, and higher TIMP1 and Cola1 levels (Figure 20a-c) during the proliferative healing stage (Figure 20b) in injured leg and in good outcome patients. Furthermore, the relationship between CFD and Col1a1 was studied, resulting in a positive association in both inflammation and proliferation phase (Figure 20). Confirmative experiment based on western blot analysis also repeated the same observation, strengthening our findings from the MS data (Figure 20g).

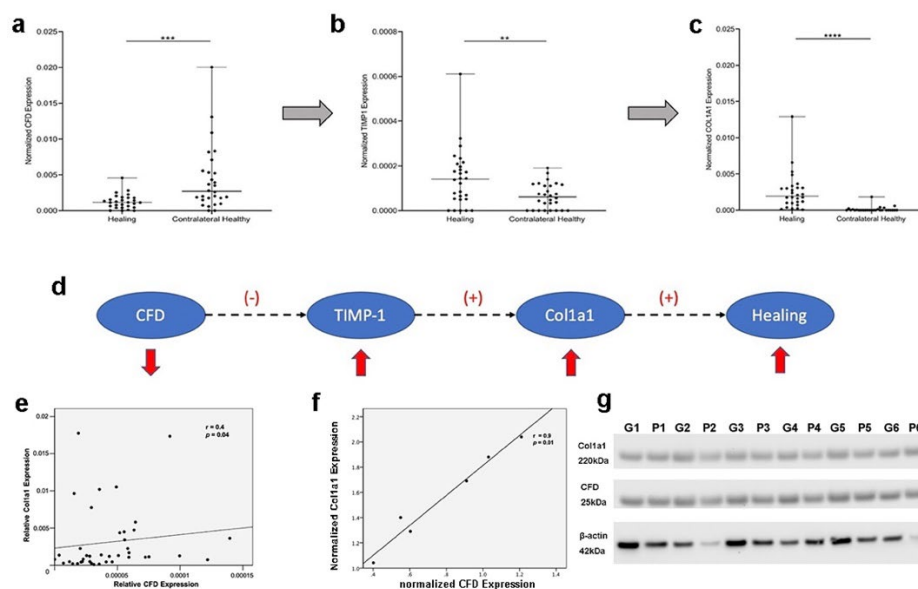


Figure 20. The relationship between CFD and Col1a1 in a-d) micro-dialysate and e-g) tissue biopsies. Expression of a) CFD, b) TIMP1, c) Col1a1 in healing and contralateral intact Achilles Tendon, 2-weeks post-surgery and, d) potential associations among CFD and Col1a1 in micro-dialysates as a representative of the proliferative healing stage; e-g) Association of CFD and Col1a1 in tissue biopsies as a representative of the inflammatory healing stage, e) correlation based on relative expression; b) correlation based on normalized

expression. c) Western blot analysis of CFD, Colla1 and beta-actin (β -actin) expression in good (G) and poor (P) outcome patients in tissues.

5.4.2 CFD Enhances Dense CT Repair by Regulating Colla1 Synthesis during both Inflammation and Proliferation Stage

After a CT injury, inflammation is the first phase of tissue repair, followed by the proliferative phase. To investigate the effect of CFD on Colla1 during CT healing, we created an inflammation-induced and an unchallenged fibroblast model to represent the inflammatory and proliferative stage of repair in both primary fibroblasts and fibroblast cell line. By using gene silencing technique, we identified that Colla1 production was significantly decreased when CFD was knocked down in the inflammatory fibroblast model. In contrast, CFD knock down lead to an increased Colla1 synthesis in unchallenged fibroblasts, highlighting that lower CFD during proliferation stage can improve CT healing by up-regulating the Colla1 production. Additionally, our findings from both the fibroblast cell line and primary fibroblasts confirmed these effects of CFD on Colla1 synthesis, highlighting the role of CFD in enhancing CT repair (Figure 21).

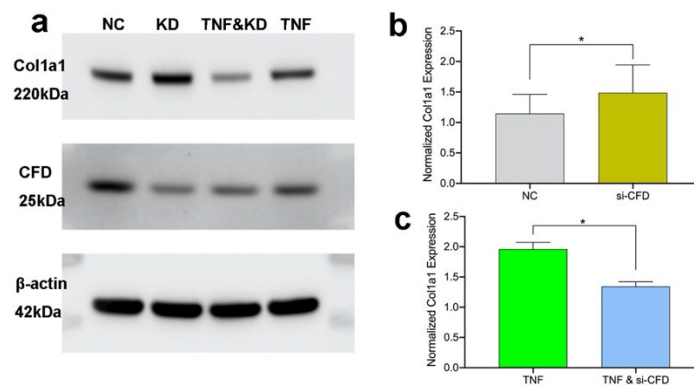
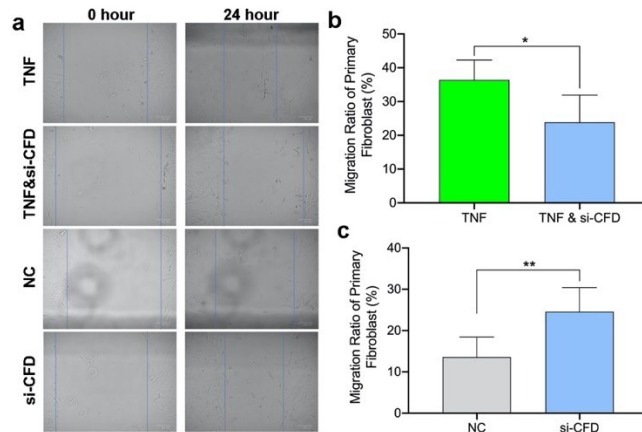


Figure 21. CFD regulates Colla1 expression during inflammation and proliferation stages among fibroblasts. Knock-down (KD=silencing (si) of CFD regulates Colla1 synthesis (a, c) during inflammation (TNF-induced) and (a, b) proliferation (NC=normal challenge). Signal intensity was used for quantitative analysis of western blot, and the intensity of the house-keeping gene (beta-actin) used for normalization. Data reported as mean \pm SD, * $p < 0.05$, 3 replicates were used for quantitative analysis. Adapted from **Paper IV**, Figure 2.

5.4.3 CFD Enhances Dense CT Repair by Regulating Cell Migration during both Inflammation and Proliferation Stage

The migration of fibroblasts to the site of injury is a vital process initiating wound healing [215]. However, Colla1 produced by fibroblasts is the major regenerative protein during the whole healing process. We then identified the role of CFD in regulating fibroblast migration during dense CT repair by gene silencing technique. For these experiments, a scratch was established in monolayer cultured fibroblasts using both the primary cells and the cell line, treated with or without si-CFD. The findings presented that CFD can up-

regulate cell migration during the inflammatory stage while fibroblasts migration was decreased at the proliferative phase (Figure 22).



Dense CT repair is a complex and overlapping process comprising of inflammation, proliferation, and remodeling phases [24]. To go insight on healing mechanisms and the related biomarkers, we, in a stepwise manner studied CFD from inflammation to proliferation stages. Our previous findings have shown that a lower expression of CFD in proliferation stage has positive effects on healing, leading to better clinical outcome [30]. Our present findings presented an improvement in proliferation phase demonstrating that CFD positively stimulated Colla1 expression during inflammation but down-regulate Colla1 synthesis in proliferation stage. Colla1 is the major element of collagen type I, which is the most vital collagen in ECM of tissues [222, 223]. Previous findings presented that higher and faster production of Colla1 is the key reason of improved dense CT healing [224]. Thus, our current findings further confirmed a dynamic effect of CFD in regulating Colla1 production in dense CT repair.

Fibroblasts play a vital role during tissue healing from the late inflammation stage by acting as a trigger of inflammation-proliferation transition [215, 227]. Previous studies have reported that the migration of fibroblasts can promote dense CT healing under the regulation of functional biomarkers [228, 229]. However, the biomarkers for mediating dense CT repair are still unknown. Our *in-vitro* investigations presented CFD as a novel biomarker which affects fibroblasts migration from the inflammatory to proliferative stage of tissue healing, demonstrating that CFD up-regulates fibroblasts migration during inflammation but reduces the migrative process at proliferation. Interestingly, both primary fibroblast and fibroblast cell line presented the same observation, confirmed and strengthened our finding.

5.5 Network analysis of Proteins as Prognostic Biomarkers and Therapeutic Target of Dense CT Repair (Study V, Manuscript submitted)

In this study, a weighted gene co-expression network analytical (WGCNA) approach was applied to the MS data to identify biomarkers or hub proteins associated with 1-year postoperative prognosis. Further, the regulatory mechanisms of identified hub proteins on Col synthesis were studied by using gene silencing technique in human fibroblasts.

5.5.1 Identification of Hub Proteins and Associated Pathway

The MS proteomic data from study III was re-analyzed by WGCNA which identified a total of 14 modules from which 2 (brown and red) were determined to be significantly related to healing prognosis after ATR. Based on an absolute value of the MM > 0.8 and GS > 0.1, 24 hub proteins from the brown and 23 from the red module were selected (Figure 23a-b). In the next step, network was imported into the Cytoscape software and CytoHubba plugin was employed. By using the MCC and Degree methods the top 10 hub proteins from the brown and red modules were detected along with their interaction. Subsequently, three common proteins, ITIH4, Serpin family F member 1 (SERPINF1), and immunoglobulin lambda variable 1-47 (IGLV1-47), were detected (Figure 23c, d). Among these, the ITIH4 expression was found to be elevated in good compared to the poor outcome group (Figure 23d). ITIH4, SERPINF1 and IGLV1-47 were further subjected to logistic regression analysis which also identified ITIH4 as a factor for prognosis. Moreover, the prognostic reliability of ITIH4, SERPINF1 and IGLV1-47 was studied by the ROC curve analysis which demonstrated ITIH4 with the highest AUC value of 0.709 as a strong predictor of good clinical outcome (Figure 23e). As Col1 is the main collagen subtype of tissue repair, the relationship between ITIH4 and Col1a1 was explored. Our results showed elevated Col1a1 levels in the group with low compared to high-risk group, indicating the positive effects of ITIH4 on collagen expression. To identify the potential pathways for connective tissue repair, GSEA was performed which selected PPAR as the highest ranked signaling pathway with an enrichment score of 0.84 (Figure 23f). Taken together, these analyses selected ITIH4 as the best predictive biomarker and PPAR as an associated signaling pathway, findings which were then subjected to further targeted investigations.

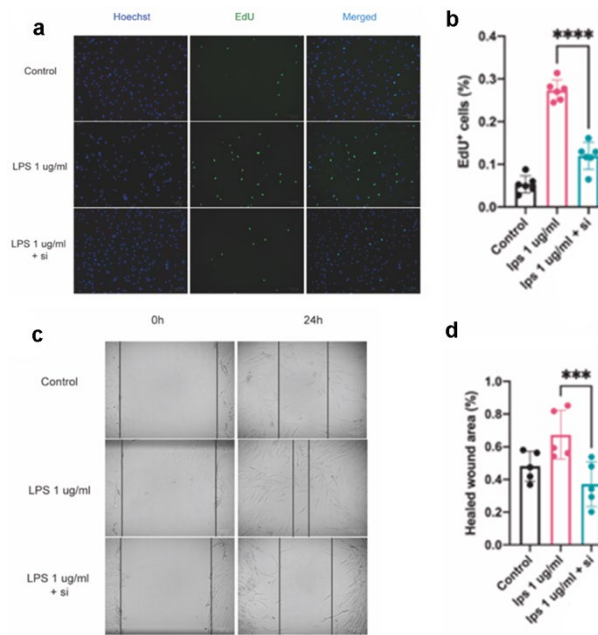


Figure 24. The effects of ITIH4 on proliferation and wound healing. of fibroblasts treated with LPS. Fibroblasts were transfected with 50 nM ITIH4 siRNA. At 48 h after transfection, fibroblasts were subjected to 72 h of LPS treatment with different concentrations. a-b) Representative images and quantitative analysis of proliferation rate assessed by EdU assay. (n=6). At 24 h after transfection, a scratch was created, and fibroblasts were subjected to 24 h of LPS treatment with different concentrations. c-d) Representative images and quantitative analysis of wound recovery rate assessed by wound healing assay. (n=5). Scale bar = 100 μ m. ns, not significant; * $p < 0.05$; ** $p < 0.01$; *** $p < 0.001$; **** $p < 0.0001$

5.5.2 ITIH4 Regulates Dense CT Repair by Mediating Cell Death and Apoptosis

Further, the role of ITIH4 on apoptosis and cell death was investigate. The analysis of activated Caspase-3/7 staining demonstrated that LPS alone can promote the activation of Caspase-3/7 in fibroblasts. During LPS treatments, knockdown of ITIH4 further increased the activation of Caspase-3/7 in fibroblasts (Figure 25a-b). These results were further confirmed by live/dead assay, showing that LPS alone or si-ITIH4 decrease survival rate. Consistently, following LPS treatments, knockdown of ITIH4 resulted in higher apoptosis rate (Figure 25c-d). Collectively, these results suggest that ITIH4 has a cytoprotective role in LPS-treated fibroblasts.

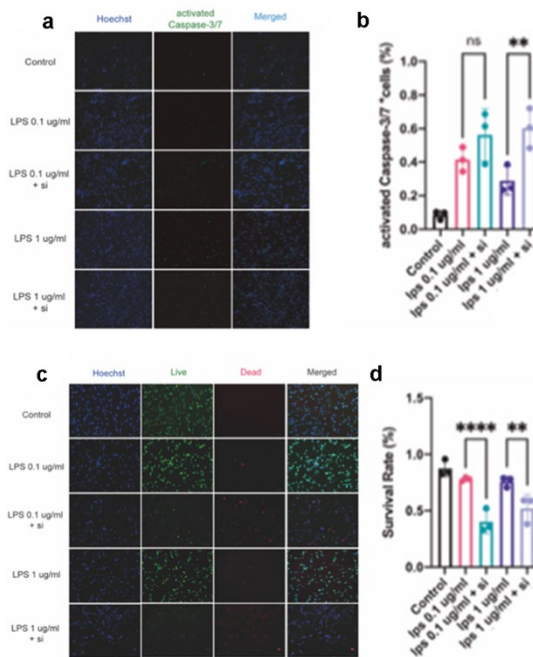


Figure 25. Knockdown of ITIH4 on apoptosis of fibroblasts. a-b) Representative images and quantitative analysis of Caspase-3/7 activation. (n=3). c-d) Representative images and quantitative analysis of cell death assessed by live/dead assay. (n=3). Scale bar = 100 μ m. ns, not significant; * $p < 0.05$; ** $p < 0.01$; *** $p < 0.001$; **** $p < 0.0001$.

5.5.2 ITIH4 Regulates Dense CT Repair by Mediating Col1a1 synthesis and PPAR Signaling Pathway

Col1a1 is the major constituent for CT matrix and ECM organization. Our bioinformatic analysis highlighted that collagen containing matrix production was one of the most enriched biological processes leading to good healing. Additionally, patients with higher ITIH4 levels exhibited elevated Col1a1 levels in the surgical biopsies.

Our bioinformatic analysis identified PPAR as the highly ranked signaling pathway associated with good healing outcomes after ATR. To confirm an association between PPAR and ITIH4, immunofluorescence analysis with anti-ITIH4 and anti-PPAR-gamma was used in LPS-stimulated fibroblasts with and without ITIH4. The results showed that LPS treatment alone downregulated the expression of PPAR γ at relatively low concentrations (1-10 μ g/ml), while it upregulated PPAR γ expression at a relatively high concentration (50 μ g/ml). However, the knockdown of ITIH4 by si-ITIH4 significantly increased PPAR γ expression in LPS-stimulated fibroblasts (Figure 26c, d). Thus, the presence of ITIH4 can impact expression of components of the PPAR pathway.

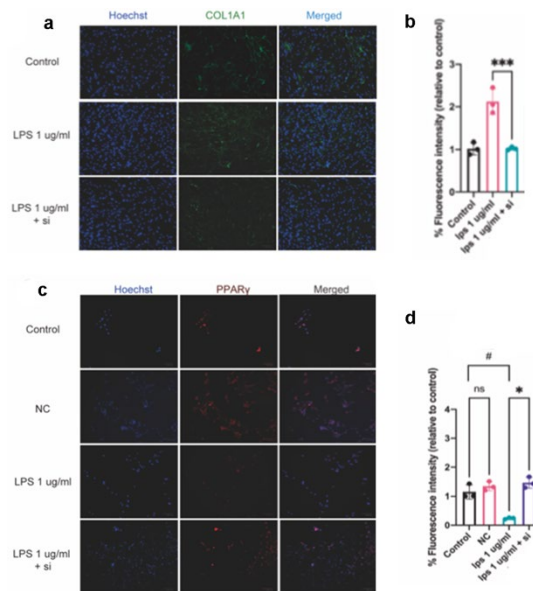


Figure 26. Knockdown of ITIH4 on levels of collagen I and PPAR γ of fibroblasts treated with LPS. Fibroblasts were transfected with 50 nM ITIH4 siRNA. At 48 h after transfection, fibroblasts were subjected to 48 h of LPS treatment with different concentrations. a-b) Representative images and quantitative analysis of expression of Col1a1 via immunofluorescence analysis. (n=3). c-d) Representative images and quantitative analysis of expression of PPAR γ via immunofluorescence analysis. (n=3). Scale bar = 100 μ m. ns, not significant; * $p < 0.05$; ** $p < 0.01$; *** $p < 0.001$; **** $p < 0.0001$.

PPAR is known to be involved in lipid catabolism, inflammation, survival, proliferation, as well as regeneration of the skin, bone and liver [230, 231]. It has been demonstrated to be an emerging target to promote wound healing and regeneration. PPARs consist of ligand-activated transcription factors belonging to the nuclear hormone receptor super-family [232]. As an important member of the super-family, PPAR γ has been reported that the expression is increased exposed to inflammation, and significantly suppress collagen production. In our study, the expression of PPAR γ is regulated by LPS in a dose-dependent manner. Moreover, the expression of ITIH4 is negatively correlated to PPAR γ in cultured fibroblasts. Taken together, our results suggest that ITIH4 regulate Col I production via regulating the expression of PPAR γ in inflammatory environments.

6 CONCLUSIONS

Connective tissues are essential to support, protect and give structure to other tissues and organs in human body [233]. CT repair follows similar healing process as other organs or tissues and can be affected by various biomarkers which are not fully understood. In this thesis, the differential expression of biomarkers and their role in regulating dense CT repair and long-term clinical outcome was studied. These studies identified four novel biomarkers that can be used as predictors for outcome prognosis and involve in potential pathways in mediating CT healing.

The first biomarker is *FGF2* with a higher gene expression in better outcome patients 1-year after ATR, and was also associated with less pain on tendon, less running limitation, and less loss of work activity (as described in **Paper I**). Previous studies have reported that FGF not only affect stem cells to release tendon-associated genes, but also directly regulate Col type I and III synthesis [193, 194]. Thus, the observed higher *FGF2* expression in the present thesis may promote *Col I* and *III* synthesis, regulates ECM degradation and formation, leading to an improved healing and long-term outcome.

The **paper II** reported the largest landscape of human healing tendon, also identified CFD as a biomarker which can be used as predictor of CT healing with high quality and sensitivity. In this study, we observed a lower CFD expression level in healing tendon when compared with the healthy contralateral side, and we also detected lower CFD expression among good compared to poor outcome patients. Predominantly synthesized and released into the bloodstream by adipocytes, macrophages and monocytes, CFD is considered to initiate body inflammation [201]. A previous study also reported that a lower CFD levels can increase TIMP1 production, leading to improved Colla1 synthesis [169]. Based on our stepwise analysis, we highly speculate that the decreased CFD regulates tendon healing by enhancing TIMP1 expression, which inhibits matrix metalloproteinase activity reducing Colla1 degradation and thereby leading to improved Colla1 production and improving healing. Further *in-vitro* investigations of CFD reported that this marker increases dense CT repair by enhancing Colla1 synthesis and cellular migration in the inflammation stage but decrease Colla1 production and cell migration during proliferation stage (as described in **Paper IV**).

Outcomes following human dense CT repair are often variable and suboptimal, resulting in compromised function and development of chronic painful degenerative diseases. In **Paper III**, we characterized the proteomic landscape of dense CT repair following human tendon rupture and its association with long-term patient-reported outcome and investigated the potential mechanisms of these healing-related biomarkers. A novel biomarker, elongation factor-2 (eEF2) was identified as being strongly prognostic of the 1-year clinical outcome. Further bioinformatic and experimental investigation revealed that eEF2 positively regulated autophagy, cell proliferation and migration, as well as reduced cell death and apoptosis, leading to improved dense CT repair and outcomes. These findings presented may lead to the

development of targeted treatments which could enhance the long-term healing outcomes for patients suffering with dense CT injuries that currently yield a poor clinical outcome.

To further gain insights into process of CT repair we utilized a quantitative proteomic and weighted co-expression network analysis of tissues acquired from ATR patients with different outcomes at 1-year postoperatively (**Paper V**). Two modules were detected to be associated with prognosis. The initial analysis identified ITIH4 as a strong biomarker or hub protein positively associated with better healing outcomes. Additional analysis further identified the beneficial role of ITIH4 in inflammation, cell viability, apoptosis, proliferation, wound healing, and production of type I collagen by cultured human fibroblasts. Functionally, the beneficial effects of ITIH4 on collagen I production were found to be mediated by PPAR γ signaling pathways. These findings suggest that ITIH4 plays an important role in prognosis and the processes of connective tissue repair.

Taken together, the findings presented in the thesis would lead to improved prognostic accuracy and development of targeted treatments, thus enhancing long-term healing outcome after dense CT injuries.

7 POINTS OF PERSPECTIVE

How can these biomarkers be benefit to Dense CT repair and clinical outcome?

In this thesis, we identified functional biomarkers in relation with long-term clinical outcome after ATR injury and assessed the mechanisms of these biomarkers in regulating human dense CT repair. Furthermore, the biomarker related processes mediating collagen 1 synthesis were investigated with *in-vitro* experiments. Our findings provide total four novel prognostic biomarkers which could pave the way for new targeted treatments to improve healing outcomes after dense CT injuries.

Are there any potential relationship among FGF, CFD, eEF2 and ITIH4 during Dense CT repair?

Our bioinformatic analysis reported that these biomarkers are sharing some biological processes: 1) CFD and eEF2 share the processes “collagen/ECM binding, regulation of wound healing, immune response, cellular proliferation and response to growth factor”. 2) FGF and CFD share the processes “ECM organization, cellular metabolism and catabolism”. 3) eEF2 and CFD share the processes “cell migration, collagen binding and wound healing response”. Additionally, we also detected a high enriched protein-protein interaction among these biomarkers, together with important intermediary Colla1 and TIMP1 (Figure 26). Although no correlation was identified for CFD in this network, our *in-vitro* investigations presented that CFD can directly regulate Colla1 synthesis during dense CT repair. Furthermore, a previous study reported that CFD can affect the activity of TIMP1 and subsequently regulate Colla1 production [169], strengthen and confirm our finding. Thus, based on our experimental and bioinformatic findings, we strongly suggest that these biomarkers in association with Colla1 and other potential intermediators, regulate dense CT repair.

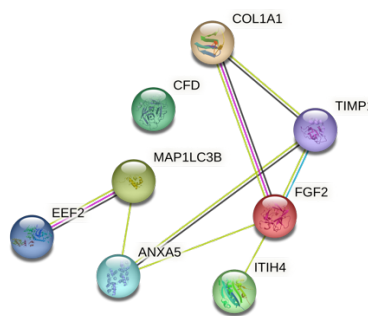


Figure 26. Protein-protein interaction among FGF, CFD, eEF2 and ITIH4.

eEF2 can be phosphorylated, if the eEF2 phosphorylation affect Dense CT repair?

eEF2 kinase can modulate the activity of phosphorylated-eEF2 (p-eEF2) [220], resulting in phosphorylating total eEF2 to p-eEF2. Our western blotting analysis investigated the ratio

of p-eEF2/total eEF2, presenting no statistical significance among good and poor outcome subgroups.

Are there any gender-specific differences for these biomarkers in regulating Dense CT repair?

Gender is a common impact factor during dense CT healing. After combining our MS data with validated clinical database, we found no gender-difference on these biomarkers' expressions. Moreover, we identified the association between these biomarkers and Col1a1 in patient samples, resulting in no gender-specific difference either. Gender difference on protein expression was identified on diseases such as chronic intermittent hypoxia (CIH) [234] and osteopenia [235]. However, we didn't observe any gender-specific effects in dense CT repair for FGF, eEF2, CFD and ITIH4. However, further studies are needed to explore whether these biomarkers present gender difference during dense CT healing.

8 ACKNOWLEDGEMENTS

It is my great fortune to complete my doctoral education at the **Department of Molecular Medicine and Surgery (MMK) in Karolinska Institutet**, a world-renowned research platform with abundant resources.

My main supervisor **Paul W. Ackermann** who has given me the opportunity to complete my PhD studies in his research group. The present thesis could not have been possible without your support and guidance. Time flies and it seems like yesterday when I arrived at Karolinska Institutet. You made these 4-years interesting with your passion, kindness and energy for scientific research. I have truly admired your passion and enthusiasm for science and your broad knowledge which you have always shared with me in our meeting. Thank you for your belief in me and giving me the freedom to work on my projects, which has given me lots of experience and an insight in orthopaedic research.

I need to say a lot of thanks to my co-supervisor **Aisha S. Ahmed** who has facilitated ways so that I could learn and improve during the 4 years' study. Thank you for always willing to help and discuss in science. Although my PhD study did not lack difficulties and confusion, you have always made me feel that you are standing with me and we can find the correct solution for all the issues. I could still remember what you said and what you did to make me calm down when I was feeling stressful. Thank you again for all the time you spent with me working in lab, scientific learning, and personal life. We are supervisor and student in the lab, and also good friends in the daily life. I would like to say, I cannot have had a better supervisor than you.

I would like to say thank you to my dissertation committee: **Ola Nilsson, Tomas Movin and Thorpe Chavaunne**, as well as my opponent **Gustav Andersson** for taking the time to review my work and contribute to an interesting discussion on the outcomes of my project. Thank you to **Ola Nilsson** for hosting the dissertation as a chairperson.

I want to say thank you to **Ann-Britt Wikström, Marietta Vaseghi and Catharina Lavebratt** in the department of MMK. Thank you for all the kindness and help during my PhD study.

I would like to acknowledge and thank for **Shuijie Li and Shaobo Jin** in Karolinska. You have participated in my PhD study and are always willing to give me your guidance in scientific research. It's hard to say in a single word how much I appreciate your help and kindness. Also, thanks to **Jianzhong Wang**, my supervisor during my master studies. You taught me a lot, not only in scientific thinking but also how to be a good clinician and researcher.

I would like to thank all the collaborators and co-authors I have had the pleasure to work with, **Joel Svensson, Carl-Johan Sundberg, Jin Wang, Xinjie Wu, Nils Simon, Camila I Svensson and Juan Yuan**. Special thanks to **David A Hart**, I am truly grateful for your

feedback to improve the quality of my scientific work and all the time and efforts to correct my manuscripts and thesis.

I would like to thank **Luigi Belcastro** for his contribution in collecting the human samples, **Akos Vegvari** for his kindness and help in MS data analysis and **Cecilia Aulin** for her help and support in lab work. All the best for your further scientific and clinical career, also wish you a good daily life.

I would express a lot of thanks to all the current and former co-workers in Paul's group: **Simon Svedman**, for introducing me about the clinical database and patient outcome assessment when I just started my project. **Robin Juthberg**, for helping me to check the patient database. **Annikka Sarrensilta & Johanna Flodin**, for introducing me to sample collection and detail information, also for all the help with my scientific writing during these years, wish you a happy career in the future.

I also want to thank all present and past CMM floor 3 colleagues: **Xinjie Wu, Nils, Harald, Zerina, Kata, Resti, Emerson, Alex, Alexandra, Nilesh, Joana, Francisca, Zhenggang, Azar, Huda, Vinko** and **Yuki**, for all the help in lab work and all the happiness you give me.

I would like to thank all the **PIs** at floor 3 CMM, for creating such a great environment for scientific research.

To all my current or previous friends at CMM, **Yueshan Fan, Qizhang Wang, Letian Zhang, Yunbin Shen, Xiaowei Bian, Long Jiang, Xinxin Luo, Guanglin Niu, Heshuang Qu, Jinming Han** and **Rebecka Heinbäck**. I appreciate our every conversation about life, culture and science.

Many thanks to my friends inside and outside Karolinska Institutet: **Yang Yu, Sailan Wang, Ying Wang, Yang Gao, Jielu Liu, Dan Wu, Yuyang Zhang, Yuanyuan You, Bowen Tang, Shengduo Pei, Zhiming Liu, Yunhan Zhao, Wenchao Shao, Richeng Jiang, Yang Cong, Sike Wan** and **Jinchan Xu**. It is great to share time with you. I will never forget all the happiness we spent during this journey.

To my **parents** and **grandparents**: Thank you so much for your support, your trust and love. I cannot finish my PhD without you.

To my lovely girlfriend, **Yi Zhang**. Thank you for your love and support all the way. I am the luckiest man who owns your love and solicitude every single day and night since 2014.11.07.

9 REFERENCES

1. El-Tallawy, S.N., et al., *Management of Musculoskeletal Pain: An Update with Emphasis on Chronic Musculoskeletal Pain*. Pain Ther, 2021. **10**(1): p. 181-209.
2. Richardson, J., *The connective tissue*. Br Med J, 1961. **1**(5234): p. 1187-90.
3. Lee, N.M., et al., *Polymer fiber-based models of connective tissue repair and healing*. Biomaterials, 2017. **112**: p. 303-312.
4. O'Brien, M., *The anatomy of the Achilles tendon*. Foot Ankle Clin, 2005. **10**(2): p. 225-38.
5. Maffulli, N., *Rupture of the Achilles tendon*. J Bone Joint Surg Am, 1999. **81**(7): p. 1019-36.
6. Hernandez-Diaz, C., et al., *Clinical anatomy of the ankle and foot*. Reumatol Clin, 2012. **8 Suppl 2**: p. 46-52.
7. Maffulli, N. and D. Kader, *Tendinopathy of tendo achillis*. J Bone Joint Surg Br, 2002. **84**(1): p. 1-8.
8. Reinherz, R.P., S.J. Zawada, and D.P. Sheldon, *Recognizing unusual tendon pathology at the ankle*. J Foot Surg, 1986. **25**(4): p. 278-83.
9. Cramer, A., et al., *Estimation of Patient Acceptable Symptom State (PASS) and Treatment Failure (TF) Threshold Values for the Achilles Tendon Total Rupture Score (ATRS) at 6 Months, 1 Year, and 2 Years After Acute Achilles Tendon Rupture*. J Foot Ankle Surg, 2022. **61**(3): p. 503-507.
10. Svedman, S., et al., *Longer duration of operative time enhances healing metabolites and improves patient outcome after Achilles tendon rupture surgery*. Knee Surg Sports Traumatol Arthrosc, 2018. **26**(7): p. 2011-2020.
11. Andarawis-Puri, N., E.L. Flatow, and L.J. Soslowsky, *Tendon basic science: Development, repair, regeneration, and healing*. J Orthop Res, 2015. **33**(6): p. 780-4.
12. Langevin, H.M., *Connective tissue: a body-wide signaling network? Med Hypotheses*, 2006. **66**(6): p. 1074-7.
13. Lin, T.W., L. Cardenas, and L.J. Soslowsky, *Biomechanics of tendon injury and repair*. J Biomech, 2004. **37**(6): p. 865-77.
14. Thorpe, C.T., et al., *The role of the non-collagenous matrix in tendon function*. Int J Exp Pathol, 2013. **94**(4): p. 248-59.
15. Barnard, K., et al., *Chemistry of the collagen cross-links. Origin and partial characterization of a putative mature cross-link of collagen*. Biochem J, 1987. **244**(2): p. 303-9.
16. Kjaer, M., *Role of extracellular matrix in adaptation of tendon and skeletal muscle to mechanical loading*. Physiol Rev, 2004. **84**(2): p. 649-98.
17. Riley, G.P., et al., *Tendon degeneration and chronic shoulder pain: changes in the collagen composition of the human rotator cuff tendons in rotator cuff tendinitis*. Ann Rheum Dis, 1994. **53**(6): p. 359-66.
18. Kjaer, M., et al., *From mechanical loading to collagen synthesis, structural changes and function in human tendon*. Scand J Med Sci Sports, 2009. **19**(4): p. 500-10.

19. Birch, H.L., *Tendon matrix composition and turnover in relation to functional requirements*. Int J Exp Pathol, 2007. **88**(4): p. 241-8.
20. Thorpe, C.T., P.D. Clegg, and H.L. Birch, *A review of tendon injury: why is the equine superficial digital flexor tendon most at risk?* Equine Vet J, 2010. **42**(2): p. 174-80.
21. Chowdhury, P., J.R. Matyas, and C.B. Frank, *The "epiligament" of the rabbit medial collateral ligament: a quantitative morphological study*. Connect Tissue Res, 1991. **27**(1): p. 33-50.
22. *Multiscale computer modeling in biomechanics and biomedical engineering*. 2013, New York: Springer.
23. Bordoni, B., N. Mahabadi, and M. Varacallo, *Anatomy, Fascia*, in *StatPearls*. 2022: Treasure Island (FL).
24. Qu, F., et al., *Repair of dense connective tissues via biomaterial-mediated matrix reprogramming of the wound interface*. Biomaterials, 2015. **39**: p. 85-94.
25. Pierer, M., et al., *Chemokine secretion of rheumatoid arthritis synovial fibroblasts stimulated by Toll-like receptor 2 ligands*. J Immunol, 2004. **172**(2): p. 1256-65.
26. Krafts, K.P., *Tissue repair: The hidden drama*. Organogenesis, 2010. **6**(4): p. 225-33.
27. Kireeva, M.L., et al., *Cyr61, a product of a growth factor-inducible immediate-early gene, promotes cell proliferation, migration, and adhesion*. Mol Cell Biol, 1996. **16**(4): p. 1326-34.
28. Ignatz, R.A. and J. Massague, *Transforming growth factor-beta stimulates the expression of fibronectin and collagen and their incorporation into the extracellular matrix*. J Biol Chem, 1986. **261**(9): p. 4337-45.
29. Nguyen, Q.T., et al., *Therapeutic Effects of Doxycycline on the Quality of Repaired and Unrepaired Achilles Tendons*. Am J Sports Med, 2017. **45**(12): p. 2872-2881.
30. Chen, J., et al., *Complement factor D as a predictor of Achilles tendon healing and long-term patient outcomes*. FASEB J, 2022. **36**(6): p. e22365.
31. Abdul Alim, M., et al., *Achilles tendon rupture healing is enhanced by intermittent pneumatic compression upregulating collagen type I synthesis*. Knee Surg Sports Traumatol Arthrosc, 2018. **26**(7): p. 2021-2029.
32. Baranzini, N., et al., *HvRNASET2 Regulate Connective Tissue and Collagen I Remodeling During Wound Healing Process*. Front Physiol, 2021. **12**: p. 632506.
33. Chen, J., et al., *FGF gene expression in injured tendons as a prognostic biomarker of 1-year patient outcome after Achilles tendon repair*. J Exp Orthop, 2021. **8**(1): p. 20.
34. Doral, M.N., et al., *Functional anatomy of the Achilles tendon*. Knee Surgery Sports Traumatology Arthroscopy, 2010. **18**(5): p. 638-643.
35. Winnicki, K., et al., *Functional anatomy, histology and biomechanics of the human Achilles tendon - A comprehensive review*. Annals of Anatomy-Anatomischer Anzeiger, 2020. **229**.
36. Carr, A.J. and S.H. Norris, *The blood supply of the calcaneal tendon*. J Bone Joint Surg Br, 1989. **71**(1): p. 100-1.

37. Gilbert, P.J., et al., *Macroscopic and microvascular blood supply of the canine common calcaneal tendon*. Vet Comp Orthop Traumatol, 2010. **23**(2): p. 81-6.
38. Xu, X., et al., *Age-related Impairment of Vascular Structure and Functions*. Aging Dis, 2017. **8**(5): p. 590-610.
39. Schweitzer, M.E. and D. Karasick, *MR imaging of disorders of the Achilles tendon*. AJR Am J Roentgenol, 2000. **175**(3): p. 613-25.
40. Hartgerink, P., et al., *Full- versus partial-thickness Achilles tendon tears: sonographic accuracy and characterization in 26 cases with surgical correlation*. Radiology, 2001. **220**(2): p. 406-12.
41. Weinfeld, S.B., *Achilles tendon disorders*. Med Clin North Am, 2014. **98**(2): p. 331-8.
42. Huttunen, T.T., et al., *Acute achilles tendon ruptures: incidence of injury and surgery in Sweden between 2001 and 2012*. Am J Sports Med, 2014. **42**(10): p. 2419-23.
43. Lopez, R.G. and H.G. Jung, *Achilles tendinosis: treatment options*. Clin Orthop Surg, 2015. **7**(1): p. 1-7.
44. Leadbetter, W.B., *Cell-matrix response in tendon injury*. Clin Sports Med, 1992. **11**(3): p. 533-78.
45. Park, Y.H., et al., *Achilles tendinosis does not always precede Achilles tendon rupture*. Knee Surg Sports Traumatol Arthrosc, 2019. **27**(10): p. 3297-3303.
46. Kannus, P. and L. Jozsa, *Histopathological changes preceding spontaneous rupture of a tendon. A controlled study of 891 patients*. J Bone Joint Surg Am, 1991. **73**(10): p. 1507-25.
47. Kvist, M., *Achilles tendon injuries in athletes*. Sports Med, 1994. **18**(3): p. 173-201.
48. Litjens, S.H.M., J.M. de Pereda, and A. Sonnenberg, *Current insights into the formation and breakdown of hemidesmosomes*. Trends in Cell Biology, 2006. **16**(7): p. 376-383.
49. Lantto, I., et al., *Epidemiology of Achilles tendon ruptures: increasing incidence over a 33-year period*. Scand J Med Sci Sports, 2015. **25**(1): p. e133-8.
50. Lemme, N.J., et al., *Epidemiology of Achilles Tendon Ruptures in the United States: Athletic and Nonathletic Injuries From 2012 to 2016*. Orthop J Sports Med, 2018. **6**(11): p. 2325967118808238.
51. Moller, A., M. Astron, and N. Westlin, *Increasing incidence of Achilles tendon rupture*. Acta Orthop Scand, 1996. **67**(5): p. 479-81.
52. Raikin, S.M., D.N. Garras, and P.V. Krapchev, *Achilles tendon injuries in a United States population*. Foot Ankle Int, 2013. **34**(4): p. 475-80.
53. Leppilahti, J., J. Puranen, and S. Orava, *Incidence of Achilles tendon rupture*. Acta Orthop Scand, 1996. **67**(3): p. 277-9.
54. Maffulli, N., P. Sharma, and K.L. Luscombe, *Achilles tendinopathy: aetiology and management*. J R Soc Med, 2004. **97**(10): p. 472-6.
55. Khan, R.J., et al., *Treatment of acute achilles tendon ruptures. A meta-analysis of randomized, controlled trials*. J Bone Joint Surg Am, 2005. **87**(10): p. 2202-10.

56. Willits, K., et al., *Operative versus nonoperative treatment of acute Achilles tendon ruptures: a multicenter randomized trial using accelerated functional rehabilitation*. J Bone Joint Surg Am, 2010. **92**(17): p. 2767-75.
57. Nilsson-Helander, K., et al., *Acute Achilles Tendon Rupture A Randomized, Controlled Study Comparing Surgical and Nonsurgical Treatments Using Validated Outcome Measures*. American Journal of Sports Medicine, 2010. **38**(11): p. 2186-2193.
58. Eliasson, P., T. Andersson, and P. Aspenberg, *Achilles tendon healing in rats is improved by intermittent mechanical loading during the inflammatory phase*. Journal of Orthopaedic Research, 2012. **30**(2): p. 274-279.
59. Hammerman, M., P. Aspenberg, and P. Eliasson, *Microtrauma stimulates rat Achilles tendon healing via an early gene expression pattern similar to mechanical loading*. J Appl Physiol (1985), 2014. **116**(1): p. 54-60.
60. Schepull, T. and P. Aspenberg, *Early controlled tension improves the material properties of healing human achilles tendons after ruptures: a randomized trial*. Am J Sports Med, 2013. **41**(11): p. 2550-7.
61. Young, S.W., et al., *Weight-Bearing in the Nonoperative Treatment of Acute Achilles Tendon Ruptures: A Randomized Controlled Trial*. J Bone Joint Surg Am, 2014. **96**(13): p. 1073-1079.
62. Hsu, A.R., et al., *Clinical Outcomes and Complications of Percutaneous Achilles Repair System Versus Open Technique for Acute Achilles Tendon Ruptures*. Foot Ankle Int, 2015. **36**(11): p. 1279-86.
63. Taylor, G.I. and J.H. Palmer, *'Angiosome theory'*. Br J Plast Surg, 1992. **45**(4): p. 327-8.
64. Ma, G.W. and T.G. Griffith, *Percutaneous repair of acute closed ruptured achilles tendon: a new technique*. Clin Orthop Relat Res, 1977(128): p. 247-55.
65. Lim, J., R. Dalal, and M. Waseem, *Percutaneous vs. open repair of the ruptured Achilles tendon--a prospective randomized controlled study*. Foot Ankle Int, 2001. **22**(7): p. 559-68.
66. Karabinas, P.K., et al., *Percutaneous versus open repair of acute Achilles tendon ruptures*. Eur J Orthop Surg Traumatol, 2014. **24**(4): p. 607-13.
67. Kakiuchi, M., *A combined open and percutaneous technique for repair of tendo Achillis. Comparison with open repair*. J Bone Joint Surg Br, 1995. **77**(1): p. 60-3.
68. Hsu, A.R., et al., *Clinical Outcomes and Complications of Percutaneous Achilles Repair System Versus Open Technique for Acute Achilles Tendon Ruptures*. Foot & Ankle International, 2015. **36**(11): p. 1279-1286.
69. Huang, J., et al., *Rehabilitation regimen after surgical treatment of acute Achilles tendon ruptures: a systematic review with meta-analysis*. Am J Sports Med, 2015. **43**(4): p. 1008-16.
70. Pajala, A., et al., *Augmented compared with nonaugmented surgical repair of a fresh total Achilles tendon rupture. A prospective randomized study*. J Bone Joint Surg Am, 2009. **91**(5): p. 1092-100.

71. Schepull, T., et al., *Autologous Platelets Have No Effect on the Healing of Human Achilles Tendon Ruptures A Randomized Single-Blind Study*. American Journal of Sports Medicine, 2011. **39**(1): p. 38-47.
72. Sanchez, M., et al., *Comparison of surgically repaired achilles tendon tears using platelet-rich fibrin matrices*. American Journal of Sports Medicine, 2007. **35**(2): p. 245-251.
73. Okamoto, N., et al., *Treating Achilles tendon rupture in rats with bone-marrow-cell transplantation therapy*. J Bone Joint Surg Am, 2010. **92**(17): p. 2776-84.
74. Adams, S.B., Jr., et al., *Stem cell-bearing suture improves Achilles tendon healing in a rat model*. Foot Ankle Int, 2014. **35**(3): p. 293-9.
75. Martin, P., *Wound healing--aiming for perfect skin regeneration*. Science, 1997. **276**(5309): p. 75-81.
76. Wang, Y., et al., *Exosomes from tendon stem cells promote injury tendon healing through balancing synthesis and degradation of the tendon extracellular matrix*. J Cell Mol Med, 2019. **23**(8): p. 5475-5485.
77. Millar, N.L., et al., *MicroRNA29a regulates IL-33-mediated tissue remodelling in tendon disease*. Nat Commun, 2015. **6**: p. 6774.
78. Molloy, T., Y. Wang, and G. Murrell, *The roles of growth factors in tendon and ligament healing*. Sports Med, 2003. **33**(5): p. 381-94.
79. Juneja, S.C., et al., *Cellular and molecular factors in flexor tendon repair and adhesions: a histological and gene expression analysis*. Connect Tissue Res, 2013. **54**(3): p. 218-26.
80. Killian, M.L., et al., *The role of mechanobiology in tendon healing*. J Shoulder Elbow Surg, 2012. **21**(2): p. 228-37.
81. Hillin, C.D., et al., *Effects of immobilization angle on tendon healing after achilles rupture in a rat model*. J Orthop Res, 2019. **37**(3): p. 562-573.
82. Alim, M.A., et al., *Achilles tendon rupture healing is enhanced by intermittent pneumatic compression upregulating collagen type I synthesis*. Knee Surgery Sports Traumatology Arthroscopy, 2018. **26**(7): p. 2021-2029.
83. Keating, J.F. and E.M. Will, *Operative versus non-operative treatment of acute rupture of tendo Achillis: a prospective randomised evaluation of functional outcome*. J Bone Joint Surg Br, 2011. **93**(8): p. 1071-8.
84. Spennacchio, P., et al., *Outcome evaluation after Achilles tendon ruptures. A review of the literature*. Joints, 2016. **4**(1): p. 52-61.
85. Deshpande, P.R., et al., *Patient-reported outcomes: A new era in clinical research*. Perspect Clin Res, 2011. **2**(4): p. 137-44.
86. Kaya Mutlu, E., et al., *The Turkish version of the Achilles tendon Total Rupture Score: cross-cultural adaptation, reliability and validity*. Knee Surg Sports Traumatol Arthrosc, 2015. **23**(8): p. 2427-2432.
87. Dams, O.C., et al., *The Achilles tendon Total Rupture Score is a responsive primary outcome measure: an evaluation of the Dutch version including minimally important change*. Knee Surgery Sports Traumatology Arthroscopy, 2020. **28**(10): p. 3330-3338.

88. Buckinx, F., et al., *French translation and validation of the Achilles Tendon Total Rupture Score "ATRS"*. *Foot Ankle Surg*, 2020. **26**(6): p. 662-668.
89. Leppilahti, J., et al., *Outcome and prognostic factors of Achilles rupture repair using a new scoring method*. *Clinical Orthopaedics and Related Research*, 1998(346): p. 152-161.
90. Carmont, M.R., et al., *Cross cultural adaptation of the Achilles tendon Total Rupture Score with reliability, validity and responsiveness evaluation*. *Knee Surg Sports Traumatol Arthrosc*, 2013. **21**(6): p. 1356-60.
91. Martin, R.L., et al., *Evidence of validity for the Foot and Ankle Ability Measure (FAAM)*. *Foot Ankle Int*, 2005. **26**(11): p. 968-83.
92. Schepull, T., J. Kvist, and P. Aspenberg, *Early E-modulus of healing Achilles tendons correlates with late function: Similar results with or without surgery*. *Scandinavian Journal of Medicine & Science in Sports*, 2012. **22**(1): p. 18-23.
93. Moller, M., et al., *Calf muscle function after Achilles tendon rupture - A prospective, randomised study comparing surgical and non-surgical treatment*. *Scandinavian Journal of Medicine & Science in Sports*, 2002. **12**(1): p. 9-16.
94. Alfredson, H., et al., *Achilles tendinosis and calf muscle strength - The effect of short-term immobilization after surgical treatment*. *American Journal of Sports Medicine*, 1998. **26**(2): p. 166-171.
95. Olsson, N., et al., *Ability to perform a single heel-rise is significantly related to patient-reported outcome after Achilles tendon rupture*. *Scandinavian Journal of Medicine & Science in Sports*, 2014. **24**(1): p. 152-158.
96. Selvik, G., *Roentgen stereophotogrammetric analysis*. *Acta Radiol*, 1990. **31**(2): p. 113-26.
97. Rosso, C., et al., *Long-term biomechanical outcomes after Achilles tendon ruptures*. *Knee Surg Sports Traumatol Arthrosc*, 2015. **23**(3): p. 890-8.
98. Frankewycz, B., et al., *Rehabilitation of Achilles tendon ruptures: is early functional rehabilitation daily routine?* *Arch Orthop Trauma Surg*, 2017. **137**(3): p. 333-340.
99. Saleh, M., et al., *The Sheffield splint for controlled early mobilisation after rupture of the calcaneal tendon. A prospective, randomised comparison with plaster treatment*. *J Bone Joint Surg Br*, 1992. **74**(2): p. 206-9.
100. Olsson, N., et al., *Stable surgical repair with accelerated rehabilitation versus nonsurgical treatment for acute Achilles tendon ruptures: a randomized controlled study*. *Am J Sports Med*, 2013. **41**(12): p. 2867-76.
101. Soroceanu, A., et al., *Surgical versus nonsurgical treatment of acute Achilles tendon rupture: a meta-analysis of randomized trials*. *J Bone Joint Surg Am*, 2012. **94**(23): p. 2136-43.
102. Willits, K., et al., *Operative versus Nonoperative Treatment of Acute Achilles Tendon Ruptures A Multicenter Randomized Trial Using Accelerated Functional Rehabilitation*. *Journal of Bone and Joint Surgery-American Volume*, 2010. **92a**(17): p. 2767-2775.
103. Wallace, R.G., G.J. Heyes, and A.L. Michael, *The non-operative functional management of patients with a rupture of the tendo Achillis leads to low rates of re-rupture*. *J Bone Joint Surg Br*, 2011. **93**(10): p. 1362-6.

104. Metz, R., et al., *Acute Achilles tendon rupture: minimally invasive surgery versus nonoperative treatment with immediate full weightbearing--a randomized controlled trial*. Am J Sports Med, 2008. **36**(9): p. 1688-94.
105. Lansdown, D.A., et al., *Preoperative IDEAL (Iterative Decomposition of Echoes of Asymmetrical Length) magnetic resonance imaging rotator cuff muscle fat fractions are associated with rotator cuff repair outcomes*. J Shoulder Elbow Surg, 2019. **28**(10): p. 1936-1941.
106. Shi, B.Y., et al., *Biomechanical Strength of Rotator Cuff Repairs: A Systematic Review and Meta-regression Analysis of Cadaveric Studies*. Am J Sports Med, 2019. **47**(8): p. 1984-1993.
107. Haviv, B., et al., *Which patients are less likely to improve after arthroscopic rotator cuff repair?* Acta Orthopaedica Et Traumatologica Turcica, 2019. **53**(5): p. 356-359.
108. Carmont, M.R., et al., *Age and Tightness of Repair Are Predictors of Heel-Rise Height After Achilles Tendon Rupture*. Orthop J Sports Med, 2020. **8**(3): p. 2325967120909556.
109. Claessen, F.M.A.P., et al., *Predictors of Primary Achilles Tendon Ruptures*. Sports Medicine, 2014. **44**(9): p. 1241-1259.
110. Aujla, R., et al., *Predictors of functional outcome in non-operatively managed Achilles tendon ruptures*. Foot and Ankle Surgery, 2018. **24**(4): p. 336-341.
111. Arverud, E.D., et al., *Ageing, deep vein thrombosis and male gender predict poor outcome after acute Achilles tendon rupture*. Bone Joint J, 2016. **98-B**(12): p. 1635-1641.
112. Ackermann, P.W., et al., *Anti-inflammatory cytokine profile in early human tendon repair*. Knee Surg Sports Traumatol Arthrosc, 2013. **21**(8): p. 1801-6.
113. Alim, M.A., et al., *Procollagen markers in microdialysate can predict patient outcome after Achilles tendon rupture*. BMJ Open Sport Exerc Med, 2016. **2**(1): p. e000114.
114. Watt, F.M. and H. Fujiwara, *Cell-extracellular matrix interactions in normal and diseased skin*. Cold Spring Harb Perspect Biol, 2011. **3**(4).
115. Tomasek, J.J., et al., *Myofibroblasts and mechano-regulation of connective tissue remodelling*. Nat Rev Mol Cell Biol, 2002. **3**(5): p. 349-63.
116. Kalluri, R. and M. Zeisberg, *Fibroblasts in cancer*. Nature Reviews Cancer, 2006. **6**(5): p. 392-401.
117. Driskell, R.R. and F.M. Watt, *Understanding fibroblast heterogeneity in the skin*. Trends Cell Biol, 2015. **25**(2): p. 92-9.
118. Bhowmick, N.A., E.G. Neilson, and H.L. Moses, *Stromal fibroblasts in cancer initiation and progression*. Nature, 2004. **432**(7015): p. 332-7.
119. Bhowmick, N.A., et al., *TGF-beta signaling in fibroblasts modulates the oncogenic potential of adjacent epithelia*. Science, 2004. **303**(5659): p. 848-51.
120. Darby, I.A. and T.D. Hewitson, *Fibroblast differentiation in wound healing and fibrosis*. Int Rev Cytol, 2007. **257**: p. 143-79.

121. Sriram, G., P.L. Bigliardi, and M. Bigliardi-Qi, *Fibroblast heterogeneity and its implications for engineering organotypic skin models in vitro*. Eur J Cell Biol, 2015. **94**(11): p. 483-512.
122. Houzelstein, D., et al., *The expression of the homeobox gene Msx1 reveals two populations of dermal progenitor cells originating from the somites*. Development, 2000. **127**(10): p. 2155-64.
123. Castor, C.W., R.K. Prince, and E.L. Dorstewitz, *Characteristics of human "fibroblasts" cultivated in vitro from different anatomical sites*. Lab Invest, 1962. **11**: p. 703-13.
124. Lynch, M.D. and F.M. Watt, *Fibroblast heterogeneity: implications for human disease*. J Clin Invest, 2018. **128**(1): p. 26-35.
125. Davidson, E.H. and D.H. Erwin, *Gene regulatory networks and the evolution of animal body plans*. Science, 2006. **311**(5762): p. 796-800.
126. Lesko, M.H., et al., *Sox2 modulates the function of two distinct cell lineages in mouse skin*. Dev Biol, 2013. **382**(1): p. 15-26.
127. James, K., et al., *Sox18 mutations in the ragged mouse alleles ragged-like and opossum*. Genesis, 2003. **36**(1): p. 1-6.
128. Maas-Szabowski, N., A. Shimotoyodome, and N.E. Fusenig, *Keratinocyte growth regulation in fibroblast cocultures via a double paracrine mechanism*. J Cell Sci, 1999. **112** (Pt 12): p. 1843-53.
129. Werner, S., T. Krieg, and H. Smola, *Keratinocyte-fibroblast interactions in wound healing*. J Invest Dermatol, 2007. **127**(5): p. 998-1008.
130. Mastrogiannaki, M., et al., *beta-Catenin Stabilization in Skin Fibroblasts Causes Fibrotic Lesions by Preventing Adipocyte Differentiation of the Reticular Dermis*. J Invest Dermatol, 2016. **136**(6): p. 1130-1142.
131. Plikus, M.V., et al., *Regeneration of fat cells from myofibroblasts during wound healing*. Science, 2017. **355**(6326): p. 748-752.
132. Jumper, N., R. Paus, and A. Bayat, *Functional histopathology of keloid disease*. Histol Histopathol, 2015. **30**(9): p. 1033-57.
133. Lee, J.Y., et al., *Histopathological differential diagnosis of keloid and hypertrophic scar*. Am J Dermatopathol, 2004. **26**(5): p. 379-84.
134. Herzlinger, D., *Renal interstitial fibrosis: remembrance of things past?* J Clin Invest, 2002. **110**(3): p. 305-6.
135. Kalluri, R. and E.G. Neilson, *Epithelial-mesenchymal transition and its implications for fibrosis*. J Clin Invest, 2003. **112**(12): p. 1776-84.
136. Zeisberg, M. and R. Kalluri, *The role of epithelial-to-mesenchymal transition in renal fibrosis*. J Mol Med (Berl), 2004. **82**(3): p. 175-81.
137. Zeisberg, M. and E.G. Neilson, *Biomarkers for epithelial-mesenchymal transitions*. J Clin Invest, 2009. **119**(6): p. 1429-37.
138. Lee, C.H., et al., *CTGF directs fibroblast differentiation from human mesenchymal stem/stromal cells and defines connective tissue healing in a rodent injury model*. J Clin Invest, 2010. **120**(9): p. 3340-9.

139. Bi, Y., et al., *Identification of tendon stem/progenitor cells and the role of the extracellular matrix in their niche*. Nat Med, 2007. **13**(10): p. 1219-27.
140. McAnulty, R.J., *Fibroblasts and myofibroblasts: their source, function and role in disease*. Int J Biochem Cell Biol, 2007. **39**(4): p. 666-71.
141. Caplan, A.I., *Mesenchymal stem cells*. J Orthop Res, 1991. **9**(5): p. 641-50.
142. Wlaschek, M., et al., *Connective Tissue and Fibroblast Senescence in Skin Aging*. J Invest Dermatol, 2021. **141**(4S): p. 985-992.
143. Krausgruber, T., et al., *Structural cells are key regulators of organ-specific immune responses*. Nature, 2020. **583**(7815): p. 296-+.
144. Forrest, L., *Current concepts in soft connective tissue wound healing*. Br J Surg, 1983. **70**(3): p. 133-40.
145. Wong, T., J.A. McGrath, and H. Navsaria, *The role of fibroblasts in tissue engineering and regeneration*. Br J Dermatol, 2007. **156**(6): p. 1149-55.
146. Bainbridge, P., *Wound healing and the role of fibroblasts*. J Wound Care, 2013. **22**(8): p. 407-8, 410-12.
147. Tracy, L.E., R.A. Minasian, and E.J. Caterson, *Extracellular Matrix and Dermal Fibroblast Function in the Healing Wound*. Adv Wound Care (New Rochelle), 2016. **5**(3): p. 119-136.
148. Addis, R., et al., *Fibroblast Proliferation and Migration in Wound Healing by Phytochemicals: Evidence for a Novel Synergic Outcome*. Int J Med Sci, 2020. **17**(8): p. 1030-1042.
149. Schultz, G.S., et al., *Dynamic reciprocity in the wound microenvironment*. Wound Repair Regen, 2011. **19**(2): p. 134-48.
150. Desmouliere, A., et al., *Apoptosis Mediates the Decrease in Cellularity during the Transition between Granulation-Tissue and Scar*. American Journal of Pathology, 1995. **146**(1): p. 56-66.
151. Kim, W.J., et al., *Effect of PDGF, IL-1alpha, and BMP2/4 on corneal fibroblast chemotaxis: expression of the platelet-derived growth factor system in the cornea*. Invest Ophthalmol Vis Sci, 1999. **40**(7): p. 1364-72.
152. Li, B. and J.H. Wang, *Fibroblasts and myofibroblasts in wound healing: force generation and measurement*. J Tissue Viability, 2011. **20**(4): p. 108-20.
153. Guido, S. and R.T. Tranquillo, *A Methodology for the Systematic and Quantitative Study of Cell Contact Guidance in Oriented Collagen Gels - Correlation of Fibroblast Orientation and Gel Birefringence*. Journal of Cell Science, 1993. **105**: p. 317-331.
154. Wojciak-Stothard, B., et al., *Adhesion, orientation, and movement of cells cultured on ultrathin fibronectin fibers*. In Vitro Cell Dev Biol Anim, 1997. **33**(2): p. 110-7.
155. Sen, C.K., et al., *Human skin wounds: a major and snowballing threat to public health and the economy*. Wound Repair Regen, 2009. **17**(6): p. 763-71.
156. Brem, H. and M. Tomic-Canic, *Cellular and molecular basis of wound healing in diabetes*. J Clin Invest, 2007. **117**(5): p. 1219-22.

157. Shah, J.M., et al., *Cellular events and biomarkers of wound healing*. Indian J Plast Surg, 2012. **45**(2): p. 220-8.
158. Martinez-Zapata, M.J., et al., *Autologous platelet-rich plasma for treating chronic wounds*. Cochrane Database Syst Rev, 2012. **10**: p. CD006899.
159. Deppermann, C., et al., *Gray platelet syndrome and defective thrombo-inflammation in Nbeal2-deficient mice*. J Clin Invest, 2013.
160. Sindrilaru, A., et al., *An unrestrained proinflammatory M1 macrophage population induced by iron impairs wound healing in humans and mice*. J Clin Invest, 2011. **121**(3): p. 985-97.
161. Loots, M.A., et al., *Differences in cellular infiltrate and extracellular matrix of chronic diabetic and venous ulcers versus acute wounds*. J Invest Dermatol, 1998. **111**(5): p. 850-7.
162. Beidler, S.K., et al., *Inflammatory cytokine levels in chronic venous insufficiency ulcer tissue before and after compression therapy*. Journal of Vascular Surgery, 2009. **49**(4): p. 1013-1020.
163. Barrientos, S., et al., *Growth factors and cytokines in wound healing*. Wound Repair Regen, 2008. **16**(5): p. 585-601.
164. Diegelmann, R.F. and M.C. Evans, *Wound healing: an overview of acute, fibrotic and delayed healing*. Front Biosci, 2004. **9**: p. 283-9.
165. Landen, N.X., D. Li, and M. Stahle, *Transition from inflammation to proliferation: a critical step during wound healing*. Cell Mol Life Sci, 2016. **73**(20): p. 3861-85.
166. Saxena, S., et al., *Connective tissue fibroblasts from highly regenerative mammals are refractory to ROS-induced cellular senescence*. Nat Commun, 2019. **10**(1): p. 4400.
167. Duncan, M.R., et al., *Connective tissue growth factor mediates transforming growth factor beta-induced collagen synthesis: down-regulation by cAMP*. FASEB J, 1999. **13**(13): p. 1774-86.
168. Montesinos, M.C., et al., *Adenosine promotes wound healing and mediates angiogenesis in response to tissue injury via occupancy of A(2A) receptors*. Am J Pathol, 2002. **160**(6): p. 2009-18.
169. Ezure, T., M. Sugahara, and S. Amano, *Senescent dermal fibroblasts negatively influence fibroblast extracellular matrix-related gene expression partly via secretion of complement factor D*. Biofactors, 2019. **45**(4): p. 556-562.
170. Aufwerber, S., et al., *Does Early Functional Mobilization Affect Long-Term Outcomes After an Achilles Tendon Rupture? A Randomized Clinical Trial*. Orthopaedic Journal of Sports Medicine, 2020. **8**(3).
171. Domeij-Arverud, E., et al., *Intermittent pneumatic compression reduces the risk of deep vein thrombosis during post-operative lower limb immobilisation: a prospective randomised trial of acute ruptures of the Achilles tendon*. Bone Joint J, 2015. **97-B**(5): p. 675-80.
172. Svedman, S., et al., *Reduced Time to Surgery Improves Patient-Reported Outcome After Achilles Tendon Rupture*. Am J Sports Med, 2018. **46**(12): p. 2929-2934.

173. Bostick, G.P., et al., *Factors associated with calf muscle endurance recovery 1 year after achilles tendon rupture repair*. J Orthop Sports Phys Ther, 2010. **40**(6): p. 345-51.
174. Olsson, N., et al., *Predictors of Clinical Outcome After Acute Achilles Tendon Ruptures*. Am J Sports Med, 2014. **42**(6): p. 1448-55.
175. Greve, K., et al., *Metabolic activity in early tendon repair can be enhanced by intermittent pneumatic compression*. Scandinavian Journal of Medicine & Science in Sports, 2012. **22**(4): p. E55-E63.
176. Norrbom, J., et al., *PGC-1 alpha mRNA expression is influenced by metabolic perturbation in exercising human skeletal muscle*. Journal of Applied Physiology, 2004. **96**(1): p. 189-194.
177. Kong, A.T., et al., *MSFragger: ultrafast and comprehensive peptide identification in mass spectrometry-based proteomics*. Nat Methods, 2017. **14**(5): p. 513-520.
178. Schwanhausser, B., et al., *Global quantification of mammalian gene expression control*. Nature, 2011. **473**(7347): p. 337-42.
179. Wang, C., et al., *LTF, PRTN3, and MNDA in Synovial Fluid as Promising Biomarkers for Periprosthetic Joint Infection Identification by Quadrupole Orbital-Trap Mass Spectrometry*. Journal of Bone and Joint Surgery-American Volume, 2019. **101**(24): p. 2226-2234.
180. Heberle, H., et al., *InteractiVenn: a web-based tool for the analysis of sets through Venn diagrams*. BMC Bioinformatics, 2015. **16**.
181. Chu, J., et al., *Rebuilding Tendons: A Concise Review on the Potential of Dermal Fibroblasts*. Cells, 2020. **9**(9).
182. Lee, J.M., et al., *Mitochondrial Transplantation Modulates Inflammation and Apoptosis, Alleviating Tendinopathy Both In Vivo and In Vitro*. Antioxidants (Basel), 2021. **10**(5).
183. Subramanian, A., et al., *Gene set enrichment analysis: a knowledge-based approach for interpreting genome-wide expression profiles*. Proc Natl Acad Sci U S A, 2005. **102**(43): p. 15545-50.
184. Liberzon, A., et al., *Molecular signatures database (MSigDB) 3.0*. Bioinformatics, 2011. **27**(12): p. 1739-40.
185. Kamarudin, A.N., T. Cox, and R. Kolamunnage-Dona, *Time-dependent ROC curve analysis in medical research: current methods and applications*. BMC Med Res Methodol, 2017. **17**(1): p. 53.
186. Alosaimy, S., et al., *Vancomycin Area Under the Curve to Predict Timely Clinical Response in the Treatment of Methicillin-resistant Staphylococcus aureus Complicated Skin and Soft Tissue Infections*. Clin Infect Dis, 2021. **73**(11): p. e4560-e4567.
187. Cai, X.R., et al., *Modified CLIP score with the albumin-bilirubin grade retains prognostic value in HBV-related hepatocellular carcinoma patients treated with trans-catheter arterial chemoembolization therapy*. J Cancer, 2018. **9**(13): p. 2380-2388.
188. Mandrekar, J.N., *Receiver operating characteristic curve in diagnostic test assessment*. J Thorac Oncol, 2010. **5**(9): p. 1315-6.

189. Gotoh, M., et al., *Increased matrix metalloprotease-3 gene expression in ruptured rotator cuff tendons is associated with postoperative tendon retear*. *Knee Surgery Sports Traumatology Arthroscopy*, 2013. **21**(8): p. 1807-1812.
190. Ireland, D., et al., *Multiple changes in gene expression in chronic human Achilles tendinopathy*. *Matrix Biol*, 2001. **20**(3): p. 159-69.
191. Majewski, M., et al., *IMPROVED TENDON HEALING USING bFGF, BMP-12 AND TGF beta(1) IN A RAT MODEL*. *European Cells & Materials*, 2018. **35**: p. 318-334.
192. Tokunaga, T., et al., *Enhancement of rotator cuff tendon-bone healing with fibroblast growth factor 2 impregnated in gelatin hydrogel sheets in a rabbit model*. *J Shoulder Elbow Surg*, 2017. **26**(10): p. 1708-1717.
193. Goncalves, A.I., et al., *Understanding the role of growth factors in modulating stem cell tenogenesis*. *PLoS One*, 2013. **8**(12): p. e83734.
194. Chan, B.P., et al., *Effects of basic fibroblast growth factor (bFGF) on early stages of tendon healing: a rat patellar tendon model*. *Acta Orthop Scand*, 2000. **71**(5): p. 513-8.
195. Najafbeygi, A., et al., *Effect of Basic Fibroblast Growth Factor on Achilles Tendon Healing in Rabbit*. *World J Plast Surg*, 2017. **6**(1): p. 26-32.
196. Li, J., et al., *The prognostic value of integration of pretreatment serum amyloid A (SAA)-EBV DNA (S-D) grade in patients with nasopharyngeal carcinoma*. *Clin Transl Med*, 2020. **9**(1): p. 2.
197. Bennet, D., et al., *Molecular and physical technologies for monitoring fluid and electrolyte imbalance: A focus on cancer population*. *Clin Transl Med*, 2021. **11**(6): p. e461.
198. Sato, N., et al., *Proteomic Analysis of Human Tendon and Ligament: Solubilization and Analysis of Insoluble Extracellular Matrix in Connective Tissues*. *J Proteome Res*, 2016. **15**(12): p. 4709-4721.
199. Zhou, H.J., et al., *Severity stratification and prognostic prediction of patients with acute pancreatitis at early phase A retrospective study*. *Medicine*, 2019. **98**(16).
200. Hajian-Tilaki, K.O., et al., *Body mass index and waist circumference are predictor biomarkers of breast cancer risk in Iranian women*. *Med Oncol*, 2011. **28**(4): p. 1296-301.
201. Huber-Lang, M., A. Kovtun, and A. Ignatius, *The role of complement in trauma and fracture healing*. *Semin Immunol*, 2013. **25**(1): p. 73-8.
202. Wang, J.H.C., Q.P. Guo, and B. Li, *Tendon Biomechanics and Mechanobiology-A Minireview of Basic Concepts and Recent Advancements*. *Journal of Hand Therapy*, 2012. **25**(2): p. 133-140.
203. McCarrel, T.M., T. Minas, and L.A. Fortier, *Optimization of leukocyte concentration in platelet-rich plasma for the treatment of tendinopathy*. *J Bone Joint Surg Am*, 2012. **94**(19): p. e143(1-8).
204. Pillitteri, D., et al., *Thrombin-induced interleukin 1beta synthesis in platelet suspensions: impact of contaminating leukocytes*. *Platelets*, 2007. **18**(2): p. 119-27.
205. Balke, N., et al., *Inhibition of degranulation of human polymorphonuclear leukocytes by complement factor D*. *FEBS Lett*, 1995. **371**(3): p. 300-2.

206. An, Y., et al., *Autophagy promotes MSC-mediated vascularization in cutaneous wound healing via regulation of VEGF secretion*. Cell Death Dis, 2018. **9**(2): p. 58.
207. Han, Y.F., et al., *Clinical perspectives on mesenchymal stem cells promoting wound healing in diabetes mellitus patients by inducing autophagy*. Eur Rev Med Pharmacol Sci, 2015. **19**(14): p. 2666-70.
208. Vescarelli, E., et al., *Autophagy activation is required for myofibroblast differentiation during healing of oral mucosa*. Journal of Clinical Periodontology, 2017. **44**(10): p. 1039-1050.
209. Ren, H., et al., *Autophagy and skin wound healing*. Burns Trauma, 2022. **10**: p. tkac003.
210. Tsuchiya, K., *Switching from Apoptosis to Pyroptosis: Gasdermin-Elicited Inflammation and Antitumor Immunity*. Int J Mol Sci, 2021. **22**(1).
211. Arulselvan, P., et al., *Role of Antioxidants and Natural Products in Inflammation*. Oxid Med Cell Longev, 2016. **2016**: p. 5276130.
212. Litwiniuk, M., et al., *Hyaluronic Acid in Inflammation and Tissue Regeneration*. Wounds, 2016. **28**(3): p. 78-88.
213. Guo, M. and B.A. Hay, *Cell proliferation and apoptosis*. Curr Opin Cell Biol, 1999. **11**(6): p. 745-52.
214. Oh, S.J., et al., *Sorafenib decreases proliferation and induces apoptosis of prostate cancer cells by inhibition of the androgen receptor and Akt signaling pathways*. Endocr Relat Cancer, 2012. **19**(3): p. 305-19.
215. Fronza, M., et al., *Determination of the wound healing effect of Calendula extracts using the scratch assay with 3T3 fibroblasts*. J Ethnopharmacol, 2009. **126**(3): p. 463-7.
216. Yang, Y., et al., *The roles of autophagy in osteogenic differentiation in rat ligamentum fibroblasts: Evidence and possible implications*. FASEB J, 2020. **34**(7): p. 8876-8886.
217. Xie, Z.Y., Z.H. Xiao, and F.F. Wang, *Inhibition of autophagy reverses alcohol-induced hepatic stellate cells activation through activation of Nrf2-Keap1-ARE signaling pathway*. Biochimie, 2018. **147**: p. 55-62.
218. Choi, H., et al., *Heterogeneity of proteome dynamics between connective tissue phases of adult tendon*. Elife, 2020. **9**.
219. Deng, Z., et al., *Myostatin inhibits eEF2K-eEF2 by regulating AMPK to suppress protein synthesis*. Biochem Biophys Res Commun, 2017. **494**(1-2): p. 278-284.
220. Knight, J.R., et al., *Rpl24(Bst) mutation suppresses colorectal cancer by promoting eEF2 phosphorylation via eEF2K*. Elife, 2021. **10**.
221. Koskinen, S.O.A., et al., *Physical exercise can influence local levels of matrix metalloproteinases and their inhibitors in tendon-related connective tissue*. Journal of Applied Physiology, 2004. **96**(3): p. 861-864.
222. Saraswati, S., et al., *Identification of a pro-angiogenic functional role for FSP1-positive fibroblast subtype in wound healing*. Nat Commun, 2019. **10**(1): p. 3027.

223. Koos, J.A. and A. Bassett, *Genetics Home Reference: A Review*. Med Ref Serv Q, 2018. **37**(3): p. 292-299.
224. Maffulli, N., H.D. Moller, and C.H. Evans, *Tendon healing: can it be optimised?* Br J Sports Med, 2002. **36**(5): p. 315-6.
225. Kaleci, B. and M. Koyuturk, *Efficacy of resveratrol in the wound healing process by reducing oxidative stress and promoting fibroblast cell proliferation and migration*. Dermatol Ther, 2020. **33**(6): p. e14357.
226. Shi, N., et al., *Eukaryotic elongation factors 2 promotes tumor cell proliferation and correlates with poor prognosis in ovarian cancer*. Tissue Cell, 2018. **53**: p. 53-60.
227. Ebeling, S., et al., *From a traditional medicinal plant to a rational drug: understanding the clinically proven wound healing efficacy of birch bark extract*. PLoS One, 2014. **9**(1): p. e86147.
228. Pitzurra, L., et al., *Effects of L-PRF and A-PRF+ on periodontal fibroblasts in in vitro wound healing experiments*. J Periodontal Res, 2020. **55**(2): p. 287-295.
229. Schreier, T., E. Degen, and W. Baschong, *Fibroblast migration and proliferation during in vitro wound healing. A quantitative comparison between various growth factors and a low molecular weight blood dialysate used in the clinic to normalize impaired wound healing*. Res Exp Med (Berl), 1993. **193**(4): p. 195-205.
230. Magadum, A. and F.B. Engel, *PPARbeta/delta: Linking Metabolism to Regeneration*. Int J Mol Sci, 2018. **19**(7).
231. Rayner, M.L.D., J. Healy, and J.B. Phillips, *Repurposing Small Molecules to Target PPAR-gamma as New Therapies for Peripheral Nerve Injuries*. Biomolecules, 2021. **11**(9).
232. Mirza, A.Z., I.I. Althagafi, and H. Shamshad, *Role of PPAR receptor in different diseases and their ligands: Physiological importance and clinical implications*. European Journal of Medicinal Chemistry, 2019. **166**: p. 502-513.
233. Voleti, P.B., M.R. Buckley, and L.J. Soslowsky, *Tendon healing: repair and regeneration*. Annu Rev Biomed Eng, 2012. **14**: p. 47-71.
234. Li, Q.Y., et al., *Gender difference in protein expression of vascular wall in mice exposed to chronic intermittent hypoxia: a preliminary study*. Genet Mol Res, 2014. **13**(4): p. 8489-501.
235. Wu, C.T., et al., *Gender difference of CCAAT/enhancer binding protein homologous protein deficiency in susceptibility to osteopenia*. J Orthop Res, 2019. **37**(4): p. 942-947.